mTORC2 controls neuron size and Purkinje cell morphology independent of mTORC1

Inauguraldissertation

zur
Erlangung der Würde eines Doktors der Philosophie
vorgelegt der
Philosophisch-Naturwissenschaftlichen Fakultät
der Universität Basel
von

Venus Thomanetz

aus

Stuttgart, Deutschland

Basel, 2012

Genehmigt von der Philosophisch-Naturwissenschaftlichen Fakultät

auf Antrag von

Prof. Dr. Markus A. Rüegg

Dr. Stephan Frank

Basel, den 18.10.2011

Prof. Dr. Martin Spiess

TABLE OF CONTENT **PAGE**

ABSTRACT

Prenatal brain development is mainly accomplished by extensive proliferation of neuronal precursor cells whereas postnatal brain growth in mammals is mainly mediated by the growth of those post-mitotic nerve cells. The neuron size and the branching pattern of the dendritic tree are highly controlled during development to enable the proper connectivity of neuronal circuits and the accurate electrical transmission in the adult which is a prerequisite for the brain to function normally. Aberrations in size, morphology or connectivity have been shown to be the cause for various brain disorders. Neuron size and dendrite development are controlled by intrinsic mechanisms, trophic factors and neuronal activity, processes that need the concerted action of a plethora of signaling molecules. A central integrator of various signaling cascades is the mammalian target of rapamycin (mTOR) and as such it contributes to brain development and function and is thus also implicated in the pathophysiology of psychiatric disorders.

mTOR is a serine threonine protein kinase that is highly conserved from yeast to humans and has been found to be part of at least two multi-protein complexes mTORC1 and mTORC2. The formation of mTORC1 is dependent on the protein raptor whereas mTORC2 assembly relies on the protein rictor. In recent years a complex picture about the function of mTORC1 has emerged by use of rapamycin, an immunosuppressive drug that acutely inhibits mTORC1 formation and activity and has attributed mTORC1 a major role in the regulation of cell size and proliferation. However, because the activity of mTORC2 is only depleted upon long term application of rapamycin, research advancement on its function was thus far impeded. Due to the early embryonic lethality of raptor or rictor knockout in mammals conditional knockout models were constructed. Whereas tissue specific knockout of raptor led to characteristic alterations, knockout of rictor in several organs such as skeletal muscle and adipose tissue provided none or only a weak phenotype. Several cell culture studies assigned mTORC2 a role in cytoskeletal modifications but *in vivo* confirmation is still lacking. The current knowledge about mTORC2 is restricted to the downstream targets Akt/PKB (proteinkinase B) and PKC (protein kinase C) which belong to the AGC kinase family. Those kinases are reported to influence cell morphology, growth and survival and are also essential regulators of brain development and function. PKCs are involved in synaptic plasticity and neurotransmitter release and, hence, also in the pathophysiological mechanisms of psychiatric disorders especially in schizophrenia and bipolar disorder. Concordantly, several psychiatric agents have been shown to alter PKC signaling. This emphasizes the urge to analyze the role of mTORC2 in the central nervous system.

In this dissertation the role of mTORC2 was analyzed in the central nervous system and in specific sub-populations of neurons by deletion of rictor. I discovered, that in contrast to all other organs analyzed so far, rictor knockout in the brain reveals a pronounced phenotype. The brain-size of those mice shows an enormous reduction to almost half of that of control mice which is caused mainly by the reduction of neuron size. The reduced cell size is observed in neurons derived from different brain areas *in vitro* and *in vivo* but is most prominent in Purkinje cells of the cerebellum, the cell type with highest rictor expression. In addition, dendrite morphology is majorly disrupted and the formation of dendritic spines is affected which correlates with a decreased neuronal activity. The Purkinje cell phenotype can also be reproduced in a Purkinje cell specific knockout of rictor and thus demonstrates that the effect of rictor deletion in neurons is cell autonomous. Moreover, Purkinje cell axonal path-finding is affected which correlates with the decrease in phosphorylation of the neuron specific PKC target protein GAP-43, a known regulator for axon growth and path-finding. Molecular analysis reveals that rictor is essential for the activity of all conventional PKC isoforms and the novel PKCε *in vivo* and *in vitro* in neurons which influences the function of downstream targets important for cytoskeleton modifications such as GAP-43, MARCKs and

neurofascin. In addition, rictor controls the phosphorylation of Akt but does not alter mTORC1 signaling towards its downstream effectors. In summary it becomes clear that rictor is important in the development and maturation of neurons and controls their size and neuron structure which influences the entire brain function and affects the behavior of the mice. Thus, these data encompass a new role of rictor in CNS disorders.

GENERAL INTRODUCTION:

Development and functional connectivity of neurons:

Like every organ, the brain is composed of specialized cells that accomplish highly specific functions and brain cells indisputably feature the most noticeable complex morphology of all cell types. To understand how the brain manages to develop an intricate behavior and enables us to think, move and communicate, a basic understanding of the cell types and their structural and functional relationship in the central nervous system (CNS) is essential.

The building units in the brain are the neurons and glial cells. A mature human brain constitutes about 100 billion neurons and even more glial cells. During brain development glial cells build the scaffold that enables neurons to migrate along to their target locations. They have stabilizing and isolating functions for neurons in the adult brain [1] and are essentially involved in the clearing of neurotransmitter from the synaptic cleft to maintain and modulate fast neurotransmission and to avoid neuronal over-excitation [2]. Although glial cells were thought to constitute mainly supportive elements in the brain, the importance of glial cells during development and in neuronal function has been appreciated more and more over the last decades. However, in this manuscript the focus is set primarily on the other cell-type, the neurons. Neurons are highly polarized cells that can be compartmentalized into three structural parts, the soma, the dendrites and the axon. The axon initiates electrical signals at the axon hillock and those signals, the action potentials, enable neurons to communicate with each other over very long distances. In humans the longest axonal range reaches from the spinal cord down to the toes.

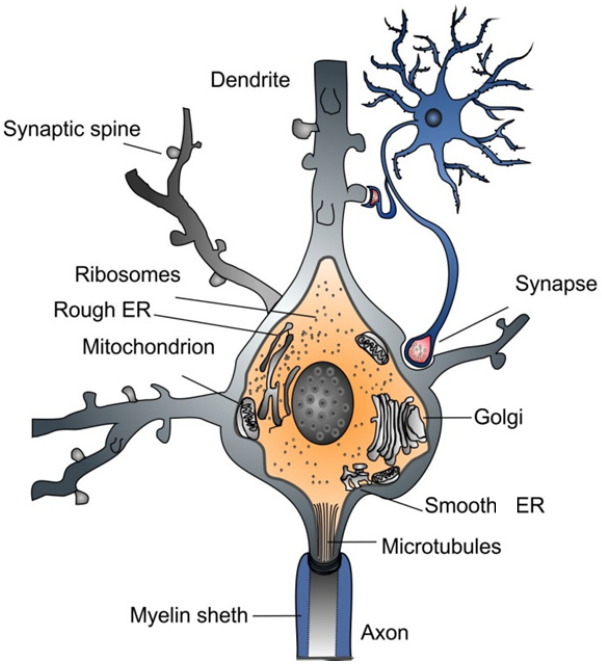

Figure 1. Sketch of a vertebrate neuron and its connections. The soma of a neuron contains all necessary components for cell survival. A neuron contains only one axon but may have many dendrites depending on the type of neuron. The dendrites are covered with synaptic spines which distinguishes them morphologically from axons. Axons can be covered by a myelin sheath which is a wrap of membrane from an oligodendrocyte. This cover enables axons to transfer electrical signals over long distances without loss of signal. All organelles are indicated in the figure.

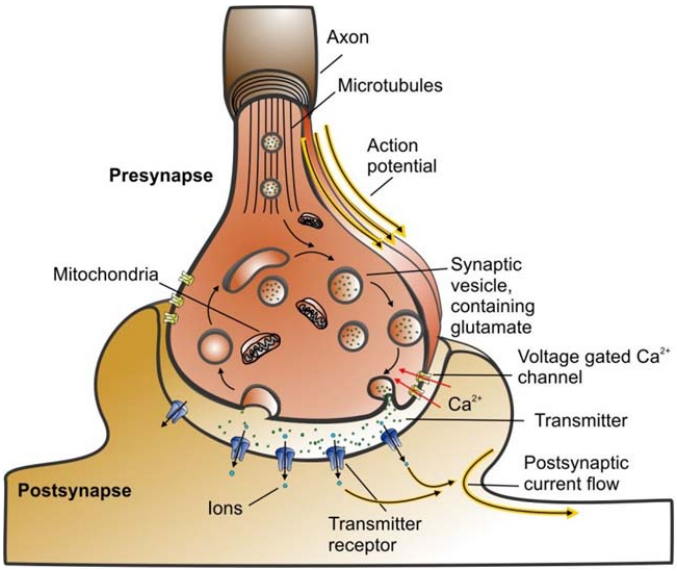

Figure 2. Schematic drawing of a typical chemical synapse. The arrival of an action potential at the presynaptic compartment opens voltage-gated Ca^{2+} channels which induces an increase in the presynaptic Ca^{2+} concentration. This causes the fusion of transmitter-containing synaptic vesicles with the membrane to release neurotransmitter into the synaptic cleft. At the postsynaptic side, the transmitter binds to neurotransmitter receptors, which causes the opening or closing of ion channels. The postsynaptic current flow induces an excitatory or inhibitory synaptic potential and leads to a change in excitability of the postsynaptic cell.

The receiving units of the neuronal network are the dendrites. Dendrites are specialized, highly ramified processes of neuronal cells which usually branch extensively but are relatively short compared to axons. Signal transfer from axon to dendrite is operated at specific compartments, the synapses. Most neurons that receive excitatory input generate highly specialized protrusions, the synaptic spines, which are mushroom-shaped extensions from dendrites that contain micro-domains of synaptic compartment. The axon terminal of a chemical synapse releases neurotransmitters, neuropeptides or combinations of both into the synaptic cleft depending on the type of neuron. The postsynapse comprises neurotransmitter receptors which are either ion channels or coupled to such. Each neuron type has a very specific composition of neurotransmitter receptors of which there are about 100 known today and this variety of receptor combinations creates a huge amount of possible responses to the signal received by the axon. The activation of neurotransmitter receptors mediates the flux of ions across the plasma membrane to evoke an electrical signal. This change in postsynaptic potential (that differs from the resting membrane potential) can be measured electrophysiologically and gives information on the number and strength of synapses. The postsynaptic membrane response which is induced by a presynaptic stimulus is referred to as excitatory postsynaptic current (EPSC) or inhibitory postsynaptic current (IPSC). The sum of all excitatory and inhibitory currents that are received by a neuron then decides if an action potential is induced by this neuron or not. EPSCs thereby increase the likelihood of an action potential to be elicited (e.g. by opening kation channels) whereas IPSCs rather inhibit this likelihood (e.g. by closing kation channels or by opening Cl-channels). In addition, those currents can trigger intracellular signaling cascades that modify the structure of the synapse and the sensitivity to neurotransmitters. Thus, an intense stimulus with the appropriate frequency can cause the maintenance of synapses or even induces the formation of new ones. The current understanding takes this structural and functional rearrangement of synapses (synaptic plasticity) as the basic concept for learning and memory formation.

A neuron can make up to 10,0000 connections with other neurons that can be of both, excitatory and inhibitory nature and thus, each neuron receives a huge amount of information which must be

integrated and redistributed to other neurons. But it becomes even more complicated when considering that in addition to their highly elaborate structure, neurons differ between each other in size, dendritic branching pattern and connectivity depending on the brain region. Importantly, the specific morphology of a neuron defines its function. This consequently means that the highly complex structure of the dendritic trees must be tightly controlled to enable the functional connectivity in the brain and to propagate the plethora of information flow from neuron to neuron. This structure to function relationship is essential and aberrations have profound consequences for the functioning of the brain [3,4]. A small composition of some neuron types is shown in Fig. 3 to exemplify the high variation in morphology of neuronal cell types.

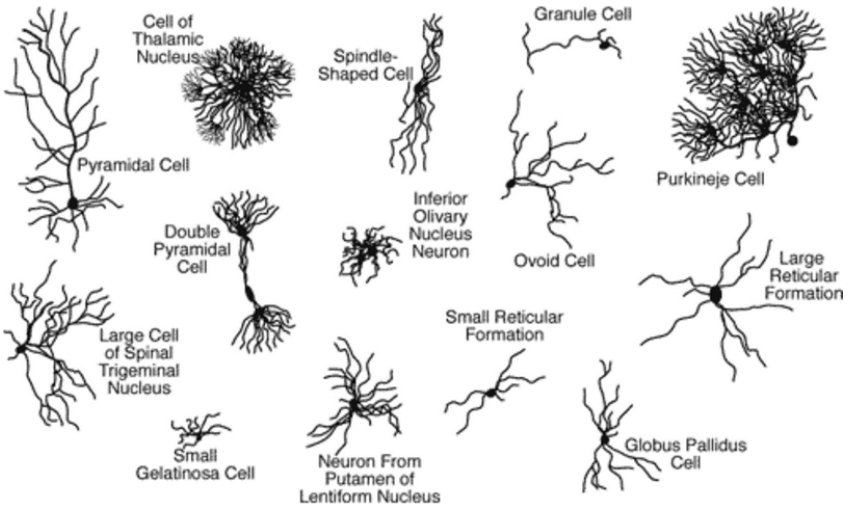

Figure 3. Schematic representation of different neuron types. Whereas some neurons are huge and contain highly branched dendrites such as the Purkinje cell, others have simple dendrite branching. The sketch is based on drawings by Cajal.

But how do neurons obtain their highly polarized morphology in axon and dendrites? And how do they grow to acquire their size and complexity?

The cell cortex of neuronal cells is composed of a cytoskeleton of actin and microtubule filaments. Thus, all factors that act on and influence the actin and microtubule structure can affect polarization, migration, growth and branching of neurons. The whole process of brain growth and neuron formation is a process that is intimately tied to the cytoskeleton. The first process in neurogenesis is the asymmetric cell division of neuronal precursor cells which is a process that depends on cytoskeleton structures [5]. Furthermore, neurons are highly motile cells that sometimes need to migrate long distances to reach their final destinations, another process that requires rapid restructuring of the cytoskeleton [6]. And also the polarization of neurons in axon and dendrites is mediated by cytoskeletal structures. The polarization of neurons starts by the elongation of several, initially undistinguishable neurites from the soma. The longest neurite elongates further and becomes the axon whereas growth of all the other neurites is inhibited. This polarization is thought to be evoked by differences in actin and tubulin dynamics. The neurites with highest actin instability but highest microtubule stability become the future axon whereas the other neurites have a rather rigid actin cytoskeleton [7,8] and destabilized microtubules and will become the dendrites. This actin destabilization is also the basis for growth and branching of neurites because only instable actin arrangement enables their rapid restructuring. Hence, although axons

and dendrites are both structures that elongate and branch during neuronal development, their actin and tubulin composition, growth rate and microtubule polarity differs considerably [9]. Whereas microtubules are tightly bundled and oriented into plus and minus ends in axons, their assembly in dendrites is loose and bidirectional [9]. This difference in composition also accounts for the difference in outgrowth.

Although differently regulated, a general mechanism which is necessary for migration, growth and branching of both, axons and dendrites, is the local actin and microtubule assembly, disassembly stabilization and destabilization and numerous intrinsic and extrinsic factors converge in regulating those processes. Since neurite growth is a central point in this manuscript, some of the molecules involved in this process will be shortly discussed in the following.

Many of the factors that have been shown to influence axonal growth and guidance come also in the focus of investigations on dendrite patterning. However, much more is known about axonal growth than is for dendrite development. Amongst the factors that influence axonal growth and migration are diffusible guidance molecules or contact-mediated cell adhesion molecules such as neuronal cell adhesion molecules (NCAM), integrins and cadherins which can have both, growth promoting or growth-inhibiting functions [10]. Extrinsic, diffusible factors that have an effect on neurite growth and branching also include growth factors such as brain derived neurotrophic factor (BDNF), Neurotrophins (NT-3 and NT-4) and nerve growth factor (NGF). But external factors are always coupled to internal signaling cascades that transfer the signal to the cytoskeleton and important players in those signaling cascades are the Rho GTPases including RhoA, Rac1 and Cdc42 [11]. Many Rho GTPases have also been implicated to regulate dendrite structure. Rac1 and Cdc42 were shown to have a growth promoting effect on axon and dendrites, whereas RhoA rather inhibits neurite growth. The proteins which finally exert the effect on the cytoskeleton by directly interacting and modifying the actin or tubulin structure are numerous and include severing or capping proteins, stabilizing and destabilizing factors and proteins that help in the assembly or disassembly of actin and tubulin [12]. In axons, one of those proteins that directly binds to and modifies actin stability is the growth associated protein 43 (GAP-43) [13]. This protein was shown to be phosphorylated by protein kinase C (PKC). It binds to actin filaments in phosphorylated and unphosphorylated state, however, in the unphosphorylated state its affinity for actin filaments is lower and it functions as a barbed-end, capping molecule that inhibits the severing of actin and thus prevents filopodia formation. Phosphorylation by PKC alters GAP-43 function and it then stabilizes actin filaments and promotes filopodia formation [14]. But this is only one example and many other proteins are also known to regulate those processes.

Dendritic growth and branching is a less well described process but it was shown to involve intrinsic genetic programs and extracellular signals. Neuronal activity seems to be important for most cell types to obtain their complex dendritic structure and there is evidence that cell contact and diffusible molecules mediate the polarization of apical and basal dendrites and the directional growth and branching [15].

In summary, any defect that may have an effect on actin or microtubule dynamics can alter the growth, migration and polarity of neurons. The morphology of neurons, however, is the key to their functions and the neuron-type specific dendritic arbors define their computational abilities [10,16,17].

In the following part, the development of one specific brain region, the cerebellum, is discussed in more detail. The requirements and growth conditions for Purkinje cells, a specific cerebellar

cell type, and the establishment of neuronal connections in the cerebellum are well defined and are thus a good example for dendrite development and circuit formation. In addition, a great part of this dissertation deals with the development, the structure and function of this brain region.

The cerebellum:

The adult cerebellum is composed of only few neuron types which assemble in a highly conserved structure. The granule cells build the granule cell layer which is topped with a monolayer of Purkinje cell somata [18]. The huge dendritic trees of Purkinje neurons extend perpendicularly to the pial surface and constitute the molecular layer where most of the synaptic contacts onto Purkinje cells are made [18]. All afferent and all efferent fibers diverge into the white matter below the granule cell layer. Importantly, the Purkinje cell axons are the only output of the cerebellar cortex [19].

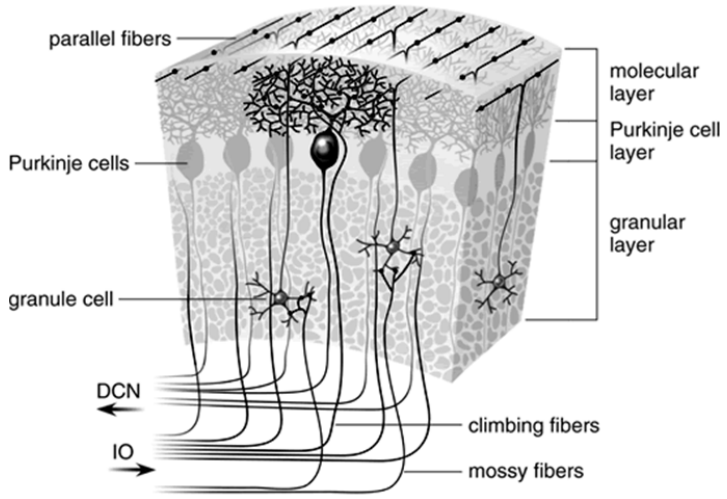

Figure 4. Schematic representation of the cellular distribution in the adult mammalian cerebellum. Purkinje cells form a monolayer on top of a dense layer of granule cells. Purkinje cell dendrites are oriented flat in the sagittal plane and give rise to the molecular layer with their huge and highly branched dendritic trees. The axons of granule cells, the parallel fibers, run perpendicular to the Purkinje cell dendrites and innervate the distal parts of those. Climbing fibers which have their somata in the deep cerebellar nuclei (DCN) innervate the proximal Purkinje cell dendrite. Mossy fibers from the inferior olive are the main afferents to granule cells. Picture derived by *current protocols.com*

The cerebellar development is unique in that the cells that constitute the cerebellum derive from two germinal centers, the ventricular zone and the rhombic lip. Purkinje cells are generated in the ventricular zone. Between embryonic day 11 (E11) and E13 they become post-mitotic [20] and start migrating radially along radial glial cells towards the structure that will develop into the cerebellum [21,22]. Shortly after birth, dendrite development of Purkinje cells begins with the evolvement of a polarized morphology (Fig.5). In the first postnatal week, Purkinje cells form multiple short processes, the so called "stellate with disoriented dendrites" and migrate outward to form a monolayer [23]. During this phase, innervations are mediated solely by climbing fibers that contact Purkinje cells perisomatically [24] and parallel fiber innervation is restricted to only some immature synapses onto the dendrites of Purkinje cells [25] (Fig.6). At the end of the first postnatal week and the beginning of the second, Purkinje cells have formed a monolayer [25]. The soma starts growing and most cells extend one primary dendrite in the molecular layer. This phase is characterized by rapid growth and branching of Purkinje cell dendrites [25,26] and strong

innervation by parallel fibers whereas climbing fiber innervation is shifted to a peridendritic location [24]. It has been shown that maturation of the dendritic tree of Purkinje cells is not simultaneous and depends on the location within the cerebellum with lobule I and X as the earliest and lobule VI, VII and VIII as the latest to mature [25]. Finally, enlargement, flattening and synaptogenesis of Purkinje cell dendrites continues until about the 4th postnatal week [25].

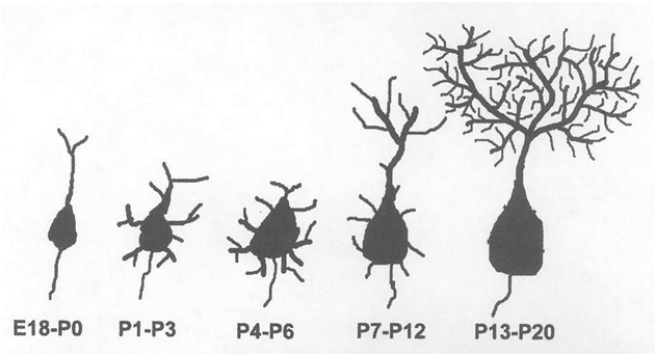

Figure 5. Sketch of postnatal Purkinje cell development in the mouse cerebellum. Developmental time points are indicated in the drawing. The Purkinje cell develops a stellate appearance during the first postnatal week. This morphology is transformed at the end of the first week to a polarized morphology with one primary dendrite whereas the other neurites are retracted. Picture derived from *Kapfhammer; 2004.*

The second germinal zone of the cerebellum is the rhombic lip which gives rise to granule cells, unipolar brush cells and some deep nuclear neurons [27,28]. Granule cells are the smallest neurons in the brain but also the most numerous (10^{10}) [29]. Granule cell precursors (GCP) migrate over the outer surface of the cerebellum to form the mitotically active external granule cell layer (EGL) which reaches its proliferative peak at postnatal day 8 (P8) [30]. At birth (P0), the first GCP's become post-mitotic and migrate tangentially inward to form the internal granule cell layer (IGL)

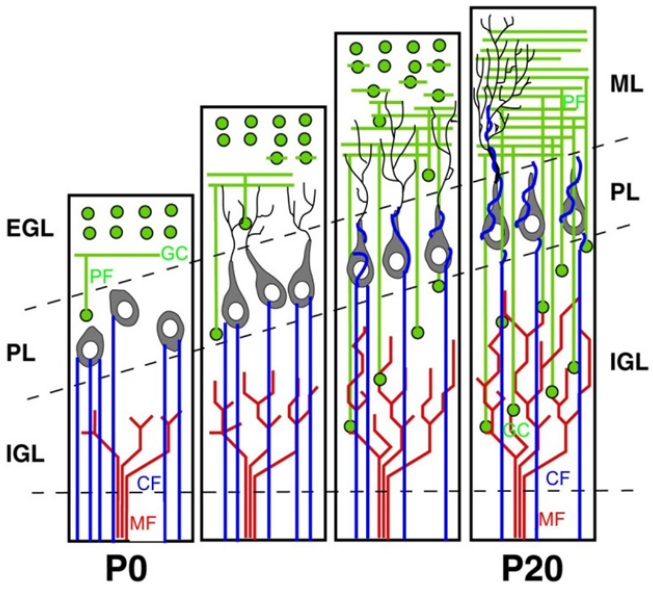

Figure 6. Sketch, depicting the postnatal cerebellar development. During the early postnatal period (P0) multiple climbing fibers (CF) innervate Purkinje cells in the Purkinje cell layer (PL). Those innervations are retracted during postnatal development and monosynaptic innervation on the proximal dendrite retains in the adult cerebellum. Mitotically active granule cells (GC) in the external granule cell layer (EGL) proliferate and then differentiate and move inward to build the internal granule cell layer (IGL). During their migration they start to form axons, the parallel fibers (PF) with which they innervate the distal dendrites of growing Purkinje cells in the molecular layer (ML). GCs are innervated on their small dendritic trees by mossy fiber axons (MF) in the IGL. Picture derived from *clifta.com* with own modifications.

[31]. During the migration process, granule cells start to form axon extensions and begin to innervate Purkinje cells [24]. This process is finished at about P20 in mice [32]. Granule cells themselves are innervated by mossy fibers which originate from several brain areas. Their axons form characteristic, rosette like synaptic structures with the small granule cell dendrites in the granule cell layer [33].

Superimposed on the excitatory synaptic connections onto Purkinje cells from parallel and climbing fibers, are the inhibitory cells of the cerebellum. Localized in the molecular layer are the stelate and basket cells which use the neurotransmitter γ-aminobutyric acid and are interneurons that make synapses onto the dendrites and the soma of Purkinje cells, respectively. The candelabrum cells reside in the Purkinje cell layer and the lugaro and Golgi cells are located in the granule cell layer. The dendrites of those inhibitory neurons are located in the molecular layer. They receive synaptic input mainly from parallel fibers [19] which are also their output targets. This inhibitory circuit generates a highly interactive loop of excitation and inhibition onto Purkinje cells and contributes to the fine tuning of motor coordination.

As mentioned above, Purkinje cells are the only output of the cerebellar cortex. Thus, proper morphology and innervations of those cells are essential for accurate signaling to other brain regions. In the adult brain, Purkinje cells receive excitatory input from granule cells and climbing fibers which use the neurotransmitter glutamate [18]. All other cerebellar neurons use the inhibitory neurotransmitter GABA, including Purkinje cells.

In the cerebellum, early postnatal innervation differs strongly from the innervation pattern in the adult. During early postnatal development the axons of climbing fibers, which have their soma in the inferior olivary nucleus in the medulla oblongata, grows and forms multiple connections to the soma of Purkinje cells. Those multiple connections are degenerated over the ongoing postnatal development. In adult brain, only one climbing fiber contacts one PC with multiple contacts along the proximal dendrite and constitutes the strongest excitatory connection in the CNS [34]. In contrast to this homosynaptic innervation, the synaptic connection between Purkinje cells and parallel fibers is very numerous. In the adult brain, one Purkinje cell is innervated by approximately 10^5- 10^6 parallel fibers but one parallel fiber forms only 1-2 synaptic connections onto one Purkinje cell [35]. This heterosynaptic innervation generates a cumulative signal transmission from parallel fibers onto Purkinje cells.

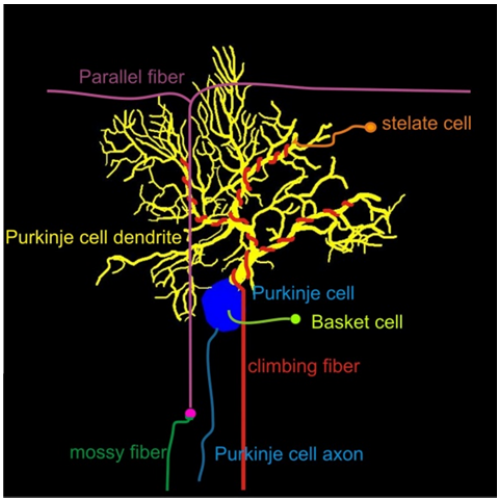

Figure 7. Purkinje cell innervation. Drawing of an adult Purkinje cell and most of its afferents. The climbing fibers which have their soma in the deep cerebellar nuclei make synaptic contacts on the proximal dendritic stem of Purkinje cells. Each climbing fiber innervates only one Purkinje cell but makes several synaptic contacts. Parallel fibers contact the distal dendrites of Purkinje cells. Each parallel fiber makes only few synapses with one Purkinje cell but also innervates numerous other Purkinje cells. Inhibitory afferents are provided by Basket, Golgi and stellate cells which also make synaptic contacts on parallel and climbing fibers.

As mentioned above, the morphology of a certain cell type is highly specific and reflects the function of this respective neuron type. The morphology of Purkinje cells is also highly regulated and the main hallmark is the large soma and the huge dendritic tree which emanates from one single primary dendrite and receives input from between 50,000 to 150,000 different axons. This highly ramified dendritic tree is flat in the sagittal plain and aligned perpendicularly to the pial surface.

Many factors have been shown to have an influence on the structure, growth and alignment of Purkinje cells. The development of one single primary Purkinje cell dendrite and the retraction of all other dendritic protrusions at about P7 correlates with the differentiation of climbing fibers and the establishment of the first parallel fiber synapses. Thus, it is presumed, that a competition through electrical activity between climbing fiber and parallel fiber synapses onto Purkinje cells is responsible for the preservation of only one single primary dendrite and the retraction of the other processes [36]. However, in the absence of parallel fiber input during development, Purkinje cells develop a rather complex dendritic tree although much smaller and mis-oriented to the pial surface. In addition they fail to form distal branches and spiny branchlets. This has been demonstrated in neonatal rats in which granule cells were subjected to X-irradiation [37] but the same Purkinje cell morphology can also be observed in the *weaver* mutation where most granule cells die before they can form synaptic contacts with Purkinje cells [38]. Those studies have led to the concept that parallel fiber input is essential for Purkinje cells to generate higher order spiny branchlets and to orient Purkinje cells into the sagittal plain. However, blockage of glutamatergic excitatory neurotransmission during the rapid growth phase of Purkinje cells by application of different glutamate receptor antagonists was demonstrated to have no profound effect on Purkinje cell dendritic structure [23] which rather indicates that other factors than just simply parallel fiber activity influence the dendritic tree development of Purkinje cells.

Important also for Purkinje cell development is the abundance of several hormones. Thyroid hormone is significantly involved in Purkinje cell morphology and hypothyroidism in neonatal rats causes a profound reduction of Purkinje cell size and branching [39]. Sex hormones such as progesterone and estrogen are important for growth and spine formation of Purkinje cells and it was even demonstrated that Purkinje cells themselves synthesize those hormones [40,41] especially at the postnatal period of highest Purkinje cell growth.

As mentioned above, cell growth can be influenced by the presence of trophic factors. The sensitivity of Purkinje cells to growth factors such as BDNF, NGF or NT is, however, controversial. The results obtained from *in vitro* studies suggest that BDNF has no effect on growth and survival of Purkinje cells [23] whereas NT-3 and NT-4 were shown to promote Purkinje cells survival but not growth [42]. Thus, the notion appears that Purkinje cell-growth and structuring is not simply dependent on growth factors or excitatory neurotransmission during the rapid growth phase of Purkinje cells but is also fueled by Purkinje cell intrinsic growth programs and endogenous electrical activity of Purkinje cells [43].

The structural conformity of neuronal cell types is also reflected in the structural consistency of the cerebellar architecture. The adult cerebellum is organized into 10 highly conserved lobules [19,44] and aberations in the anatomy of this structure were shown to cause defects in motor coordination.

But how does this morphology develop? The formation of the lobules and sub-lobules was demonstrated to also depend on Purkinje cells and their axonal anchorage to the base of the

fissures. During development, Purkinje cells locate at the future base of the fissure whereas Purkinje cell axons are anchored in the deep cerebellar nuclei [45]. The anchorage causes the rapidly proliferating granule cells to bulge out in between the fissures which results in the structuring of those lobules and sublobules [45]. Hence, morphology and organization of Purkinje cells assigns the shape of folia and this in turn has a major influence on the proper functioning of the cerebellum.

In summary, the cerebellum is a highly conserved structure and aberrations in the morphology are implicated to cause motor defects. The cerebellar shape is indispensably linked to the size, morphology and function of the cell types that constitute the cerebellum in particular the Purkinje cells. The size and morphology of those neurons is controlled by intrinsic genetic growth programs and by extrinsic cues and neuronal activity during cerebellar development.

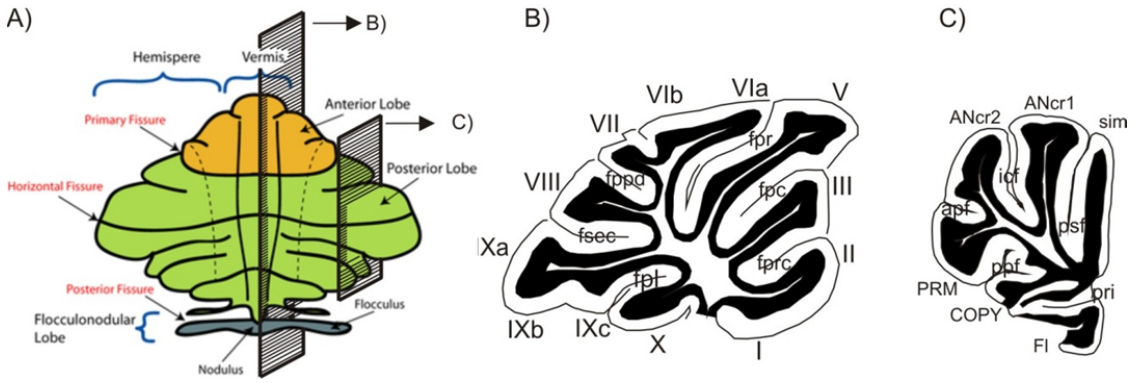

Figure 8. The cerebellar structure is highly conserved. (**A**) Schematic drawing of the major anatomical subdivisions of the mouse cerebellum (picture derived from *Wikipedia* with own modifications). (**B**) Cerebellar structure in a mid-sagittal section, in the vermal part of the cerebellum. The inner white area represents the white matter, the black layer the granule cell layer and the outer white area the molecular layer. (**C**) Cerebellar structure in the cerebellar hemisphere in sagittal plain. Abbreviations: fpl: posterolateral fissure, fsec: secondary fissure, fppd: prepyramidal fissure, fpr: primary fissure,fprc: precentral fissure. Vermal lobules are numbered from I-X. Lateral lobules: Ancr: Ansiform cruciform lobule, COPY: Copula pyramidis, Fl: Flocculus, PRM: paramedian lobule, Sim: simple lobule, apf: ansoparamedian fissure, icf: intercrural fissure, psf: posterior superior fissure, ppf: prepyramidal fissure, pri: primary fissure

Development and function of neurons has been studied for over a century already. However, much of the knowledge that we have today has been discovered since genetic manipulation enabled the ablation of specific gene products. Therefore, the following section introduces one technique which enables the analysis of the function of specific proteins in selected organs such as the brain.

Cre-Lox-recombination

In the last decade, the generation of several genetic and molecular-biological methods has aided the research on the function of specific proteins by the deletion of those. Knockout of a functionally important protein in an organism gives rise to a phenotype that is distinct to the wild type. If the gene is vital, deletion of it will be lethal to the organism. If it has a specific function

for example the reception of insulin, loss of this receptor function will make the animal unable to sense insulin which has severe consequences for the entire metabolism and the survival of the animal. The cause for the development of a disease is frequently an alteration of gene function. Targeted deletion of genes in model systems such as mice or flies are tools to discover the function of proteins and to find possible treatments for diverse ailments. Because proteins can exert different functions in different organs, the discovery of the Cre-Lox-system was of great benefit to study the function of proteins *in vivo* in specific organs and cell types. This system enables the site-specific recombination of genomic DNA which means that certain gene sequences can be eliminated by genetic manipulation. This is accomplished by insertion of a DNA construct into the genomic DNA of the model organism. The construct comprises the gene sequence of interest (mostly one or more exons), flanked by so called LoxP sites (locus of X-over P1). Those LoxP sites are known DNA sequences (from the Bacteriophage P1) of about 50 bp length which do not alter the function of the protein when inserted into the intron sequence of the gene of interest. However, those LoxP sites are recognized by a specific enzyme, the Cre (cyclization recombination) recombinase which excises the DNA sequence that lies between the loxP sites. For recombination a mouse containing loxP sites must be crossed with a mouse that comprises the Cre enzyme otherwise no recombination takes place. Importantly, the tissue or cell type in which the Cre recombinase will be activated is dependent on the promoter region, a gene sequence that sequesters proteins for transcription. Therefore, a specific promoter region is coupled to the Cre gene. Because the activity of a promoter region depends on the cell type, the promoter determines the location of the tissue- specific knockout to occur. Thus, the promoter of

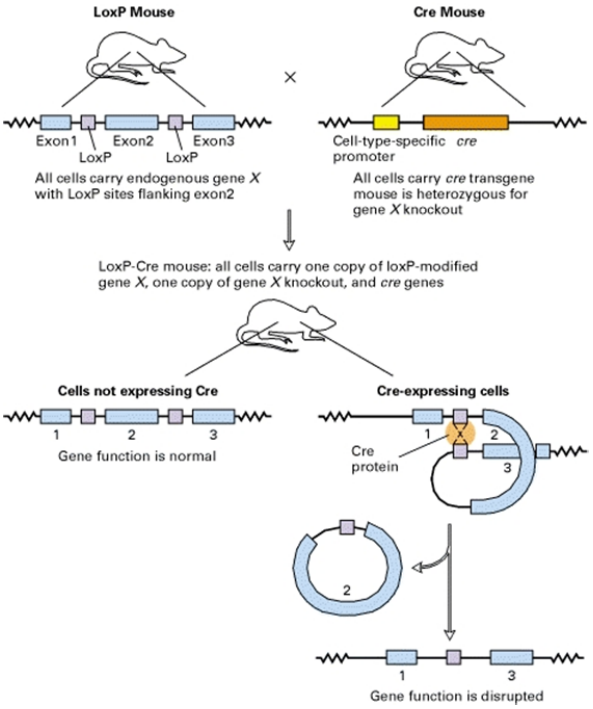

Figure 9. Sketch of the mechanisms of constitutive gene knockout by the Cre-lox-system. The exon of interest (blue) is flanked by the LoxP sites (grey) on both alleles in the LoxP mouse, which does not disrupt gene function. The Cre transgene containing the Cre-recombinase (orange) and the cell type specific promoter (yellow) is heterozygously inserted into the Cre-mouse. Crossing the LoxP-mouse with the Cre-transgenic mouse induces recombination of the LoxP sites in those mice that express the Cre recombinase. Recombination and thereby functional deletion of the gene takes only place in those cells that are able to activate the promoter. Picture derived from *Molecular Cell Biology. 4th edition. Lodish H, Berk A, Zipursky SL, et al. New York:W.H.Freeman; 2000.*

a brain specific protein such as nestin will cause LoxP recombination in brain cells only from early embryonic development on because the promoter starts to be active at around E10.5. Other promoters are cell type specific such as the Pcp2/L7 promoter which is only active in Purkinje cells and retinal bipolar cells and starts to be active during late embryonic development. The LoxP system has been proven to be especially advantageous in cases where full body knockout of a gene is lethal to the organism and impedes research on the function of the protein *in vivo*. But it has also aided in understanding cell autonomous effects in complex tissues.

In this manuscript, the function of one specific protein, rictor, is analyzed which is part of a signaling complex, mTORC2. This complex is highly abundant in neurons and regulates the activities of proteins which are linked to neuronal development and function and hence also to the development of brain diseases. To understand the implications of the results obtained in this study, one must be familiar with some of the proteins that play a role in the cellular signaling cascade in which rictor is a part of. Thus, the following part summarized most of the payers that are supposed to be involved in mTORC2 signaling.

The mTOR pathway

Eukaryotic cells are constantly controlling and optimizing their energy status to maintain cellular conditions for survival, growth and proliferation. The sensing of the cellular environment and internal cellular status is therefore essential and is mediated by various receptors. They perceive the availability of amino acids, hormones and growth factors like FGF (fibroblast growth factor), NGF or BDNF or cellular stress such as DNA damage, heat shock or ischemia. Those signals are then transferred via signaling pathways to generate an adequate cellular response. The availability of nutrients and growth factors trigger protein, nucleic acid and lipid synthesis which are necessary for growth and proliferation. On the other hand, low energy supply induces protein degradation (autophagy) and recycling [46]. Importantly, most of those signals involved in energy sensing were shown to converge onto one protein, the target of rapamycin, TOR [47]. The name originated in the sensitivity of TOR to the macrolide of a soil bacterium, rapamycin, nowadays used as immunosuppressant drug [47,48]. Its inhibitory action on the evolutionarily conserved kinase TOR fueled the possibilities in this research field and led to the fast discovery of the pathways involved in TOR signaling [49].

In mammals, the serine/threonine protein kinase mTOR assembles into at least two multi-protein complexes, mTORC1 and mTORC2 but most of its actions have been attributed to mTORC1. This is due to the insensitivity of mTORC2 to rapamycin which hampered research of this complex [50-52]. Both complexes have a distinct protein composition, mTORC1 comprising the necessary component regulatory-associated protein of mTOR (raptor) and mTORC2 comprising the rapamycin-insensitive companion of mTOR (rictor) as essential and complex defining proteins, respectively [53-55]. In addition, mTORC1 includes the 40 kDa Pro-rich Akt substrate (PRAS40) as negative regulator that blocks substrate accessibility of mTORC1 by regulating the raptor-mTOR binding [56]. mTORC2 on the other hand contains protein observed with rictor (PROTOR1) and PROTOR2, implicated in helping complex assembly and the mammalian stress-activated map kinase-interacting protein 1 (mSIN1), most likely involved in localizing mTORC2 to membranes [57-59]. They also share the positive regulator mammalian lethal with SEC13 protein 8 (mLST8) and the recently identified, negative regulator DEP domain-containing mTOR-

interacting protein (DEPTOR) [60,61]. Importantly, however, rictor is essential for complex assembly and activity of mTORC2. Concerning the activity, it is well documented that mTORC2 controls the activation of the protein kinases Akt, also known as protein kinase B (PKB) [59,62] and the protein kinase C (PKC) by inducing phosphorylation at several important amino acid residues [51,63]. The effect of this regulation is, however, scarcely elucidated because both protein kinases have numerous substrates themselves and exert many different functions in cell systems. Nevertheless, some of the roles of Akt and PKC are illuminated in the following.

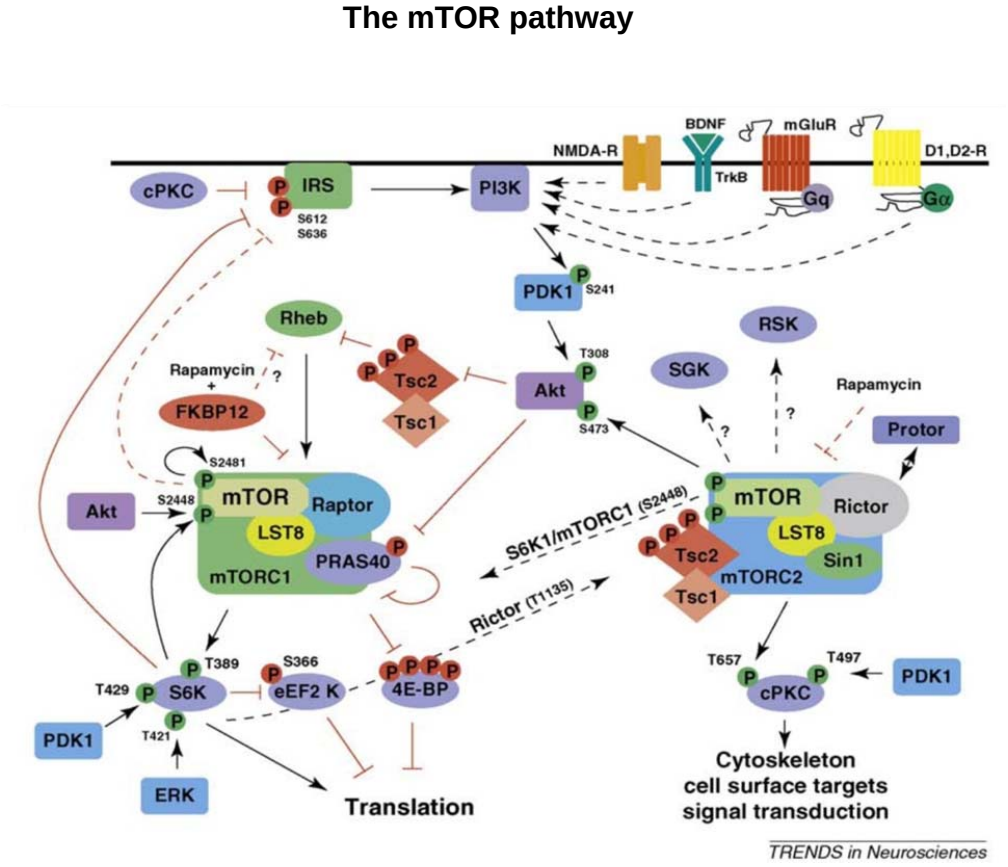

Figure 10. Proposed mTOR signaling pathway in neurons. mTORC1 is activated by activation of neuronal receptors and channels through a pathway involving Akt. In normally functioning neurons, Akt inhibits the TSC1/TSC2-complex by phosphorylation which further circumvents the replacement of GTP in Rheb and keeps this protein in an active state. GTP-boud Rheb activates mTORC1 which phosphorylates its downstream effectors causing transcription events to occur. A feedback loop towards the insulin receptor substrate (IRS) negatively controls mTORC1s own activity. The mechanism that leads to mTORC2 activation is not known. It is supposed that S6K1/2 can also phosphorylate rictor and thereby alters mTORC2 activity. Conversely, mTORC2 is supposed to mediate mTORC1 phosphorylation at a specific residue. However, the consequences of this crosstalk are not fully understood. mTORC2 regulates the phosphorylation of the hydrophobic motif and turn motif of Akt and the hydrophobic and turn motif phosphorylation of PKC and thereby controls their activity. Whether this phosphorylation is direct or indirect is not known. mTORC2 mediated regulation of PKC activity is thought to have an influence on the actin cytoskeleton whereas Akt activity is thought to control cell survival. See text for detailed description. Picture derived from *C. A. Hoeffer and E.Klann; 2009; Cell press*

Akt signaling

Akt is a central player in the mTOR signaling pathway. Akt is a member of the AGC family of kinases and can be activated by extracellular signals such as hormones, trophic factors and mitogens. Those molecules bind to and activate receptor tyrosine kinases at the plasma membrane. Upon receptor activation, the phosphatidylinositol-3-kinase (PI3K) generates phosphatidylinositol-2-4-5-triphosphate (PIP3) which consequentially leads to the recruitment of the protein kinase Akt to the plasma membrane. This translocation to the membrane determines the level of Akt that can be activated [64]. Once at the membrane, Akt is activated by dual phosphorylation at two amino acid residues, the activation loop at Thr308 and a highly conserved C-terminal domain, the hydrophobic motif at Ser473 [65]. Phosphorylation of Akt at the hydrophobic motif was shown to be accomplished by mTORC2 and was suggested to prime and stabilize the activated kinase [59,62]. Further phosphorylation of the activation loop is then mediated by 3-phosphoinositide-dependent protein kinase 1 (PDK1).

Many Akt substrates have been described in literature but the most well studied ones are the tuberous sclerosis complex (TSC) [66, 63,67, Long, 2005 #63], PRAS40 which was shown to inhibit mTORC1 independent of TSC [68], the glycogen synthase-kinase (GSK3ß) and the Forkhead family of transcription factors (FoxO1 and FoxO3). Phosphorylation of Tuberin (TSC2) by Akt causes the assembly of Hamartin (TSC1) to build the tuberous sclerosis complex which is a GTPase activating protein (GAP) towards the protein Ras homologue enriched in brain (Rheb) [69-72]. Thus, Akt phosphorylation causes complex assembly and thereby inactivation of TSC which consequently leads to an increase in GTP-bound Rheb [73]. Active Rheb then stimulates mTORC1 which further phosphorylates and thereby modulates two proteins, the S6 kinase 1 and 2 (S6K1/2) and the eIF4E-binding protein (4E-BP) causing mRNA translation initiation and progression and hence the regulation of protein synthesis [74]. In addition, S6K1/2 targets and inhibits also the insulin receptor substrate at the plasma membrane, generating a negative feedback loop that regulates mTORC1`s own activity [47]. However, Akt does not only have a regulatory role on mTORC1 but also has a direct impact on the activity of this complex by phosphorylation and thereby activation of the mTORC1 constituent PRAS40 [68].

The other Akt target, the FoxO`s, are thought to be responsible for the effect of Akt on cell survival [75]. Because mTORC2 has been shown to be the main kinase for hydrophobic motif (HM) phosphorylation of Akt an involvement of mTORC2 in apoptosis has been suggested. Relocation of FoxO1 and 3 from the cytoplasm to the nucleus causes the transcription of apoptosis inducing genes. Thus, phosphorylation by Akt mediates retention of the FoxO`s in the cytoplasm to promote cell survival [76]. Although many Akt substrates are described in literature, some Akt substrates seem to be more dependent on the HM phosphorylation than others. In this context, depletion of the Ser473 phosphorylation by knockdown of rictor was shown to affect only the phosphorylational activation of the FoxO`s whereas TSC1/2 and GSK3 seemed to be unaffected [77,78] which suggests that HM phosphorylation of Akt defines its substrate specificity.

The function of Akt in neurons

Akt has been implicated in various aspects of neuronal development, survival and function of neurons [79-82]. During brain development, neurons form an immense number of synaptic connections and neurons that make inappropriate attachments die by apoptosis. An important factor for the survival of developing neurons is the signaling by neurotrophins and the Akt

pathway is activated by those [83]. As mentioned above Akt mediated survival of cells is regulated by transcription factors such as the FoxOs or Bcl-2 family members [84,85]. Thus Akt links neurotrophic factor signaling to neuronal survival.

Another important role assigned to Akt function during brain development is the regulation of neuronal growth including neurite length, diameter and branching and neuronal migration. In this context it was shown that in growing cells, Akt is located at the tips of the growth cones [81]. Other aspects of neuronal development include the function of Akt in neuronal differentiation by regulation of GSK3ß, cyclic AMP response element binding protein (CREB) [86] or mTOR [87]. The effects on the cytoskeleton mediated by Akt involve the regulation of actin and tubulin modifying proteins that are involved in the severing or stabilization of filaments [88, 89,90]. One of those Akt targets is the p21 activated-kinase (Pak1) which is substrate of the Rho GTPases Cdc42 and Rac1. Those molecules are well known for their function in the organization of cytoskeletal structures and their growth promoting effect [91]. Thus, Akt signaling is required for various aspects of neuronal development and Akt dysfunction has been proposed to play an important role in brain dysfunction such as autism spectrum disorders and neurodegenerative diseases.

PKC signaling

Further regulation of AGC kinases by mTORC2 includes the protein kinase C (PKC) [63,92]. There are at least ten different PKC isoforms that are grouped into three categories classified by their structural and enzymatic properties. These include the conventional isoforms (cPKC: PKCα, -β and –γ), the novel isoforms (nPKC: PKCε, -δ and –η) and the atypical isoforms (aPKC: PKCζ, -λ, -ι and –μ) [93]. The cPKC isoforms are activated by phosphorylation and second messengers [elevated Ca^{2+} concentrations and diacylglycerol (DAG)], whereas the novel isoforms are regulated only by DAG and phosphorylation [94] and the atypical PKC`s are regulated independent of calcium and DAG. cPKC's and nPKC's are phosphorylated initially after translation at the turn motif (TM) and absence of this phosphorylation causes rapid, ubiquitin dependent degradation of the kinase [95,96]. In addition, hydrophobic motif (HM) phosphorylation of classical and novel PKC's stabilizes and increases the kinase activity [97]. Importantly, the main kinase for TM, HM and A-loop phosphorylation of PKCα is mTORC2 and mTORC2 was also demonstrated to regulate the activity of all conventional and the novel PKCε [63]. Because A-loop phosphorylation is normally targeted by PDK1 [98,99] an indirect effect of mTORC2 on this motif has been suggested.

PKC expression and function in the brain

PKC isoforms differ in their cellular distribution, in their sub-cellular localization and in their temporal expression during development [100]. Although they often share overlapping functions they can also antagonize each other and each isoform serves a unique biological role. In the brain, the occurrence of different PKC isoforms is also spatially and temporally regulated. During embryonic development, PKCα and PKCβ are considerably highly expressed in brain whereas PKCγ expression is low at birth and increases in the first 2-3 postnatal weeks. PKCα and PKCε are distributed in the entire brain whereas PKCγ is localized only in certain neurons such as cerebellar Purkinje cells and hippocampal neurons [101,102]. The function of a specific PKC isoforms is not only defined by their cellular but also by their sub-cellular distribution in different cellular

compartments and proximity to other proteins. Sub-cellular distribution of PKC isoforms reveals that PKCγ is localized to soma, dendrites and axon whereas PKCε is mainly found in presynaptic terminals. In the mammalian CNS, most PKC isoforms have been investigated by genetic deletion of the respective isoform. In those, PKCα was discovered to play a role in certain learning paradigms, the cerebellar long term depression (LTD) [103] and PKCγ knockout induced deficits in LTP (long term potentiation) and LTD [104]. PKCβ deficiency caused defects in fear conditioning [105], a test that is used to detect anxiety disorders, and PKCε proofed to be important in ischemic preconditioning and pain sensation [102,106]. Both, PKCγ and PKCε have been found to modulate $GABA_A$ receptor signaling and have been shown to play a role in pain response and the pharmacological tolerance to Ethanol [104]. However, because of their closely related roles and overlapping functions, only marginal effects are obtained by knockout of one PKC isoform which is attributed to the compensational mechanism of another PKC. This compensatory activity also impedes the research on specific subtypes of PKCs *in vivo.*

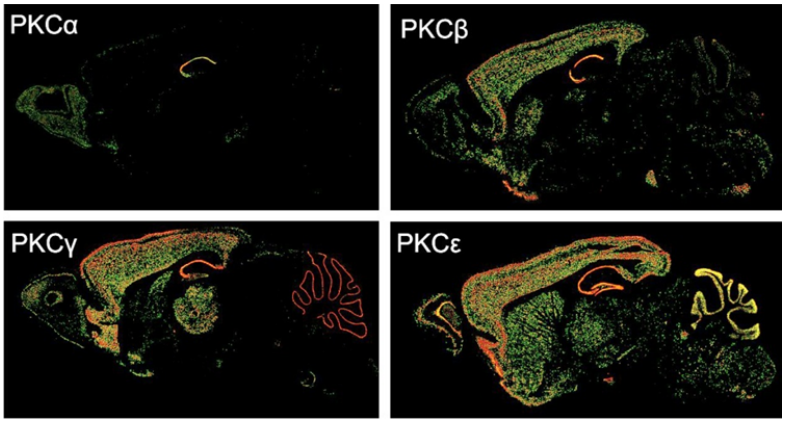

Figure 11. Expression profile of PKCα, β, γ and PKCε in adult brain. Midsagittal brain sections where the blue signal represents the lowest and red the highest expression. Data obtained by *Allen institute for brain science.*

PKC is a protein kinase that was shown to have an effect on the cellular actin cytoskeleton and as discussed above, proteins which influence the actin structure also interfere with cell morphology. Several lines of evidence from yeast studies and cell culture experiments also indicate that rictor is involved in cytoskeleton organization [51,107] and this function of rictor has been attributed to changes in the activation of PKCs [51]. However, the exact mechanism of how rictor affects the actin cytoskeleton is not known and interestingly *in vivo* no change in the actin cytoskeleton has ever been detected upon loss of rictor [108]. Furthermore, there have never been any suggestions on PKC substrates that mediate the effects in actin remodeling upon rictor depletion.

In neurons, the major substrate of PKCs is the growth associated protein 43 (GAP43) [109-112] and as actin-binding protein [113], GAP-43 was shown to directly influence the structure of the cytoskeleton [14,112] and to contribute to growth cone spreading, branching and adhesion of neurons. The organization of the brain during development is highly dependent on GAP-43 and knockout of the protein is lethal in the first postnatal days due to axon path finding defects. Interestingly, GAP-43 was shown to be located in presynaptic terminals of parallel and climbing fibers and depletion of GAP-43 led to defective cerebellar structure [114]. Hence, PKC signaling plays a

substantial role in the structuring of the neuronal actin cytoskeleton by directly binding to actin structures and by modulating actin interacting proteins.

Upstream regulation of mTORC2

Not much is known about the upstream signaling factors that lead to the activation of mTORC2. It has been demonstrated that mTORC2 regulates the activity of Akt by phosphorylating its hydrophobic motif. This suggests that mTORC2 activity might be controlled by growth factors which signal through the PI3K-Akt pathway and recently, direct activation of mTORC2 by PI3K was demonstrated [58,59,115]. Further evidence for this hypothesis emerged with the finding that mTORC2 phosphorylates the turn motif of Akt. This posttranslational modification is necessary for adequat protein folding and deficient phosphorylation causes the rapid ubiquitin dependent degradation of the nascent kinase. Furthermore, mTORC2 mediated phosphorylation of this residue requires its association with translating ribosomes and this association is stimulated by Insulin-PI3K signaling [116]. However, the mechanism of activation of mTORC2 by ribosome binding is not yet understood.

Another pathway that is induced by growth factor stimulation is the GTPase Rac 1 signaling [117] which also elicits a regulatory effect towards mTORC1 and mTORC2. Rac1 supposedly binds to mTOR in the active and the inactive state. Upon stimulation by growth factors, Rac1 together with mTORC2 is translocated to the membrane where the close proximity to activating proteins facilitates Rac1 activation. However, the mechanism of this process is so far unknown.

The TSC1-TSC2-complex which negatively regulates mTORC1 has been implicated in activating mTORC2 by direct complex binding. This action was supposed to be mediated independent of the GAP activity of TSC towards Rheb [118]. Hence, the exact mechanism of mTORC2 activation remains to be elucidated.

mTORC2 deletion mutants

In contrast to mTORC1, mTORC2 can be inhibited with rapamycin only in long-term treatment [52]. This inhibition is also only effective in certain cell types and was thought to be caused by the binding of rapamycin to free mTOR which consequently represses synthesis of new mTOR that is available for mTORC2[119]. Thus, rapamycin treatment always includes mTORC1 inhibition. Therefore various other mTORC2 inhibitors have been designed in the last years but so far none of them seems to be specific enough to repress only mTORC2 and all of the mTORC2 downstream factors. Hence, the physiological role of mTORC2 is not very well defined also because genetic deletion of *rictor* in mammals is embryonically lethal [120]. In flies and in *C.elegans* ablation of mTORC2 produces only minor growth impairments [64,121]. In rictor deficient

Figure 12. Deletion of rictor in drosophila causes only a slight growth reduction of about 10%. However, cell size is not altered in those mutant flies. Picture derived from *Gina Lee, Jongkyeong Chung, 2007*

C.elegans an increased fat storage was observed that was presumed to be caused by loss of the serum and glucocorticoid inducible kinase SGK1 and was not linked to loss of Akt or PKC [121]. In mammals, it was expected that conditional deletion of rictor would provide some more insight into the function of this complex. However, in mammalian muscle, rictor deletion did not evoke an overt phenotype in the morphology of the muscle although insulin-stimulated glucose transport was impaired [122,123]. As expected, Akt failed to be phosphorylated at the hydrophobic motif in muscle specific rictor knockout mice. Interestingly, however, double knockout of raptor and rictor in muscle tissue caused an increase in phosphorylation at this residue, indicating that mTORC2 might not be the only kinase able to phosphorylate Akt at Ser 473[122]. In adipose tissue, loss of rictor was found to increase body size due to an increase in organ size which the authors attributed to the increased insulin growth factor (IGF1) levels in the blood of their mice. However, fat tissue mass and fat cell size did not differ[124]. Mice with a deletion of rictor in pancreatic β-cells showed a reduction in cell mass and proliferation which led to reduced insulin synthesis and secretion [125]. The proliferative effect was ascribed to mTORC2 activity towards Akt whereas the reduction in cell mass was attributed to enhanced Akt-308 phosphorylation due to increased mTORC1 signaling. Hence, due to the lack of a stark phenotype and the involvement of mTORC1 function in some of the analyzed tissues, the progress in elucidating mTORC2 functions was thus far hindered.

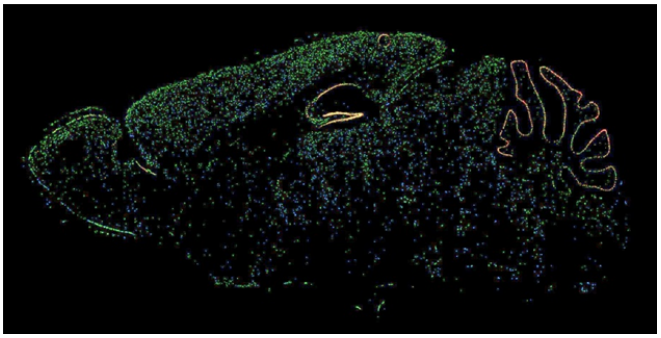

Figure 13. Rictor expression in the adult mouse brain. Mid-sagittal section shows that rictor is abundant throughout the adult brain with highest expression in Purkinje neurons of the cerebellum. Expression signal is scaled from blue to red with blue representing the lowest and red the highest levels. Data obtained by *Allen institute for brain science.*

mTOR signaling in disease

The regulation of protein synthesis places mTOR in the focus of many investigations concerned with diverse diseases. In fact, mTORC2 was shown to be up-regulated in various forms of cancer. Concordantly, studies have indicated a role of mTORC2 in tumorigenesis, specifically in the development of prostate cancer [126]. In addition, the role of mTORC2 in the regulation of Akt and PKC activity also denotes this complex as important factor in cancer induction because both kinases are known for their tumorigenic activity. mTOR is also studied intensively in the central nervous system (CNS) and is thought to be involved in physiological processes such as synaptic plasticity, learning and memory processing and brain control of food uptake [127]. CNS dysfunctions such as Alzheimer, Parkinson, Huntington, Tuberous sclerosis, fragile X syndrome and mental retardation were also suggested to involve mTOR signaling and neurodevelopmental disorders like autism spectrum disorders and schizophrenia all hint to an involvement of mTOR signaling [128]. Alzheimer, Parkinson and Tuberous sclerosis were so far associated with mTORC1

due to the autophagocytotic activity of this complex [128]. However, recent evidence also suggests a role for mTORC2 in autophagy [129]. Most studies where mTOR inhibitors are applied attribute their findings to the function of mTORC1. But general mTOR inhibitors can also interfere with mTORC2 function when administered for prolonged time-periods and thereby mTORC2 might contribute to the observed effects. Hence, it is not at all known whether some of those diseases are due to dysregulation of mTORC1 or mTORC2 because *in vivo* no data exists on the physiological relevance of mTORC2 in brain. However, it is known that rictor is highly expressed in brain tissue, especially and exclusively in neurons [120]. The first indication of rictor function in the brain was recently provided by Siuta et al.[130] where mice with a brain-specific deletion of *rictor* have been shown to exhibit schizophrenia like behavior that was associated with decreased dopamine levels. Those mice showed defective prepulse inhibition, a widely used technique to study defects in sensory motor gating and are noted in Alzheimer or Schizophrenia patients. Although the study concentrated mainly on one brain area and the dopamine and noradrenergic release, they missed out basic information on the overall phenotype of their mice. However, their data indicate an involvement of mTORC2 in brain function and provide evidence for a participation of mTORC2 in neurodevelopmental disorders. In addition to altered dopamine levels another hallmark in schizophrenic brain tissue is the reduction in neuronal cell soma size and a decrease and alteration in dendrite arborisation [128,131,132], both characteristic features that were not described in the publication by Siuta.

In summary, the mammalian TOR was found to play an important role in the development of the brain and in the function of neurons but the contribution of mTORC2 thereby is still unknown. mTORC2 regulates the activities of Akt and PKC. In the brain, those AGC kinases have been implicated in the regulation of neuron size, neuron morphology and function and they are known to exert important roles during neuronal circuit assembly and plastic adaptations in the adult [79,133-135]. It was therefore tempting to hypothesize that mTORC2 could play an essential role in the development of neurons and the structuring and establishment of neuronal connections to enable the complex functions of the brain. Hence, this manuscript describes the implication of neuronal rictor knockout for neuron and brain morphology and for the behaviour of those mice.

mTORC2 controls neuron size and Purkinje cell morphology independent of mTORC1

Venus Thomanetz[1], Dimitri Cloëtta[1], Regula M. Lustenberger[1], Manuel Schweighauser[1], Filippo Oliveri[1], Noburu Suzuki[2] and Markus A. Rüegg[1]

[1]Biozentrum, University of Basel, CH-4056 Basel, Switzerland, [2]Mie University Life Science Research Center of Animal Genomics, Functional Genomics Institute, Japan

ABSTRACT

The mammalian target of rapamycin (mTOR) is well known to regulate cell and organismal size because of its central role in the control of protein translation. According to the current concept, this function is rather mediated by mTOR complex 1 and not by mTOR complex 2. Instead, *in vitro* studies have implicated mTORC2 in the control of the actin cytoskeleton and the activation of members of the AGC kinase family such as Akt and PKC. However, mice with a tissue-specific deletion of the essential mTORC2 component *rictor* have not revealed any change in the actin cytoskeleton and show only a subtle or no phenotype. Nonetheless, the mTOR pathway seems to be important in central nervous system diseases such as autism spectrum disorder or schizophrenia. Thus, the mTOR pathway is central to several essential functions in many tissues but the contribution of mTORC2 to those is largely unknown.

We eliminated *rictor* in mice during brain development and in postnatal Purkinje cells. We describe a new function of mTORC2 in the regulation of neuron size, dendritic development and synapse function and provide first *in vivo* evidence of a role of mTORC2 in actin remodeling. Importantly, the influence on neuron size is independent of mTORC1. We also find that deletion of mTORC2 causes an almost complete loss of all conventional PKCs and a reduction in phosphorylation of several PKC targets that are important for actin cytoskeletal arrangements, such as GAP-43, MARCKS and fascin.

INTRODUCTION

Neurons are the most complex cell types in the mammalian organism as they differ between each other in size, dendritic branching pattern and connectivity. The plethora of information propagation from neuron to neuron can only be accomplished by the highly elaborate structure of dendritic trees. To enable functional connectivity in the brain, the size and morphology of neurons is therefore tightly controlled.

One molecule that is involved in cell size and cell cycle control is the mammalian target of rapamycin (mTOR), a serine/threonine protein kinase that assembles into two multi-protein complexes, called mTOR complex 1 (mTORC1) and mTORC2 [53,136]. Whereas mTORC1 is known to regulate growth and proliferation in response to growth factors, nutrients or stress [137,138], the role of mTORC2 is less well defined. An essential component for the function of mTORC2 is the "rapamycin-insensitive companion of mTOR" (rictor) [50,51]. In flies and in *C.elegans* ablation of rictor produces only minor growth impairments [64,121]. Deletion in mammals is embryonically lethal [120] and inhibition with rapamycin is only effective in long-term treatment [52]. In mammalian muscle, *rictor* deletion does not evoke an overt phenotype [122,123] and in adipose tissue, loss of *rictor* was found to increase body and organ size [124] although not caused by a change in cell size.

mTORC2 controls phosphorylation of the hydrophobic motif of the AGC kinase family members Akt/Protein kinase B (Akt/PKB) and protein kinase C (PKC) [62,92]. In the brain, both kinases have been implicated in the regulation of neuron size, morphology and function and they exert important roles during neuronal circuit assembly and plastic adaptations in the adult [79,133-135].

Several lines of evidence from yeast studies and cell culture experiments also indicate that rictor is involved in cytoskeleton organization [51,107]. This function has been attributed to changes in the activation of PKCs [51]. However, the exact mechanism of how rictor affects actin arrangement is not known and *in vivo* no change in the actin cytoskeleton has ever been detected upon loss of rictor. Interestingly, thus far also no downstream targets of PKC have been discovered.

Here, we report on the phenotype of two mouse models where *rictor* was conditionally deleted either in the developing central nervous system (CNS) or in cerebellar Purkinje cells, the cell type with highest rictor expression in the brain [120]. We show that rictor is involved in the regulation of brain and neuron size and that this phenotype is independent of mTORC1 signaling. We also show that deletion of rictor affects the activation of all PKCs. In addition, phosphorylation of the PKC substrate GAP-43 is diminished *in vivo* and phosphorylation of the MARCKS and fascin is impaired in cultured hippocampal neurons, indicating that those proteins might be involved in the observed changes in the actin cytoskeleton.

RESULTS

Sub-cellular localization of rictor in the mammalian brain

Deletion of *rictor* causes embryonic lethality at embryonic day 11.5 [120]. In the adult brain, rictor is expressed in all brain regions (Fig. 1A) and is enriched in the membrane fraction (Fig. 1B). To investigate the role of rictor in the developing brain, we bred homozygous, floxed *rictor* mice (*rictor*$^{fl/fl}$) [122] with mice that express the Cre recombinase under the control of the neuron-specific

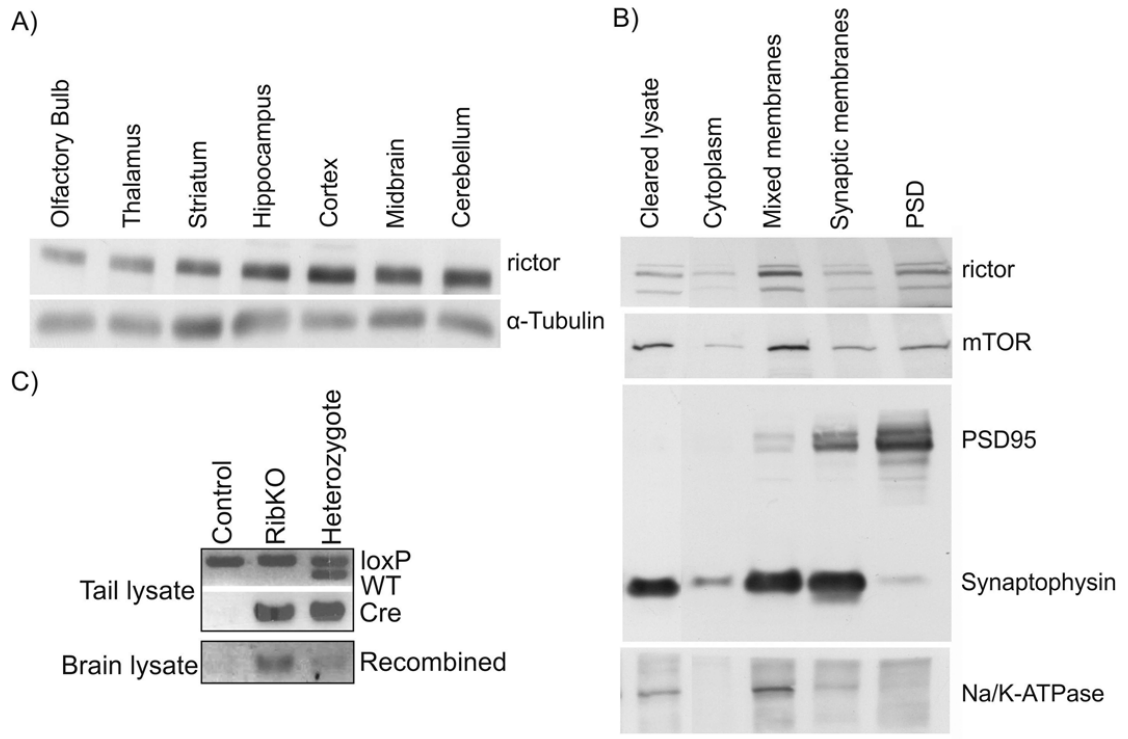

Figure 1. Sub-cellular localization of rictor and mTOR in the brain. (**A**) Western blot of tissue lysates prepared from different brain regions as indicated. α-tubulin was used as loading control. (**B**) Sub-cellular localization of rictor and mTOR as detected by Western blot analysis. Fractionation of brain tissue in postsynaptic density (PSD), synaptic fraction, mixed membranes, cytoplasm and cleared lysate. Rictor and mTOR are mainly localized in the membrane fraction with highest abundance in the postsynaptic density. Na/K-ATPase was used for identification of all cellular membranes, PSD95 for postsynaptic structures and Synaptophysin for presynaptic compartments. (Data by D. Cloëtta). (**C**) PCR with tail lysate of control, RibKO and heterozygous mice, detecting the WT, the floxed allele and Cre, and corresponding PCR with brain tissue to visualize recombination.

enhancer of the nestin promoter, which recombines the targeted allele at embryonic day 10.5 (E10.5) in all neural tube-derived cells [139]. The genotypes of the resulting offspring were determined by PCR from toe DNA (Fig. 1C). Mice that carried both transgenes (*rictor*$^{fl/fl}$; nestin-Cre^{+}), showed recombination of the targeted *rictor* allele in genomic brain DNA, whereas mice carrying the floxed allele but lacking Cre (*rictor*$^{fl/fl}$; nestin-Cre^{-}) did not show recombination (Fig.

1C). For simplicity, *rictor*$^{fl/fl}$; nestin-Cre^{+} mice will be called RibKO (for rictor brain knockout) mice.

Ablation of *rictor* in the developing brain results in microcephaly

Successful recombination of the floxed *rictor* allele was further demonstrated by the complete loss of the rictor protein (Fig. 2A), whereas loss of rictor did not affect expression of raptor or mTOR (Fig. 2A). RibKO mice were born in a Mendelian ratio and were viable. However, soon after birth they were significantly lighter (Fig. 2B) and showed some locomotory defects. At 12 months of age RibKO mice showed a clasping phenotype when lifted at the tail whereas their littermate controls displayed the normal escaping reflex and spread out their hind limbs (Fig. 2C).

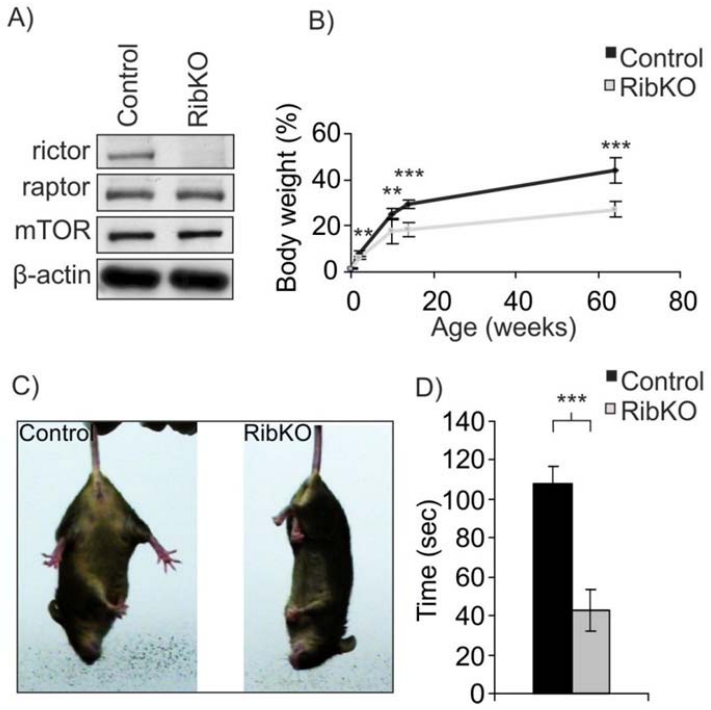

Figure 2. Rictor knockout in brain causes growth defects and motor impairments. (**A**) Western blot with whole brain lysate from adult control and RibKO mice detecting rictor, raptor and mTOR. In RibKO mice, rictor protein is undetectable whereas raptor and mTOR levels are unchanged. β-actin was used as loading control. (**B**) Body weight of control and RibKO mice at different postnatal ages. At birth, the body weight of RibKO and control mice is identical whereas after one week, significant weight differences are detected that remain throughout adulthood. (**C**) Clasping test in 1 year-old control and RibKO mice. Photograph shows the normal response of a control mouse (left) and the typical clasping reflex (right), conducted by a motor impaired RibKO mouse when lifted by the tail. Clasping reflex was seen in 11 out of 12 RibKO mice. (**D**) Performance of control and RibKO mice on the accelerating rotarod. Speed was accelerated from 5 up to 30 rpm in 120 seconds (data represent mean ± s.e.m. Student's *t-test*, *** $p < 0.001$, N = 8 mice per genotype).

This test is used to assess neurological impairments especially concerned with motor defects. To further test motor coordination abilities we used the widely applied accelerating rotarod test in 10 week-old mice. This performance task was difficult to accomplish by RibKO mice and some mice fell from the rod before the rotation had started (Fig. 2D).

Interestingly, the brains of adult RibKO mice were smaller and their weight was only half of that of control animals (Fig.3A). Despite the large difference in brain size, the overall architecture of the brain was maintained (Fig.3B) giving rise to a miniature edition of a brain. To analyze whether the microcephaly affected all brain regions equally, we measured the volumes of the cortex, the hippocampus, the striatum, the olfactory bulbs and the ventricles. As shown in Figure 3C, all analyzed brain regions were reduced to the same extent, indicating that all brain regions

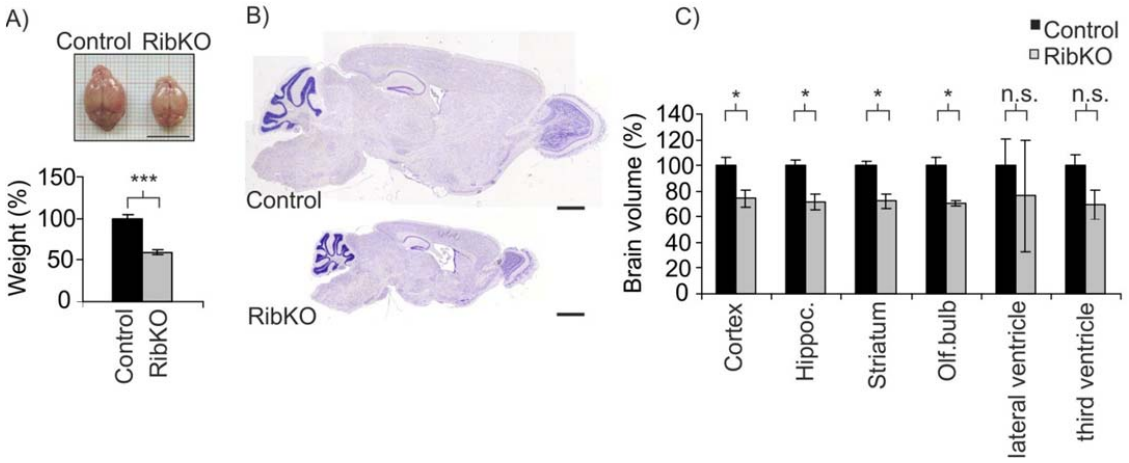

Figure 3. RibKO mice develop microcephaly. (**A**) Photograph of brains from adult control and RibKO mice and quantification of the relative brain weight (data represent mean ± s.e.m. Student's *t-test*, *** $p < 0.001$, n =7 control and 6 RibKO mice). Scale bar = 1 cm. (**B**) Cresyl violet-stained mid-sagittal sections of brains from adult RibKO and control mice. Brain proportions are maintained even though the size of the brain of RibKO mice is strongly decreased. Scale bar = 1 mm. (**C**) Quantification of the volumes of several brain areas in one year-old mice (data represent mean ± s.e.m., Student's *t-test*, * $p < 0.05$; n.s.: non-significant, n = 3 mice for each genotype).

were affected similarly. In contrast, the ventricles had a comparable volume as in control mice. These results thus reveal that mTORC2 is required for the proper sizing of the brain and differ from those obtained in other organs, such as skeletal muscle and adipose tissue [122,124], where deletion of *rictor* did not affect the size of the targeted organ.

Microcephaly is induced by a reduction in cell size

The size and mass of an organ is determined by cell size and cell number [140]. To investigate whether loss of rictor affects cell size, we analyzed the brains of control and RibKO mice by Golgi staining, which visualizes single neurons in the intact brain. Because of the relatively high levels of rictor in the hippocampus [120], we chose this brain region for investigation. As shown in Figure 4A, the apical dendrite of CA1 pyramidal cells in the hippocampus had a shorter dendritic tree in RibKO mice and analysis of the length of the basal and apical dendrites showed a reduction by more than 20% (Fig. 4B). Reconstruction of the entire neurons by camera lucida and quantification of higher order apical dendrite length revealed a striking reduction by almost 40% (Fig. 4C). Moreover, secondary dendrites of pyramidal cells of RibKO mice were sometimes devoid of any spines (Fig. 4D), suggesting that the reduction in neuron size additionally affects neuronal connectivity and spine formation.

To investigate whether the neuron density was affected in the brains of RibKO mice, we next stained sagittal brain sections with the neuron-specific antibody NeuN. The width of the cortex was strongly decreased but cell density appeared to be increased (Fig. 4E). When we counted the number of NeuN-positive neurons in an area of the retrosplenial and visual cortex, the cell density in RibKO mice was increased to more than 150% of that in control cortex (Fig. 4F). Thus, the reduction in brain size is likely caused by the decrease in neuronal size which further induces an increase in cellular density. As an independent measure we also analyzed the proliferation rate in

neurospheres that were derived from single stem/progenitor cells. The diameter of such neurospheres depends on the number of cells and thus can serve as a measure for the proliferative capacity of stem/progenitor cells [141,142]. However, neurospheres derived from brains of newborn RibKO mice were of the same size as those derived from control mice (Fig. 4 G, H) indicating that the proliferative capacity of neuronal progenitors is unchanged in RibKO mice. To measure proliferation directly, we also pulsed the neurospheres with 5-bromo-2'-deoxyuridine (BrdU) for 4 hours and then counted the number of BrdU-positive cells per sphere. BrdU is a thymidine analogue which is incorporated into the DNA during the replication process of cells and is therefore used for the detection of proliferation. Again, no difference was detected (Fig. 4 I, J),

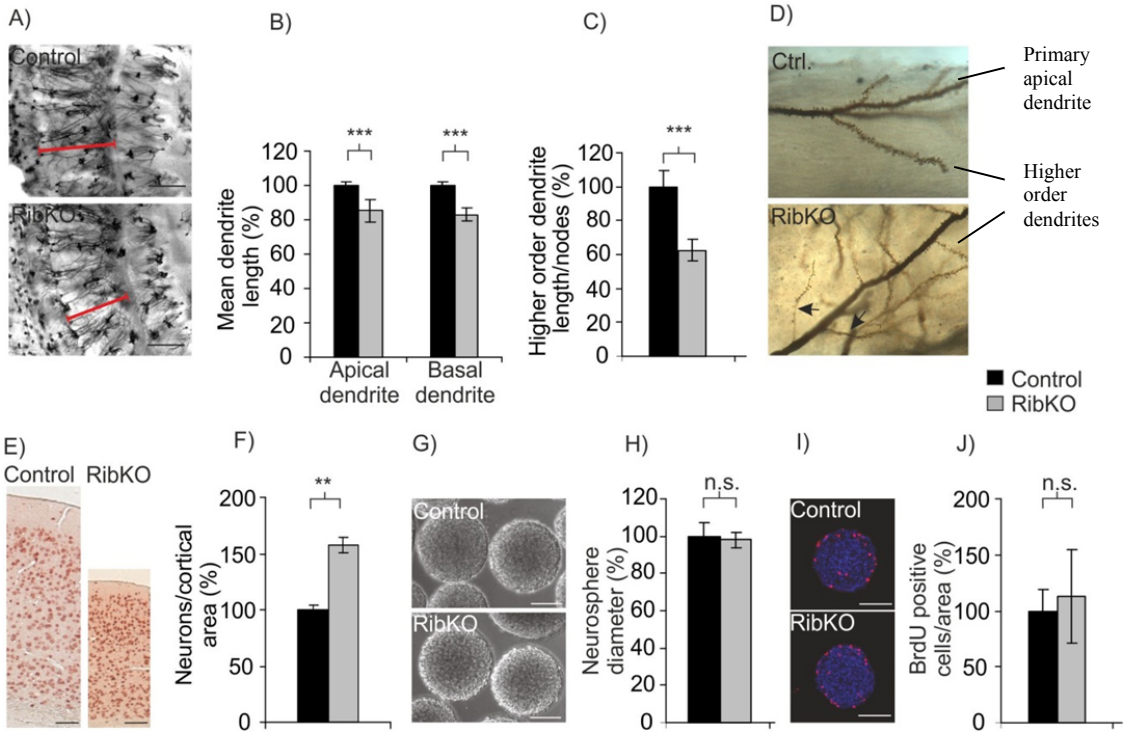

Figure 4. Microcephaly is caused by a reduction in cell size but not number. (**A**) Microscopic pictures of hippocampal sections from control and RibKO mice stained with the Golgi impregnation method. Red bar indicates the length of CA1 pyramidal dendrites. Scale bar = 200 µm. (**B**) Quantification of the mean length of apical and basal dendrites in Golgi-stained sections (data represent mean ± s.e.m. Student's *t-test*, *** $p < 0.001$, N = 4 mice for each genotype, n = 38 control neurons, n = 32 RibKO neurons). (**C**) Quantification of the total length of all higher order dendrites from Neurolucida-reconstructed neurons (data represent mean ± s.e.m. Student's *t-test*, *** $p < 0.001$, N = 4 mice, n = 38 control neurons, n = 32 RibKO neurons). (**D**) Representative images of hippocampal pyramidal cells in Golgi impregnated sections which show the reduction in spine number in cells of RibKO brains. (**E**) Representative microscopic picture of NeuN-stained cortex sections. Scale bar = 100 µm. (**F**) Quantification of neuron density in RibKO and control cortex (data represent mean ± s.e.m. Student's *t-test*, ** $p < 0.01$, N = 3 control mice, n = 36 areas, N = 4 RibKO mice, n = 58 areas). (**G**) Representative microscopic picture of neurospheres isolated from control and RibKO brains. Scale bar = 100 µm. (**H**) Quantification of neurosphere diameter (data represent mean ± s.e.m., Student's *t-test*, n.s.: $p > 0.05$, N = 5 mice for each genotype, n = 613 control spheres, n = 538 RibKO spheres). (**I**) Representative picture of neurosphere cryosections, labeled with BrdU for 4 h prior to fixation and stained with antibodies to BrdU and with Hoechst. Scale bar = 100 µm. (**J**) Quantification of the number of BrdU-positive cells/ neurosphere (data represent mean ± s.e.m., Student's *t-test*, n.s.: $p < 0.05$, N = 3 mice per genotype). (Data in (B) and (C) by M. Schweighauser).

suggesting that proliferation of neuronal progenitor cells is indeed not altered in the brains of RibKO mice. Because the size of the neurospheres was indifferent, these data additionally signify that neuronal growth rather than initial sizing of neuronal precursor cells is hampered in the brains of RibKO mice. Taken together, these data indicate that the microcephaly in RibKO mice is induced by a reduction in cell size and not in cell number.

Rictor is involved in the regulation of Purkinje cell size and shape

The severe motor coordination problems of RibKO mice suggested functional alterations in areas concerned with motor function such as the cerebellum. Moreover, expression of rictor was shown to be highest in cerebellar Purkinje neurons in the adult brain [120]. To investigate whether Purkinje cells were indeed altered in RibKO mice, we analyzed their structure during postnatal development and in the adult. In wild-type mice, Purkinje cells migrate into the periphery and start to align in a monolayer in the first postnatal week [23]. At this time point, most cells have formed one primary dendrite, which spreads out perpendicularly to the pial surface into the molecular layer where it forms numerous side branches [23]. At postnatal day 7 (P7), this alignment and the spreading of the primary dendrites was clearly detected in control mice (Fig. 5A, top), whereas Purkinje cells from RibKO mice were smaller, appeared abnormally shaped with dendritic swellings (arrows in Fig. 5G) and extended several primary dendrites into the molecular layer (Fig. 5A, bottom). Moreover, the cell bodies of Purkinje cells were aggregated in some regions of the cerebellum while in other areas, they were discontinuous (data not shown). For a closer examination of the morphological appearance of this cell type, adult Purkinje cells were analyzed in more detail by Golgi staining (Fig.5B, left) and entire neurons were reconstructed using the camera lucida (Fig. 5B, right). Quantification of the different cell parameters revealed a significant reduction of the mean dendrite length (Fig. 5C) and of the mean volume of Purkinje cells (Fig. 5D) to 32% and 28%, respectively. In addition, the soma size of Purkinje cells was quantified in sections stained with antibodies to calbindin and was found to be much smaller in cells of RibKO mice (Fig. 5E). Thus, also Purkinje cells show a considerable cell size reduction.

Besides the difference in size, one of the most striking differences between Purkinje cells from RibKO and from control mice was the increase in the number of primary dendrites, from one in control to an average of 3 dendrites in knockout cells (varying from two to six branches per cell; see Fig. 5B as an example). Some of those primary dendrites were highly ramified like in control neurons while others were simplified with hardly any branching (see the camera lucida drawing in Fig. 5B, purple and orange branches). Consistent with the simplification of many dendrites and the reduction in terminal branchlets, the number of dendritic endings was decreased in RibKO mice (Fig. 5F). In addition, high magnification pictures of Golgi-stained Purkinje cells indicated dendritic swellings and a reduction in spine density in those higher-order dendrites with a simplified pattern (Fig. 5G; see arrows as example). Finally, as described for P7 Purkinje cells, the orientation of the dendritic tree sometimes diverged from its perpendicular orientation to the pial surface and Purkinje cells were occasionally found in the molecular layer (Fig. 7D black arrow). In summary, these data demonstrate that the entire volume of Purkinje cells (i.e. length and diameter of dendrites and the soma) is significantly smaller in RibKO mice, confirming the

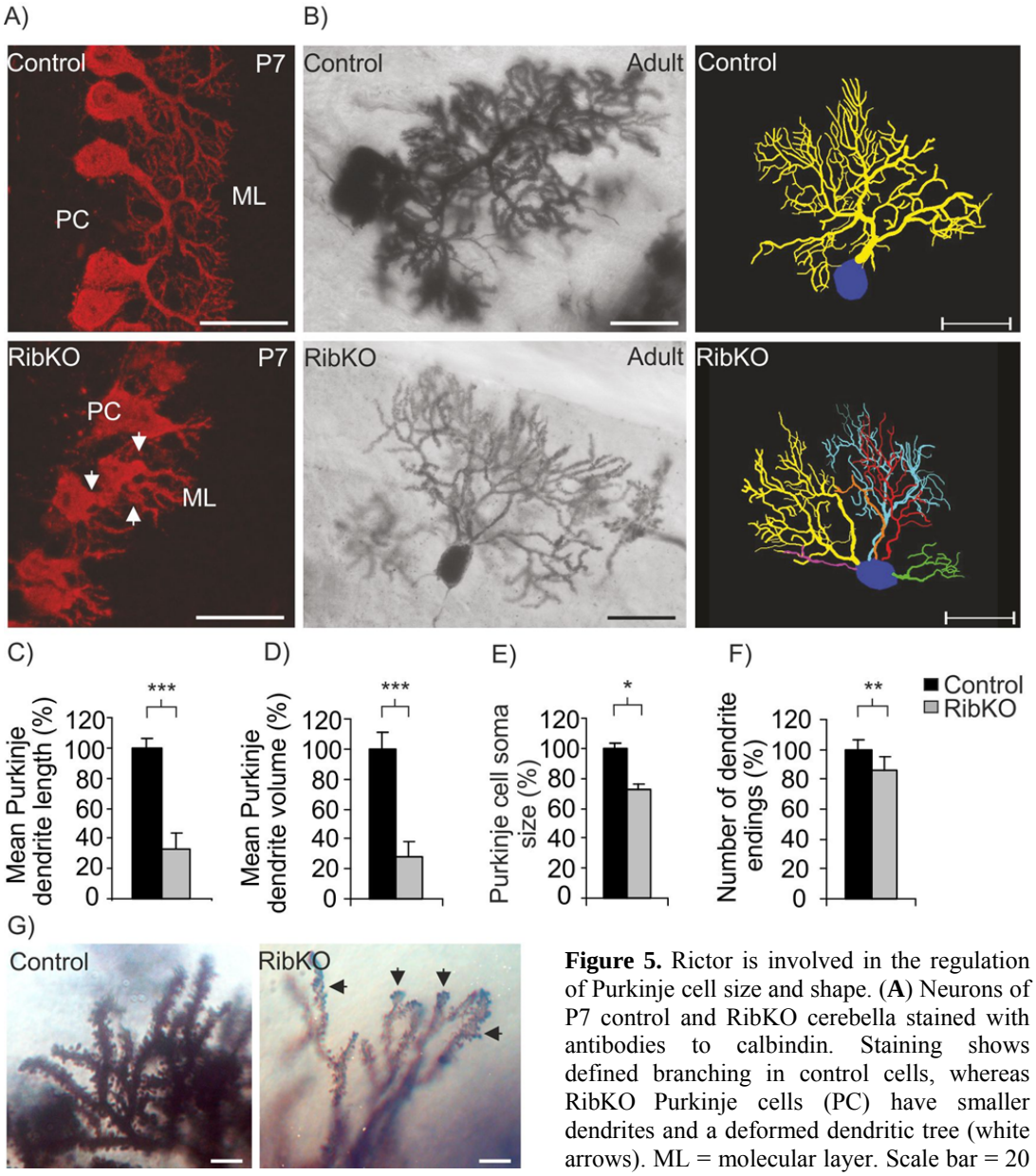

Figure 5. Rictor is involved in the regulation of Purkinje cell size and shape. (**A**) Neurons of P7 control and RibKO cerebella stained with antibodies to calbindin. Staining shows defined branching in control cells, whereas RibKO Purkinje cells (PC) have smaller dendrites and a deformed dendritic tree (white arrows). ML = molecular layer. Scale bar = 20 µm. (**B**) Representative pictures of Golgi-stained Purkinje cells from adult control and RibKO mice. The right panels depict neurolucida reconstructions of Purkinje cells. Cells from RibKO mice have several primary dendrites (visible by differently colored dendrites) and dendritic trees with little or no higher order branches (violet and orange branch). Scale bar = 50 µm. (**C**) Quantification of the mean Purkinje cell dendrite length and (**D**) the mean dendrite volume (data represent mean ± s.e.m. Student's *t-test*, *** $p < 0.001$, N = 4 mice per genotype). (**E**) Quantification of the Purkinje cell soma size. The cell soma perimeter was measured in sections of adult mice stained with antibodies to calbindin (data represent mean ± s.e.m., Student's *t-test*, * $p < 0.05$, N = 4 mice per genotype). (**F**) Quantification of the total number of Purkinje dendrite endings in neurolucida-reconstructed neurons (data represent mean ± s.e.m., Student's *t-test*, ** $p < 0.01$, N = 4 mice per genotype). (**G**) High resolution microscopic picture of control and RibKO Golgi-stained Purkinje cell terminals. Purkinje cell dendrites are deformed as marked by black arrows, and show a reduced number of spines. Scale bar = 10 µm.

results obtained from the CA1 pyramidal cells which are also reduced in length. Furthermore, Purkinje cells are often misaligned and show morphological changes, such as an increased number of primary dendrites, a reduction of terminal dendrites, deformations of the dendritic shaft and a reduction in spine density. Unfortunately, spine density could not be quantified in those Golgi-stainings. However, spineless dendrites were only observed in neurons of RibKO mice and never in those of controls.

The changes in Purkinje cell shape were also observed in organotypic cerebellar slices. There, Purkinje cells from RibKO mice appeared much smaller and had much thinner dendrites

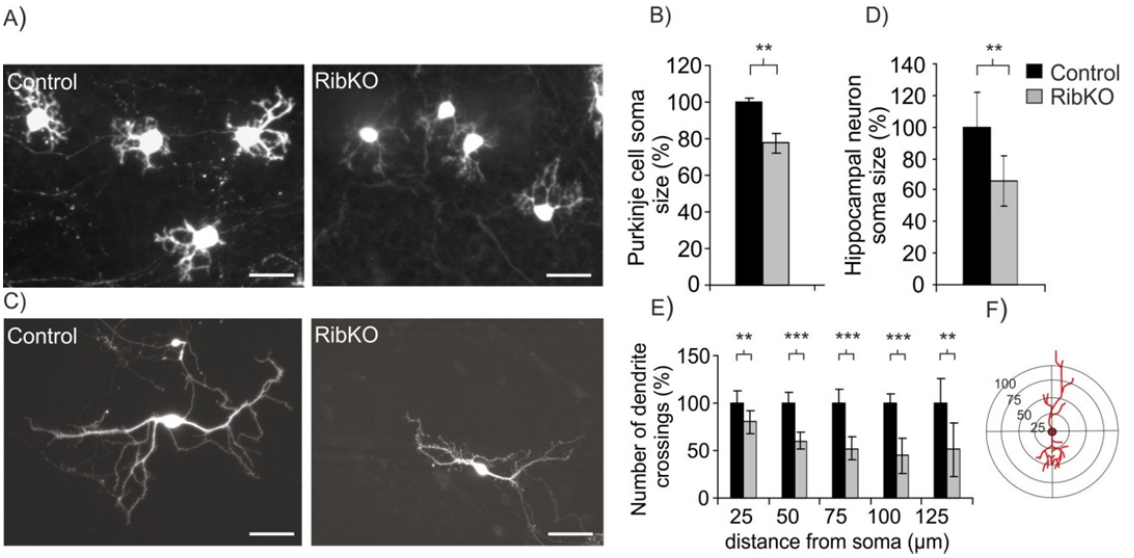

Figure 6. Neuron size in RibKO brains is reduced *in vitro*. (**A**) Microscopic pictures of calbindin-positive control and RibKO Purkinje cells in organotypic cerebellar slice cultures, derived from P0 mice and cultured for 14 days. Scale bar = 50 µm. (**B**) Quantification of Purkinje cell soma size in organotypic cerebellar slice cultures (data represent mean ± s.e.m., Student's *t-test*, ** $p < 0.01$, N = 4 control and N = 3 RibKO mice). (**C**) Representative picture of dissociated hippocampal neurons derived from P0 mice, transfected with GFP and actin-RFP after 7 days and grown for 14 days. Scale bar = 50 µm. (**D**) Quantification of hippocampal neuron soma size in dissociated hippocampal cultures grown for 14 days (data represent mean ± s.d., Student's *t-test*, ** $p < 0.01$, N = 6 mice per genotype). (**E**) Sholl analysis of hippocampal neurons (data represent mean ± s.d., Student's t-test, ** $p < 0.01$, *** $p < 0.001$, N = 6 mice per genotype). (**F**) Sketch of the Sholl blot analysis. Neuron complexity is assessed by counting the dendrite intersections on the concentric circles which are arranged in 25 µm distance and are centered at the soma.

(Fig. 6A). Quantification of the soma size also revealed a reduction by more than 20% (Fig. 6B). Unfortunately, the formation of primary dendrites could not be analyzed in cerebellar slice cultures as Purkinje cells in culture always retain several primary dendrites due to the absent climbing fiber input [23]. To assess if the reduction in cell size could also be observed in other types of neurons *in vitro*, we analyzed the size and complexity of hippocampal pyramidal cells in 14 day old, dissociated cultures derived from newborn control and RibKO brains. As shown in Fig. 6C, a strong reduction in size was visible and further analysis also showed a reduction in the soma size of those neurons (Fig. 6D). To quantify neuronal characteristics, we applied the Scholl

analysis on those hippocampal neuron cultures which assesses the number of dendritic crossings over concentric circles drawn in certain distances around the soma (Fig 6F). In this test, Pyramidal neurons of RibKO mice displayed a decrease in the number and length of dendrites (Fig. 6E). These data indicate that loss of rictor hampers neurite growth and supports the suggestion that overall neuron reduction causes the microcephaly in RibKO mice.

Rictor deficiency leads to foliation defects in the cerebellum

The changes in Purkinje cell size and shape in RibKO mice at early postnatal stages suggested to us that mTORC2 might be involved in cerebellar development and maturation. It is known that mutant mice with Purkinje cell defects develop simplified lobule patterns [143,144]. Moreover, the structure of lobes is highly conserved and aberrations in morphology can cause defects in motor behavior [19]. To test whether this would also be the case in RibKO mice, we analyzed the overall structure of the cerebellum. At birth (P0), the cerebellum only contains the five cardinal lobes, which will then develop into ten mature lobules within the following 21 days [44]. In cerebella of

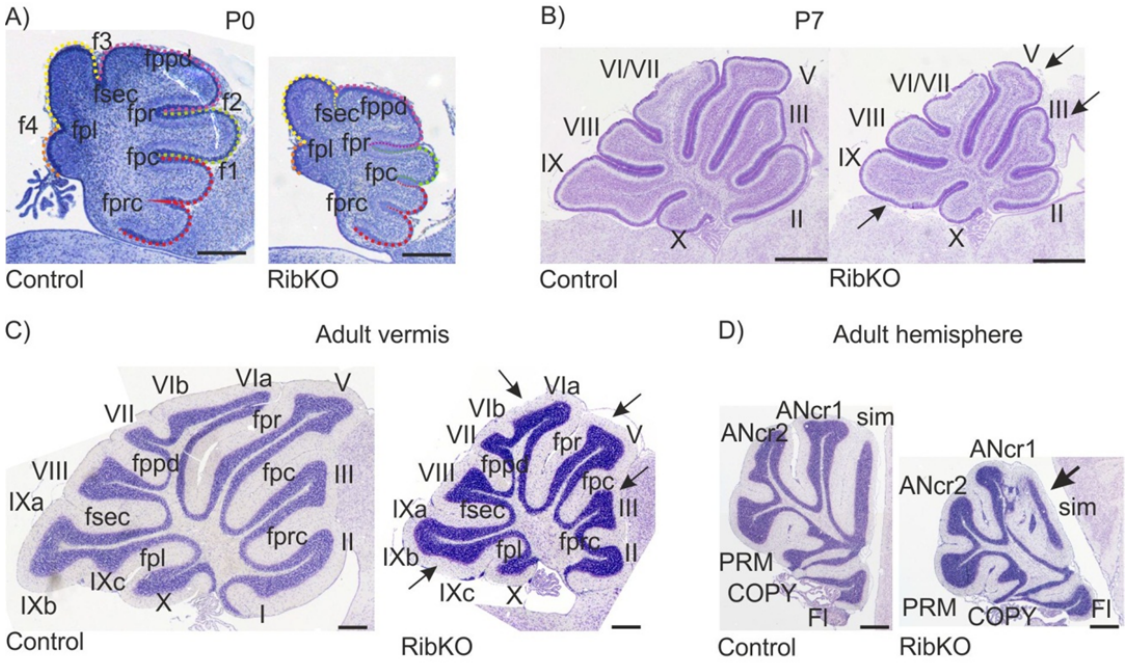

Figure 7. Rictor deficiency leads to foliation defects in the cerebellum. (**A**) Cresyl violet staining of cerebella from P0 control and RibKO mice. Brain size is slightly reduced but foliation is fairly normal and all cardinal lobes are formed as depicted by the large colored outline. (**B**) Midsagittal, Cresyl violet staining of P7 cerebella from control and RibKO mice. Foliation defects are obvious in cerebella of RibKO mice (black arrows). Scale bar = 250 µm. (**C**) Sagittal sections of cerebellar vermis from adult control and RibKO mice stained with Cresyl violet. Lobules II - VII are strongly reduced in length (black arrows) and the granular cell layer appears more densely packed. (**D**) Sagittal sections of the lateral cerebellar lobules of adult control and RibKO mice. Lobules are simplified and show cell dispersion in the molecular layer. The ansiform cruciform lobule 1 and the simple lobule are fused. Scale bar = 1mm. Abbreviations: fpl: posterolateral fissure, fsec: secondary fissure, fppd: prepyramidal fissure, fpr: primary fissure, fprc: precentral fissure. Vermal lobules are numbered from I-X. Lateral lobules: Ancr: Ansiform cruciform lobule, COPY: Copula pyramidis, Fl: Flocculus, PRM: paramedian lobule, Sim: simple lobule.

newborn RibKO mice, lobule formation was unchanged (Fig. 7A). At P7, cerebellar defects became clearly visible as the cerebella were smaller and lobules III to VII of the cerebellar vermis showed structural deformations (Fig. 7B). In 8 to 10 week-old RibKO mice the cerebellar size was strongly decreased (Fig. 7C). In addition to the reduction in size, morphological abnormalities were obvious in the vermal lobules II - VII and IX. These lobules appeared shortened compared to those of control mice and in some mice cerebellar lobules developed deformations (black arrows). Closer examination revealed that the cerebellar hemisphere was even more affected than the cerebellar vermis. In addition to the reduction in size, the simple lobule (Sim) and the Ansiform cruciform lobule 1 (ANcr1) were disrupted. These two lobules appeared to be fused and could not be distinguished as separate lobules anymore (Fig. 7D). Thus, mTORC2 affects cerebellar lobule formation and this defect most likely contributes to the motor deficits observed in RibKO mice.

Purkinje cells of RibKO mice exhibit synaptic alterations

Migration and maturation in the cerebellum is dependent on proper synaptic connections between granule cell parallel fibers and Purkinje cells as well as between climbing fibers and Purkinje cells. To analyze whether synaptic connectivity in the cerebellum was affected in RibKO mice, we labeled the climbing fiber synapses with antibodies to the vesicular glutamate transporter protein 2 (vGLUT2) [145,146] and the Purkinje cells with antibodies against calbindin. As shown in Figure 8A, the density of vGLUT2-positive puncta in the molecular layer was strongly decreased in RibKO mice, indicating that their Purkinje cells form fewer synapses with climbing fibers. To also examine the synaptic connections with parallel fibers, which are so numerous that counting of synapses after staining is not possible [35], we performed Western blot analysis from cerebellar lysates using antibodies against vGLUT1, a transporter protein enriched in parallel fiber synapses [145,146]. As seen for vGLUT2 in the immunostainings, vGLUT1 was significantly reduced in Western blots of brain lysate from RibKO mice compared to control brain lysates (Fig. 8B), indicating also a reduction of parallel fiber synapses onto Purkinje cells.

To functionally test the excitatory and inhibitory connections onto Purkinje cells, we also measured miniature excitatory- (mEPSCs) and inhibitory postsynaptic currents (mIPSCs), respectively. As shown in Figure 8C-J, frequency and amplitude of mEPSCs and mIPSCs were strongly diminished in Purkinje cells from RibKO mice. This indicates a reduction in the number and/ or size of functional excitatory and inhibitory synapses onto Purkinje cells and supports the presumption that the connectivity of neurons in the cerebellum of RibKO mice is strongly diminished and that this might be the cause for the ataxia-like phenotype of RibKO mice.

Biochemical analysis of RibKO mice

The main regulator of cell size is mTORC1 and deletion of the rapamycin sensitive companion of mTOR, *raptor,* in the developing brain also leads to severe microcephaly (DC et al.; personal communication). To test whether the deletion of *rictor* affected mTORC1 signaling and contributes to the observed phenotype of RibKO mice, we performed Western blot analysis on adult whole brain lysates. As expected, no change in the amount of mTOR was detected (Fig. 9A). Phosphorylation of mTOR at Ser2481 was diminished while phosphorylation at Ser2448 remained unchanged, consistent with the recent finding that those phosphorylation sites

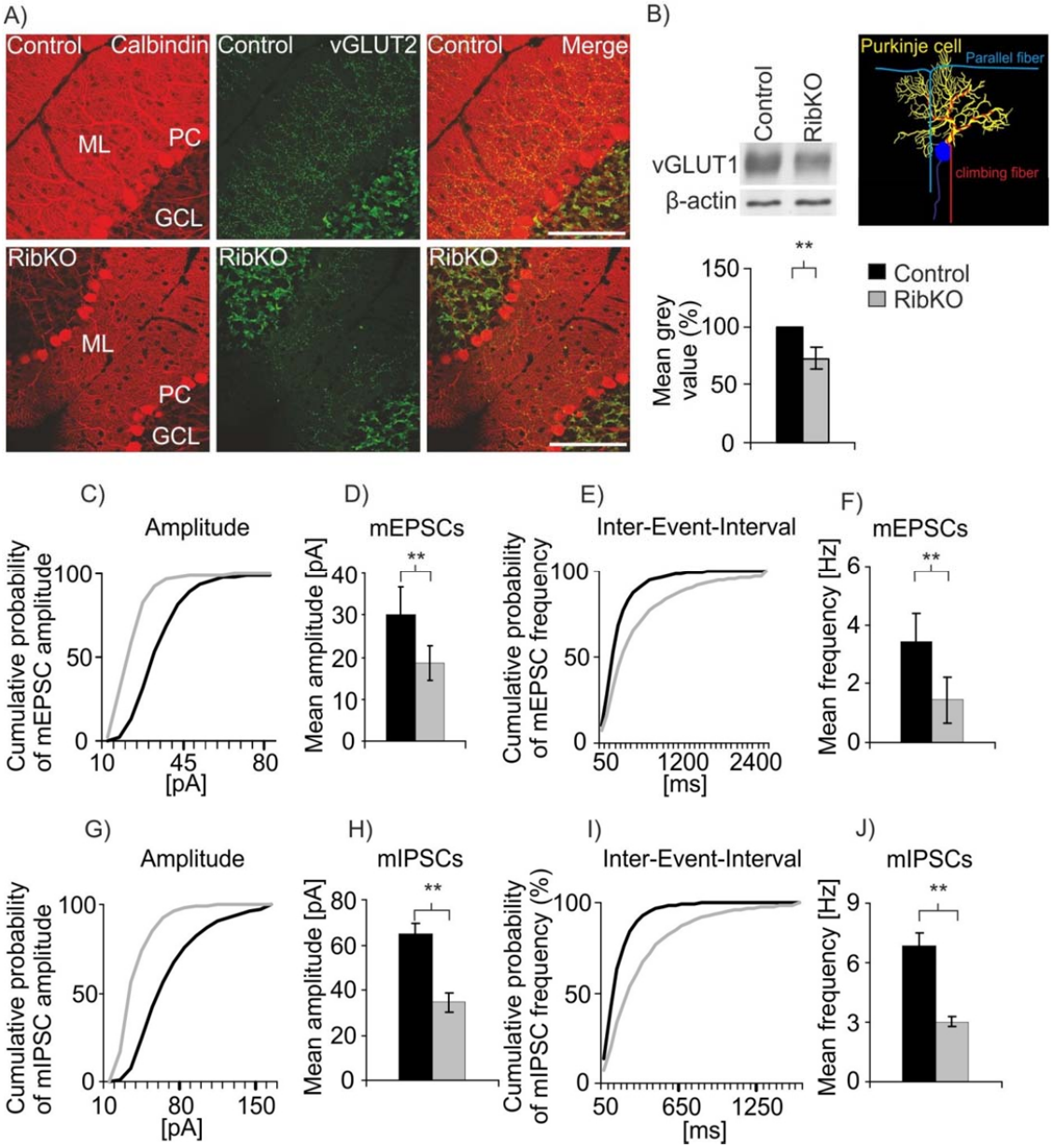

Figure 8. RibKO mice show synaptic changes in Purkinje cells. (**A**) Confocal image of cerebellar vermal lobule III of adult control and RibKO mice stained with antibodies to calbindin to visualize Purkinje cells (PC; red) and antibodies to vGLUT2 for climbing fiber terminals (green). Synaptic contacts from climbing fibers on Purkinje cells are reduced in cerebella of RibKO mice. Scale bar = 25 µm. Abbreviations: ML: molecular layer, GCL: granule cell layer, PC: Purkinje cell. (**B**) right: Schematic of Purkinje cell innervation by parallel and climbing fibers. Left: Western blot analysis of vGLUT1 in cerebellar lysates of control and RibKO mice and corresponding quantification of the mean grey values at the bottom. β-actin was used as loading control (data represent mean ± s.e.m., Student's *t-test*, ** $p < 0.01$, N = 6 control and N = 7 RibKO mice). (**C-F**) Miniature excitatory postsynaptic currents (mEPSC`s) and (**G-J**) miniature inhibitory postsynaptic currents (mIPSC`s) recorded from Purkinje cells in 250 µm sagittal sections of 25 day-old control and RibKO mice. The mEPSC recordings were performed at -70 mV, the mIPSC recordings at 0 mV, both in the presence of 0.5 µM TTX (tetrodotoxin). (**C,E,G,I**) cumulative probability plot of mEPSC and mIPSC amplitude (**C**, **G**) and inter-event interval (**E**, **I**). (**D**, **F**, **H**, **J**) Mean amplitude and mean frequency of both, excitatory and inhibitory currents were reduced in Purkinje cells of RibKO mice (data represent mean ± s.e.m. Student's *t-test*, ** $p < 0.01$, N = 4 control and N = 3 RibKO mice). Black bars/lines are from control; grey bars/lines are from RibKO mice. (Data in (C-J) by R. Lustenberger)

are indicative of the activation state of mTORC2 and mTORC1, respectively [147]. Importantly, phosphorylation of the main mTORC1 downstream targets S6K1and 4E-BP as well as the S6K1 target, the ribosomal protein S6, was also not altered in RibKO brain lysates (Fig. 9A, data not shown and Table 1 for quantification) indicating that the decrease in neuronal size does not involve altered mTORC1 activity.

Rictor deficiency was found in previous studies to reduce the phosphorylation status of the AGC kinases, including Akt [51]. Indeed, phosphorylation of Akt on Ser473 was strongly reduced and surprisingly, also the phosphorylation of Thr308 (Fig. 9A, Table1). Despite the change in phosphorylation of Akt at Ser473, phosphorylation of known Akt downstream targets such as FoxO1 [148] and GSK3β [149] was not altered in brain lysates of RibKO mice which indicates that the substrate specificity of Akt could be different in brain tissue.

Another group of AGC kinases, the protein kinase C (PKC) family was also shown to be regulated by mTORC2 [62,150]. There are at least nine different PKC isoforms that are grouped into three categories classified by their structural and enzymatic properties. These include the conventional isoforms (cPKC: PKCα, -β and –γ), the novel isoforms (nPKC: PKCε, -δ and –η) and the atypical isoforms (aPKC: PKCζ, -λ, -ι and –μ). The cPKC isoforms are activated by phosphorylation and second messengers [elevated Ca^{2+} concentrations and diacylglycerol (DAG)], whereas the novel isoforms are regulated only by DAG and phosphorylation [94]. As Figure 9C and Table 1 demonstrate, protein and phosphorylation levels of all cPKCs and the nPKCε were diminished in RibKO brain tissue whereas other PKCs are unaffected (data not shown).

In neurons, the main PKC downstream target is the growth-associated protein 43 (GAP-43). Interestingly, the phosphorylation of GAP-43 was diminished in brain lysate of RibKO mice (Fig. 9C). This demonstrates on the one hand that PKC activity is indeed diminished and on the other hand provides a first PKC substrate which is affected upon knockout of *rictor*. The reduction in PKCα could also be observed in cultured hippocampal neurons that were grown for 14 days (Fig. 9D). Importantly, there, phosphorylation of the three known PKC substrates, GAP-43, the myristoylated alanine-rich protein kinase C substrate (MARCKS) and fascin also showed lower phosphorylation levels (Fig. 9D). Phosphorylation of GAP-43 has been implicated in neurite formation, regeneration and synaptic plasticity [151] and MARCKS is assumed to be involved in actin cross-linking and thus in cell adhesion and morphology of neurons [152]. Fascin was shown to firmly bundle filamentous actin in protrusive cellular structures such as filopodia and dendrites and thus plays an important role in the cellular guidance and motility of cells [153,154]. Importantly, phosphorylation by PKCα inhibits this bundling activity [155]. Hence, all analyzed PKC substrates which exhibit decreased phosphorylation in brain lysate of RibKO mice are involved in the shaping of the actin cytoskeleton.

In summary, the biochemical data demonstrate that mTORC1 is most likely not involved in the neuronal size reduction observed in RibKO mice because neither the activity nor the downstream targets of this complex are altered. Furthermore, the data show that Akt phosphorylation, although highly reduced at Ser473, does not result in altered phosphorylation of its downstream targets FoxO1 and GSK3β. Furthermore, we demonstrate that the amount and activity of all cPKCs and of one nPKC are diminished *in vivo.* This deficiency alleviates the phosphorylation of PKC substrates involved in actin cytoskeleton morphology, pointing to an essential role of PKCs in the morphological changes of neurons in RibKO mice.

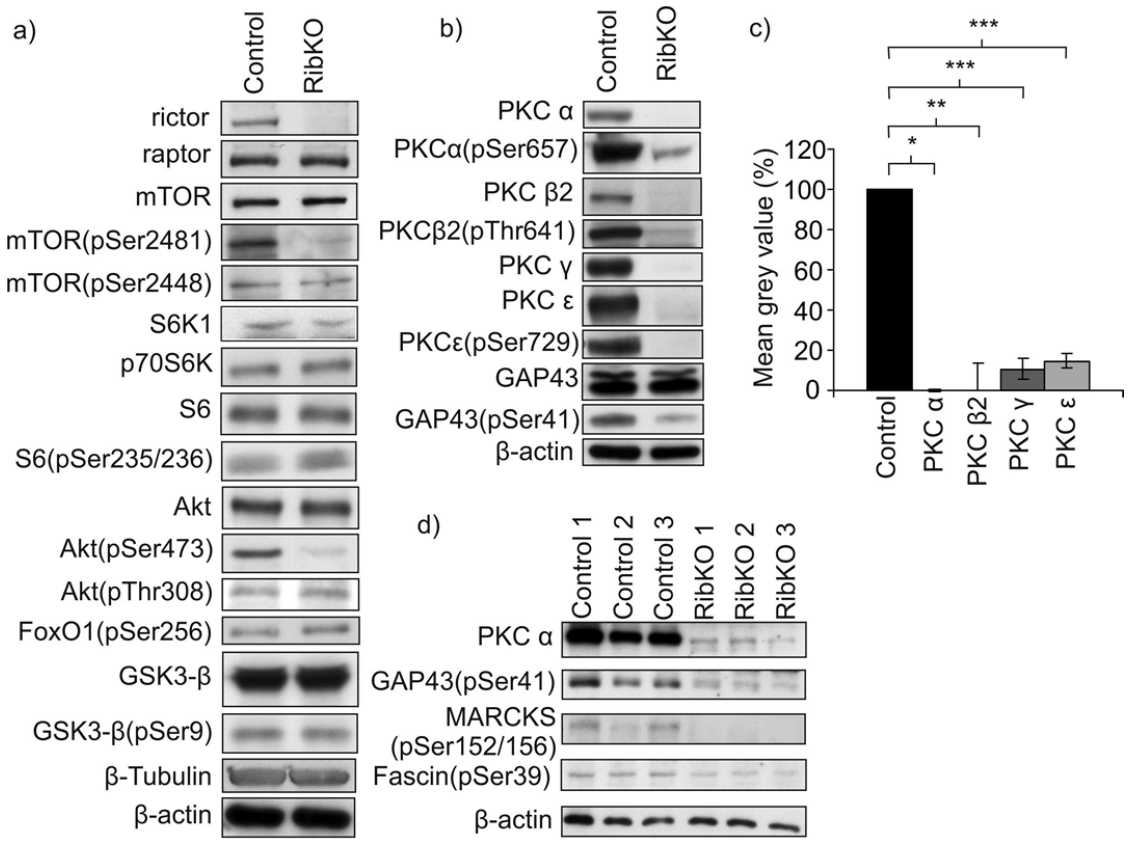

Figure 9. Biochemical analysis of RibKO brains. (**A**) Western blot analysis of whole brain lysates from adult control and RibKO mice, detecting mTORC1 and mTORC2 constituents and downstream targets. Rictor protein signal is completely lost in brain tissue of RibKO mice whereas total mTOR and raptor levels are unchanged. mTOR phosphorylation at Ser2448 is unaltered whereas mTOR phosphorylation at Ser2481 is decreased. Phosphorylation of mTORC1 targets S6K1 and the ribosomal protein S6 are unaffected in RibKO mice. Akt fails to be phosphorylated on Ser473, whereas total Akt and Akt phosphorylation at Thr308 are unchanged. Phosphorylation of Akt downstream targets FoxO1 (Ser256) and GSK3β (Ser9) is unchanged. (**B**) Western blot analysis of different PKC isoforms and their phosphorylated states and Western blot of PKC substrate GAP43 in whole brain lysates of adult control and RibKO mice. Blots reveal a decrease in phosphorylation and protein level of all conventional (α, β, γ) and one novel PKC isoform (PKCε). GAP-43 phosphorylation is also decreased. (**C**) Quantification of the mean grey value of PKC isoforms from whole brain (α, β, ε) or cerebellar lysates (PKCγ). PKCα and PKCβ2 are below detection level in RibKO brains (data represent mean ± s.d., Student's *t-test*, *** $p < 0.001$, PKCα: N = 5 control mice, N =7 RibKO mice, PKCβ2: N = 3 control and 4 RibKO mice). PKCγ is reduced to 11.8% in cerebellar lysates (data represent mean ± s.d., Student's *t-test*, *** $p < 0.001$, PKCγ: N= 4 control, N = 5 RibKO mice), and PKCε to 14.8% in whole brain lysates (data represent mean ± s.d. Student's *t-test*, *** $p < 0.001$, PKCε: N = 4 mice per genotype). (**D**) Biochemical analysis of PKCα and PKC substrate phosphorylation such as GAP43, MARCKS and Fascin in lysates of hippocampal cultures that were grown for 14 days. Amount of PKC is strongly decreased and phosphorylation of the PKC targets is diminished. β-actin was used as loading control. The data are derived from two experiments.

The role of rictor on cell size and cell morphology is cell autonomous

As the alterations in cell size and cell morphology were most prominent in Purkinje cells, we finally tested whether this effect was cell autonomous. To address this, we took advantage of another mouse model in which *rictor* was deleted under the Purkinje cell-specific Pcp2/L7 promoter (called L7rictor$^{-/-}$ mice). Pcp2/L7 is a protein of unknown function, which was reported to be expressed mainly postnatally in cerebellar Purkinje and retinal bipolar cells [156,157]. Hence, Cre-mediated ablation of *rictor* in Purkinje neurons is induced later during embryonic development compared to RibKO brains. Moreover, it has been shown that the Cre recombinase is not expressed in all Purkinje cells, thus resulting in a mosaic pattern [157] which enables the direct comparison of Purkinje cells that express the rictor protein and Purkinje cells that lack rictor. Recombination of the floxed *rictor* allele was tested by Western blot analysis for rictor and the Purkinje cell-specific isoform PKCγ, using cerebellar lysates of L7rictor$^{-/-}$ and control mice (Fig. 10A). Despite only partial deletion of *rictor*, protein levels of rictor and PKCγ were significantly reduced (Fig. 10B). Probably because of only partial and late onset deletion of *rictor* in Purkinje cells, we could not detect a locomotor phenotype in L7rictor$^{-/-}$ mice. Moreover, Cresyl violet-stained cerebellar sections did not show any gross morphological changes in the cerebellar lobules (data not shown) and also the width of the molecular layer did not differ from that of control mice (Fig. 10C). However, a closer examination of the Purkinje cell morphology revealed that L7rictor$^{-/-}$ mice recapitulated several of the hallmarks of RibKO mice. Staining of cerebellar sections from 8 week-old control and L7rictor$^{-/-}$ mice for calbindin and PKCγ revealed that between 30 and 70% of the Purkinje cell somata had lost the immunoreactivity for PKCγ in L7rictor$^{-/-}$ mice (Fig. 10D). This mosaic pattern of PKCγ immunostaining is likely due to only partial recombination of the floxed *rictor* allele [157], although we could not confirm this hypothesis because of the lack of appropriate antibodies to rictor (data not shown). However, because also in RibKO mice the PKCγ expression is diminished to almost undetectable levels, we assumed that the PKCγ deficient Purkinje cells in L7rictor$^{-/-}$ mice would be the ones that also lack rictor. Importantly, cells that were negative for PKCγ also had a reduced soma size, whereas PKCγ-positive cells from the same animal were not significantly smaller than cells in control mice (Fig. 10E). In addition, some of the PKCγ-negative Purkinje cells in L7rictor$^{-/-}$ mice were also mislocalized in the molecular layer (white asterisk in Fig. 10D, G) and their dendrites were deviated from the perpendicular plane (Fig. 10D). Moreover, PKCγ-negative Purkinje cells sometimes contained several primary dendrites (arrowheads in Fig. 10D) and the average diameter of dendrites of the PKCγ-negative neurons was significantly smaller (Fig. 10F). Interestingly, we also noticed that the dendritic area occupied by the PKCγ-positive Purkinje cells was increased compared to that of PKCγ-negative cells (Fig. 10G) when set in proportion to the number of PKCγ-positive cell soma in this area. This might indicate that the rictor-expressing, PKCγ-positive Purkinje cells compensate for the decreased dendritic tree area of the PKCγ-negative cells which would also explain the invariable molecular layer width observed in the L7rictor$^{-/-}$ mice. In conclusion, the similarity of the phenotype of Purkinje cells in L7rictor$^{-/-}$ and the Purkinje cells in RibKO mice strongly indicates that rictor acts cell autonomously.

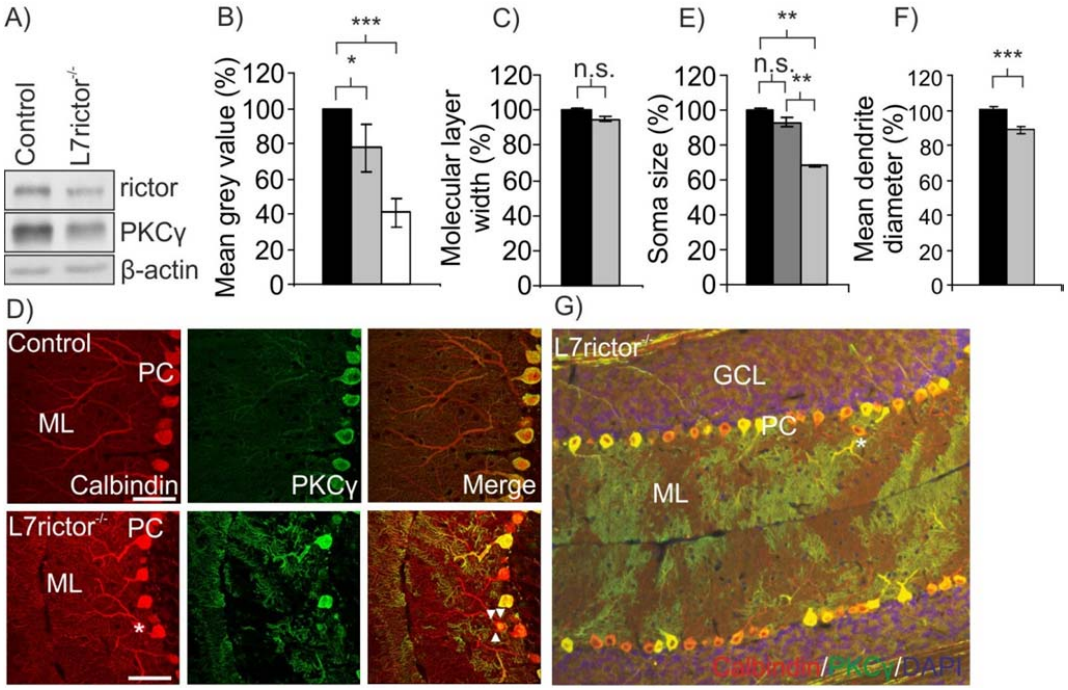

Figure 10. The role of rictor on cell size and morphology is cell autonomous. (**A**) Western blot analysis of cerebellar lysates from control and L7rictor$^{-/-}$ mice for rictor and PKCγ. β-actin was used as loading control. (**B**) Quantification of the mean grey value of Western blot bands, detecting rictor and PKCγ (values for rictor and PKCγ were set as 100% (black bar); values in L7rictor$^{-/-}$ mice: rictor: light grey bar; PKCγ: white bar). Data represent mean ± s.e.m. Student's *t-test,* * $p < 0.05$, *** $p < 0.001$, N = 5 mice per genotype. (**C**) Quantification of the molecular layer width in vermal lobules II, III and V of control and L7rictor$^{-/-}$ mice. Control mice: black bar, L7rictor$^{-/-}$: light grey bar (Student's *t-test*, n.s.: $p < 0.05$, N = 3 mice for each genotype). (**D**) Immunostaining of control and L7rictor$^{-/-}$ cerebella for calbindin (red) and PKCγ (green). Note that in L7rictor$^{-/-}$ cerebella the PKCγ staining is lost in some, but not all Purkinje cells indicating partial recombination of the *rictor* allele. The PKCγ negative (PKCγ-) cells have more than one primary dendrite (white arrowheads) and some of those are misaligned and diverge from the perpendicular plain (white asterisk). (**E**) Quantification of the Purkinje cell soma size of control (black bar), L7rictor$^{-/-}$ PKCγ-positive cells (PKCγ+) (dark grey) and L7rictor$^{-/-}$ PKCγ- cells (light grey). There is no significant change between control and PKCγ+ cells from L7rictor$^{-/-}$ mice. In contrast PKCγ- cells are significantly smaller than both PKCγ+ and control cells. (data represent mean ± s.e.m. Student's *t-test*, *** $p < 0.001$, ** $p < 0.01$, n.s. $p > 0.05$, N = 3 mice for each genotype). (**F**) Quantification of the dendrite diameter of control and L7rictor$^{-/-}$ PKCγ- Purkinje cells (data represent mean ± s.e.m. Student's *t-test*, * $p < 0.05$, N = 3 mice). (**G**) Representative picture of the Purkinje dendrites in the ML of L7rictor$^{-/-}$ mice, stained for calbindin (red) and PKCγ (green). Note that the dendritic area covered by PKCγ+ cells is larger than the number of cells expressing PKCγ in the cell body, indicating that PKCγ+ Purkinje cells compensate for the reduced size of cells. Some PKCγ-Purkinje cells diverge from the perpendicular plain (white arrowheads). Scale bar = 50 µm.

Table 1

Western blot quantification	
	adult brain lysates
	RibKO in %
rictor	n.d. ***
mTOR	64.9 ± 26.5
P-mTOR (Ser2481)	n.d. ***
P-mTOR (Ser2448)	101.4 ± 35.9
p70S6K	91.4 ± 45.7
P-p70S6K (Thr389)	95.7± 47.9
S6	169.3 ± 84.7
P-S6 (Ser235/236)	105.2 ± 52.6
Akt	115.6 ± 14.6
P-Akt (Ser473)	18.3 ± 4.8 ***
P-Akt (Thr308)	36.9 ± 8.1 **
P-FoxO1(Ser256)	152.9 ± 26.7 *
GSK3	116.8 ±14.4
P-GSK3 (Ser9)	103.7 ± 5.1
PKC a	19.3 ± 15.7 **
PKC ß2	1.2 ± 0.9 **
PKC γ	12.7 ± 5.2 **
PKC ε	15.4 ± 3.3 **
GAP-43	118.2 ± 7.5
P-GAP-43 (Ser41)	19.5 ± 4.7 ***

Quantification of Western blots from adult control and RibKO mice as shown in Fig. 9. Antibodies used for detection are listed on the left. The percentage of Western blot band intensity from RibKO mice was set in proportion to the intensity of the one in control mice (100%). T stars indicating the significance. Data represent mean ± s.d. from N > 3 up to 14 mice for each genotype.

SUPPLEMENTARY MATERIAL

Generation of floxed rictor mice

For the generation of brain specific rictor knockout mice, loxP constructs were inserted into the rictor gene flanking exons 4 and 5. The sketch below demonstrates the specific locations of the inserted fragments and their excision by enzymes.

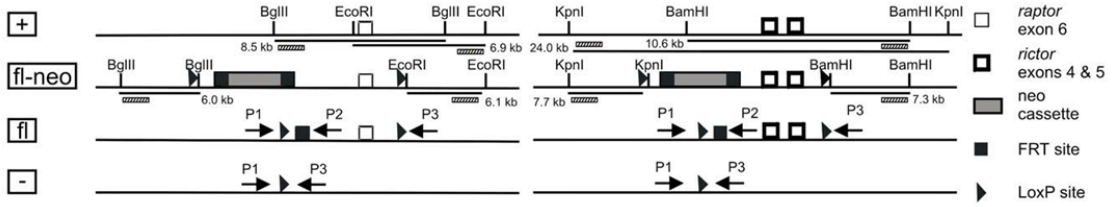

Supplementary Figure 1. Schematic presentation of wild-type and targeted alleles of raptor (left panel) and rictor (right panel) before and after recombination. As indicated in the drawing, differentially sized DNA fragments are obtained by digestion with specific restriction enzymes. Hatched bars represent the probes used for Southern blot analysis. PCR primers for genotyping are indicated by arrows. Legend: +: wild-type allele; fl-neo: targeted allele; fl: alleles after recombination by Flp-: alleles after recombination by Cre

As mentioned in the results part, RibKO mice were viable. However, soon after birth they were significantly lighter (Fig. 2B) and needed a special, nutrient rich diet to maintain their weight. As soon as they were able to walk, they showed locomotory defects and constant twitching. In young animals, tail posture was elevated and developed to a ring like tail in older animals (1 year) (Fig.S2A). They manifested some behavioral abnormalities such as defective attention upon cage opening and sudden overexcited, random running. In addition they displayed repetitive scratching behavior. In adult animals several tests for the assessment of general motor function and motor coordination were carried out including the clasping reflex (Fig.2C), the balance beam (Fig.S2B) and the accelerating rotarod (Fig.2D) and RibKO mice exhibited strong defects in all motor tasks that were executed. Defective motor function, however, can be caused on different CNS and peripheral nervous system (PNS) levels. Several brain areas are involved in the proper functioning of motor coordination involving the basal ganglia, the motor cortex, the cerebellum and the neuromuscular connections. Defects in the development of motor neurons can cause abnormal or reduced formation of the neuromuscular junction and this might lead to defects in synaptic transmission and reduced muscle control. Because of the impaired motor abilities of RibKO mice we examined their neuromuscular junctions by analyzing the formation of acetylcholine receptor clusters on the muscle membrane because their structure is indicative for the innervation-pattern by motor neurons. As shown in figure S2C, the typical pretzel-shaped acetylcholine receptor clusters did not differ in size or number in RibKO mice, indicating that there is no alteration on the level of neuromuscular connections in RibKO mice.

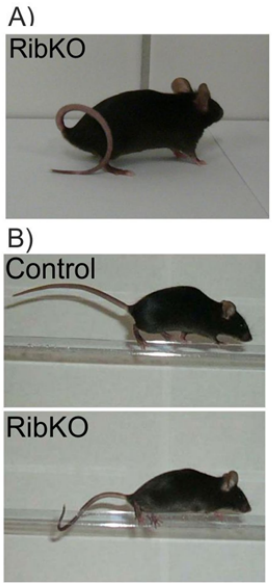

Supplementary Figure 2. RibKO mice have motor impairments (**A**) Photograph of a 1 year old RibKO mouse that has developed a ring like tail. (**B**) Photograph of a control and a RibKO mouse walking over a balance beam. RibKO mice have considerable difficulties performing this task and need to support themselves with their tail. They grab the bar from underneath and rob over it instead of walking on it. (**C**) Staining of neuromuscular junctions with antibodies to acetylcholine in control and RibKO mice. The number and structure of the pretzel-shaped neuromuscular junctions from RibKO mice are indifferent from those of control mice. (Data in (C) by S. Lin).

Mice with a brain specific knockout of rictor are infertile

Because of the apparent difference in body size and the marked reduction in brain mass, the question arose if other organs were also affected. When we measured the weight of heart, lung, kidney, liver, spleen and ependymal fat pads in male mice, we did not detect any difference when normalized to the body weight. However, a striking weight and size reduction was observed in testis which constituted only about 1/10 of the normal testis weight and resembled the size of testis in juvenile mice (Fig.S3). This strongly suggested that male RibKO mice were sterile. To determine this, and to also examine the fertility of female mice, we mated male RibKO mice, with female controls and vice versa. As we obtained no offspring in any of the breedings it seemed likely that RibKO mice were infertile.

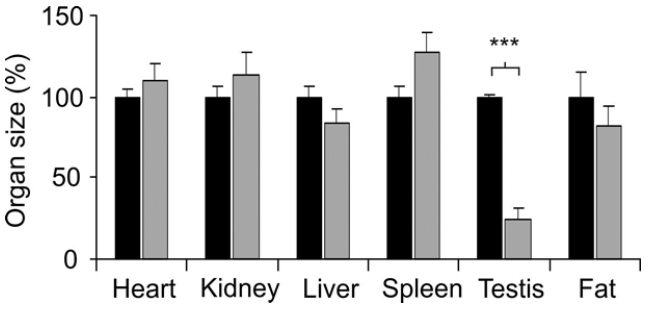

Supplementary Figure 3. Brains and balls. (**A**) Quantification of organ weight shows a reduction of testis from RibKO mice to 10% of the normal weight. (data represent mean ± s.e.m., Student's *t-test*, *** $p < 0.001$; n.s.: non- significant, $p \geq 0.05$; N= 6 mice for each genotype).

Rictor regulates cell size of dopaminergic neurons

Because of the reduction in soma size that we observed in hippocampal neurons and cerebellar Purkinje cells (Fig. 5E, 6D) we were interested if this would apply also for other cell types in other brain regions. The dopaminergic midbrain neurons can be easily distinguished with antibodies to the Tyrosine hydroxylase, an enzyme that is majorly involved in the synthesis of the

neurotransmitter dopamine. Staining of coronal brain sections revealed a reduction in the size of the ventral tegmental area and the substantia nigra in RibKO mice (Fig.S4A). Analysis of the soma size of dopaminergic neurons in this brain region revealed a decrease in size to 67% (Fig.S4B). Although the quantification represents preliminary results, the strong reduction indicates that microcephaly is indeed caused by an overall reduction in neuronal size in RibKO mice.

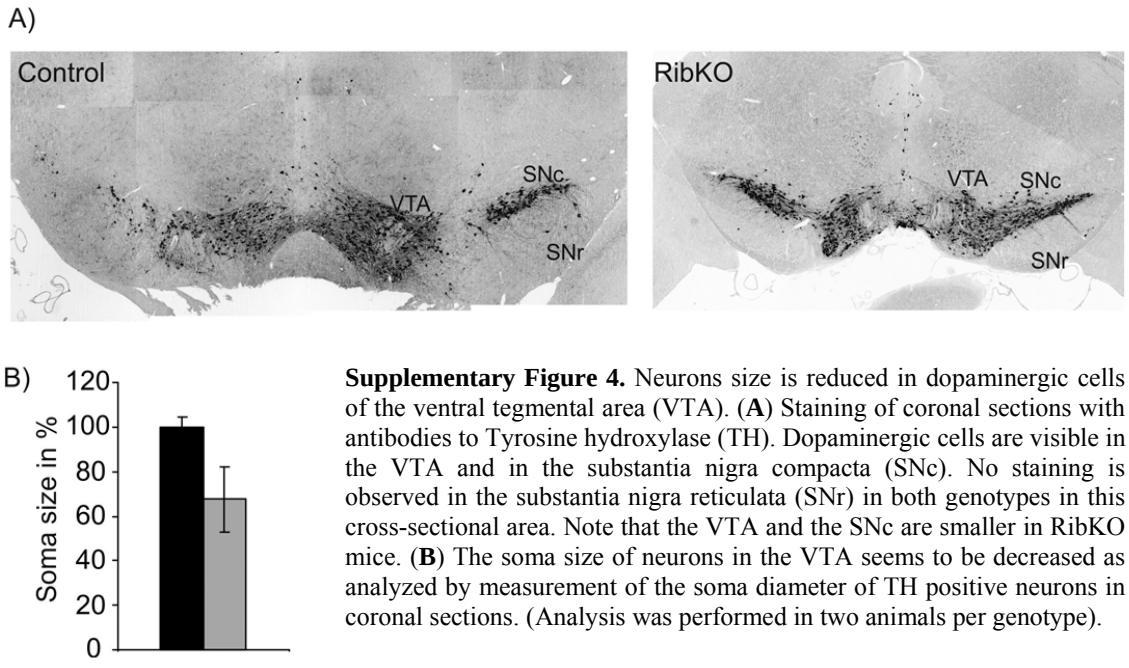

Supplementary Figure 4. Neurons size is reduced in dopaminergic cells of the ventral tegmental area (VTA). (**A**) Staining of coronal sections with antibodies to Tyrosine hydroxylase (TH). Dopaminergic cells are visible in the VTA and in the substantia nigra compacta (SNc). No staining is observed in the substantia nigra reticulata (SNr) in both genotypes in this cross-sectional area. Note that the VTA and the SNc are smaller in RibKO mice. (**B**) The soma size of neurons in the VTA seems to be decreased as analyzed by measurement of the soma diameter of TH positive neurons in coronal sections. (Analysis was performed in two animals per genotype).

Apoptosis and proliferation in cerebella of RibKO mice

During early postnatal brain development, a huge number of neurons are added and contribute to brain growth. In the rat, around 150 million neurons are generated in the cerebellum in the first postnatal week, which represent mainly granule cells [158]. Thus, if proliferation is impaired, cerebellar size will be decreased. To examine the cause for the reduced cerebellar size in RibKO mice we analyzed the proliferative rate of granule cells in cerebellar sections at different postnatal developmental stages. At birth, no difference could be observed in the staining pattern of the proliferative marker Proliferating Cell Nuclear Antigen (PCNA) (Fig. S5A), the same were true at P7, where the cerebellum was already smaller (Fig. S5B) and also BrdU labeling at postnatal day 14 revealed no difference in the proliferative rate of granule cell precursors (Fig. S5C). These data indicate that the decrease in cerebellar size is not caused by delayed or reduced proliferation and confirm the neurosphere experiments (Fig. 4G-J).

A decrease in cerebellar size could also be caused by an increased number of dying cells. To investigate if apoptosis plays a role in the cerebellar size reduction in RibKO mice, we analyzed the number of apoptotic cells in P14 cerebella. Quantification of the number of cells that were immunoreactive for the apoptotic marker protein cleaved-Caspase-3 revealed no alteration between control and RibKO mice (Fig. S5D). These findings indicate that the decreased

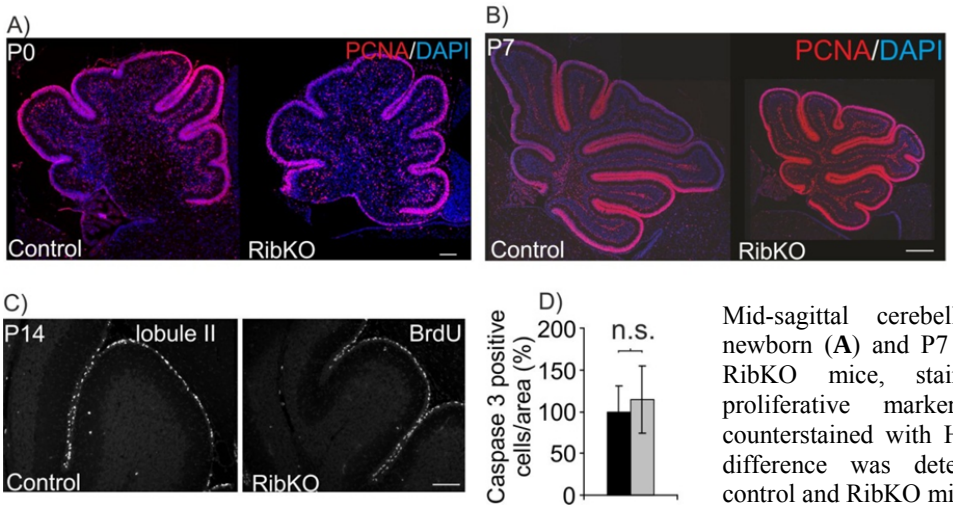

Supplementary Figure 5. Cerebellar size reduction is not caused by reduced proliferation or increased apoptosis. Mid-sagittal cerebellar section of newborn (**A**) and P7 (**B**) control and RibKO mice, stained with the proliferative marker PCNA and counterstained with Hoechst dye. No difference was detectable between control and RibKO mice. (**C**) Sagittal section of cerebellar lobule II in 14 day old control and RibKO mice stained with antibodies to BrdU. Mice were injected with BrdU 2 hours prior to tissue dissection. No difference in BrdU staining was observed. (**D**) Quantification of cleaved-caspase-3 stained cells per area in cerebella of P14 control and RibKO mice for apoptosis assessment. No significant difference was detected. Scale bar = 100 µm. (Data represent mean ± s.e. Student's *t-test*, n.s. $p > 0,05$ $N \geq 3$ mice per genotype).

cerebellar size of RibKO mice is generated by a reduction in cell size and neither by proliferative defects nor by apoptotic mechanisms.

RibKO mice develop deformations in cerebellar foliation

In addition to the overall reduction in cerebellar size, the cerebella of RibKO mice have strong defects in lobule formation and this can be observed in all lobules throughout the cerebellum, especially in the cerebellar hemisphere (Fig S6A). The normally highly conserved cyto-architecture is profoundly disrupted and specific lobule features are no more comparable to control cerebella. Examinations of the cell types that contribute to this defect show mis-localized granule and Purkinje cells. Because defective lobule structure is already obvious at P7 when Purkinje cell migration has already ceased, and granule cell migration is on its peak this indicates that the disrupted foliation is primarily based on migration defects of Purkinje cells and further signifies that rictor is involved in cell migration.

RibKO mice display increased inhibitory neuron density in the cerebellum

Because of the dramatically decreased cell size and the reduced spine density on Purkinje cells, we have investigated electrophysiologically the functional innervation of this cell type by measuring the EPSCs and the IPSCs. The currents of both afferents was greatly diminished which could on the one hand indicate a reduction in functional synapses from excitatory and inhibitory fibers and on the other hand it could signify a reduced number of excitatory and inhibitory neurons. To investigate the cause for the impaired IPSCs in RibKO mice, we counted the number of inhibitory, GABAergic interneurons in the molecular layer of the cerebellum which stain positive for the calcium binding protein Parvalbumin. As shown in Fig S7A and B we

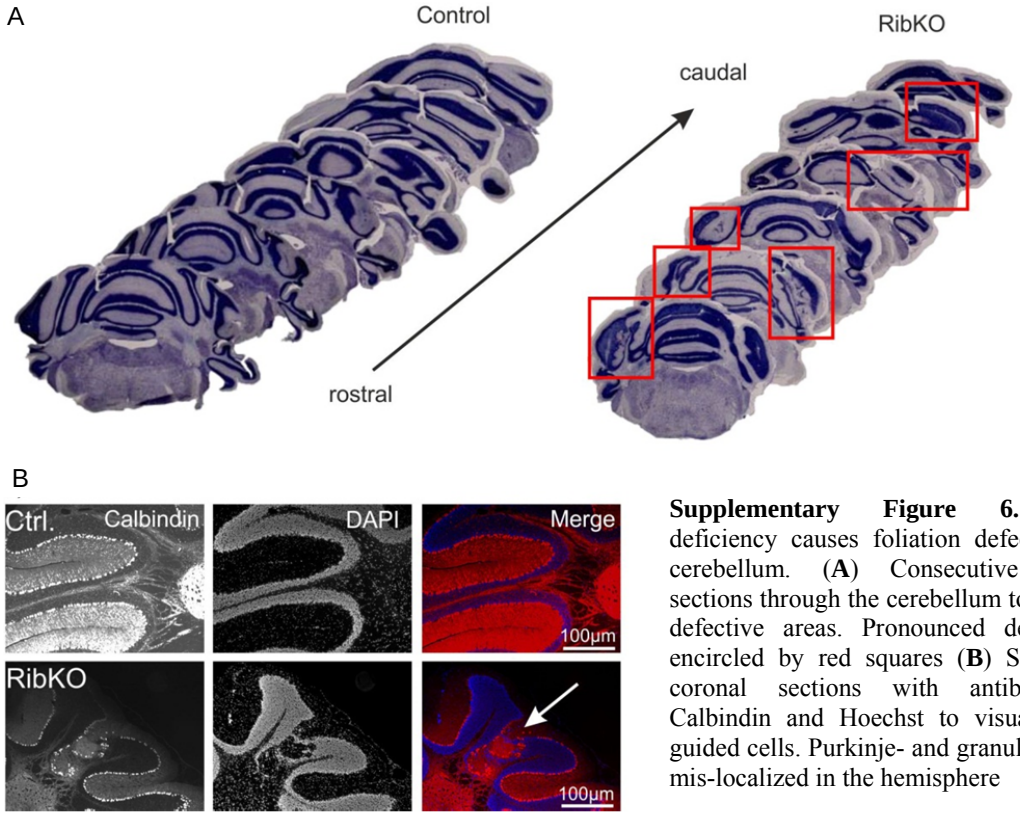

Supplementary Figure 6. Rictor deficiency causes foliation defects in the cerebellum. (**A**) Consecutive coronal sections through the cerebellum to visualize defective areas. Pronounced defects are encircled by red squares (**B**) Staining of coronal sections with antibodies to Calbindin and Hoechst to visualize mis-guided cells. Purkinje- and granule cells are mis-localized in the hemisphere

detected an increase in the density of those parvalbumin-positive neurons in the molecular layer of the cerebellum in RibKO mice suggesting that the decrease in inhibitory current is induced by deficient synapse formation and not by decreased inhibitory cell numbers. In addition, those data also support the results on the increased neuron density in the cortex and indicate that in RibKO mice an increased neuron density contributes to the microcephaly.

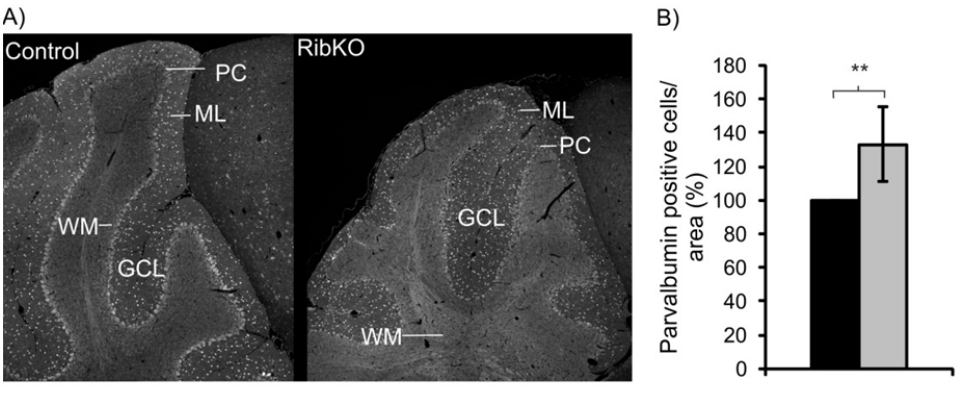

Supplementary Figure 7. The density of inhibitory neurons in the cerebellum is increased. (**A**) Immunohisto-chemical staining of sagittal cerebellar sections from control and RibKO mice for Parvalbumin. The white dots in the molecular layer represent the inhibitory parvalbumin positive cells Abbreviations: ML: molecular layer, PC: Purkinje cells, GCL: granule cell layer, WM: white matter.(**B**). Quantification of the density of parvalbumin positive cells in the cerebellum (data represent mean ± s.e.m. Student's *t-test,* ** $p < 0.01$, N= 5 control and N= 7 RibKO mice).

Axonal complexity is affected in rictor deficient brains

During the course of our studies on the morphology of Purkinje cells in organotypic cerebellar slice cultures, we observed a strong reduction of the axonal network. Whereas a strongly stained axonal network was readily visible in control slices, the axons of neurons in RibKO mice appeared fragile, less numerous and chaotically arranged (Fig.S8A). Importantly, the number of Purkinje cells in the slice did not differ between genotypes (Fig.S8B), indicating that the loss of axonal structures was not caused by a reduction in Purkinje cell number. Those data denote that in addition to the aberrant dendrite structure, Purkinje cells have also defects in axonal development. In this context it is also interesting to note that GAP-43, a protein known to be majorly involved in axonal growth and path-finding is inadequately phosphorylated in RibKO mice, further strengthening the role of PKC in the phenotype.

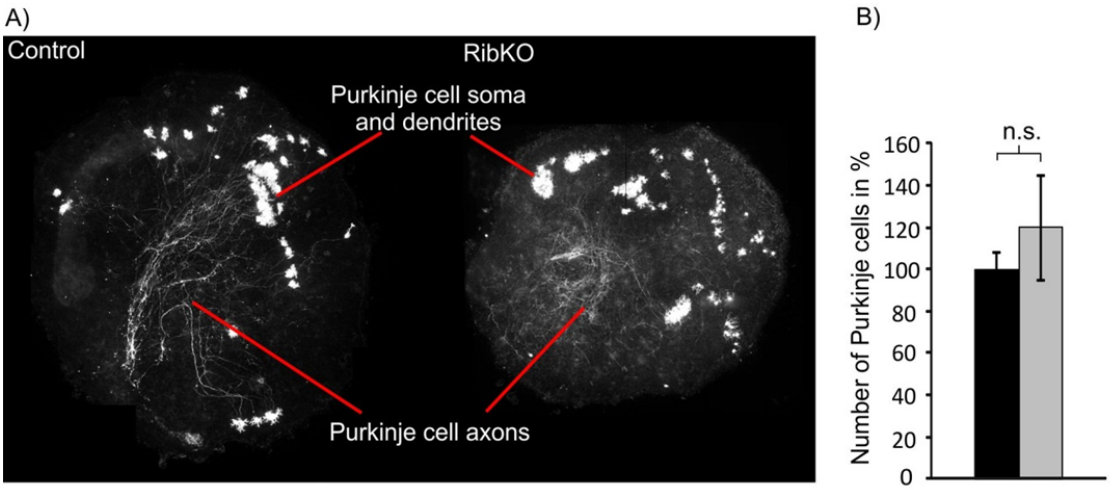

Supplementary Figure 8. Axonal development in the cerebellum of RibKO mice is impaired. (**A**) Overview of organotypic cerebellar slice cultures, stained with Calbindin. Purkinje cell soma and dendrites are brightly stained although cells appear smaller. In contrast to the thick axon tracks visible in control slices, the axonal network in RibKO slices is strongly diminished and appears disorganized. These observations were made in more than 3 animals in more than 3 experiments. (**B**) Quantification of the number of Purkinje cells in cerebellar slices of control and RibKO mice reveals no significant change in cell survival. . (Data represent mean ± s.e.m. Student's *t-test*, n.s. $p > 005$, $N \geq 3$ mice per genotype).

Detection of the PKC substrate GAP-43

We have detected impaired protein abundance of all conventional PKC isoforms in the brains of RibKO mice (Fig.9B, C). Although cell culture experiments have previously shown that loss of mTORC2 compromises PKC activity and this influences the structure of the actin cytoskeleton, there have never been suggestions on PKC substrates that might exert those modifications. To analyze which downstream targets are affected by the loss of PKCs we performed Western blot analysis on whole brain lysates of control and RibKO mice with a phospho-specific PKC substrate antibody. Thus, all proteins that are phosphorylated at the PKC specific amino acid sequence are detected by the antibody. Since PKC activity is significantly lowered in RibKO mice we expected to find some unphosphorylated PKC targets and indeed we obtained several

protein bands with reduced signal (Fig. S9A). Those bands were excised from protein gels and analyzed by mass spectrometry for phosphorylated peptides. Interestingly, one peptide sequence from the protein band between 40 and 50 kDa (kilo Dalton) featured reduced phosphorylation (Fig. S9B) and sequence analysis and database alignment identified this protein as GAP-43. Because GAP-43 is one of the major PKC downstream targets in neurons, this protein provided a reasonable result and was thus further analyzed by Western blot. We found that the phosphorylated GAP-43 was indeed diminished in brain lysates of RibKO mice and in lysates of dissociated hippocampal cultures (Fig. 9C, D). In addition, phosphorylated GAP-43 was hardly detectable in immunofluorescent staining in cerebella of young (P7) RibKO mice (Fig. S9C). Importantly, at this postnatal developmental stage, the neurons in the cerebellum undergo strong migration and rapid axonal growth and branching which are highly dependent on phosphorylated

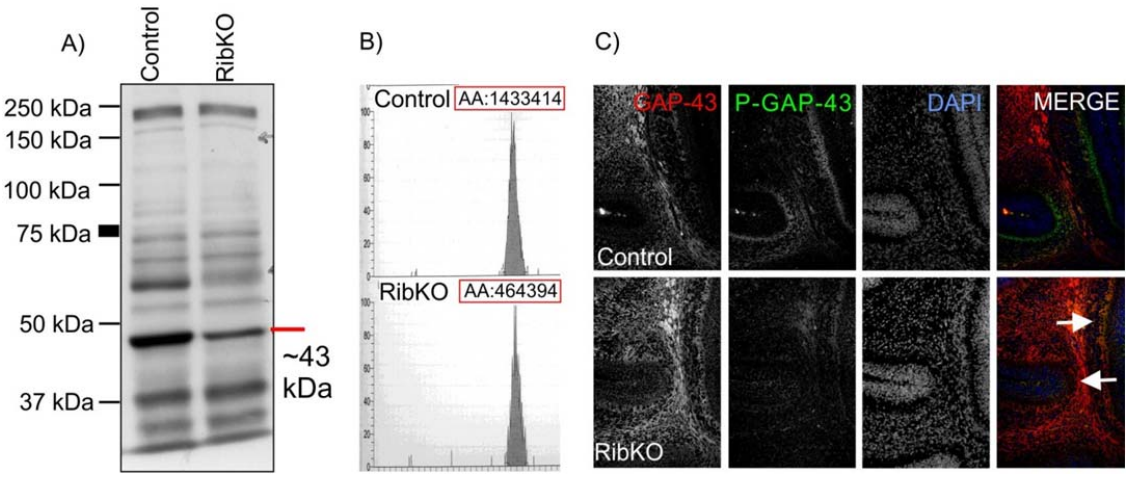

Supplementary Figure 9. Phosphorylation of GAP-43 is impaired in RibKO mice. (**A**) Western blot detecting phosphorylated PKC substrates in whole brain lysate of control and RibKO mice. A protein band at around 40-50 kDa shows decreased phosphorylation. (**B**) Mass spectrometric analysis of the protein band, detected by Western blot in **A**) reveals a protein that is about 32% less phosphorylated in RibKO mice. Database alignment identifies the protein as GAP-43. (**C**) Immunofluorescent staining of P7 sagittal cerebellar sections for GAP-43 and phosphorylated GAP-43. Whereas GAP-43 is highly expressed in both genotypes, the phosphorylated form is attenuated in cerebella of RibKO mice (white arrows). DAPI was used as nuclear marker. (Data in (B) by P. Jenö and S. Moes).

GAP-43. Hence, those data provide a PKC substrate that is substantially diminished in its phosphorylation in rictor deficient brains and furthermore was shown to be involved in the structuring of the neuronal cytoskeleton. Although we cannot provide a direct link between GAP-43 and alterations in cytoskeletal structures in the brains of RibKO mice, the data show for the first time that rictor deletion has an influence on PKC targets.

Neuronal knockout of rictor does not influence abundance of neuronal markers or Rho GTPase activity

Because of the reduction in cell size and the pronounced decrease in EPSCs and IPSCs we were wondering if the amount of specific proteins involved in neurotransmitter reception such as the glutamate receptor (GLUR2) or the *N*-methyl *D*-aspartate receptor 1 (NR1) would be affected by

loss of rictor because their expression and localization has also been shown to be dependent on PKC and Akt signaling, respectively. Neurotransmitter transport in specific neuron populations can be analyzed with proteins to the vesicular GABA transporter (vGAT) or the Glutamate ASpartate transporter (GLAST) which would show differences in the availability of neurotransmitters at the synapse or differences in the abundance of certain neuron populations. In addition, neurotransmitter synthesis is dependent on specific proteins which can be used as marker proteins for the detection of certain neuron types such as Tyrosine hydroxylase (TH) or glutamic acide decarboxylase (GAD67) and certain scaffolding molecules are known to influence the structure of the synapse in certain neuron types such as Gephyrin. Analysis of all those proteins, however, revealed no change in Western blot of adult whole brain lysates of RibKO mice (Fig.S10A). Interestingly also the TH levels did not differ in Western blots although we have seen a reduction in the size of neurons and in the size of the VTA (Fig. S6, Fig. S10A).

Modifications in cell size and morphology often involve a differential expression of actin and tubulin modifying proteins. In addition, it was proposed that mTORC2 affects Rho GTPase signaling and it is well known that PKC and Akt both influence some of the Rho GTPases [159,160]. The suggested role of rictor in actin cytoskeleton structuring therefore disposed us to analyze the role of Rho GTPases in RibKO mice. Exchange of GDP for GTP induces activation of the proteins and influences cytoskeleton rearrangement. Whereas Rac1 and Cdc42 are known to positively influence neurite outgrowth, RhoA has a negative regulatory role on neurite growth. When we analyzed the activation state of Rho, Rac1 and Cdc42 in brain tissue of RibKO mice we could not detect a difference in activity compared to control lysates (Fig. S10B). Also the direct Rac1 and Cdc42 downstream target, Pak1 which is phosphorylated upon Rac1 and Cdc42 activation, was unchanged in brain lysates of RibKO mice, suggesting that those Rho GTPases do not contribute to the modifications on the cytoskeleton.

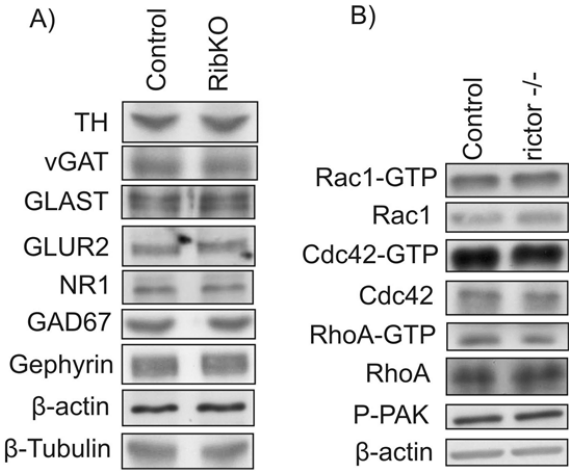

Supplementary Figure 10. Proteins involved in neuronal signaling and neuronal structure are unchanged in RibKO mice. (**A**) Western blot detecting several neuronal markers. None of the analyzed proteins is changed in whole brain lysates of RibKO mice. (**B**) Activity of Rho GTPases is indifferent in brain tissue of RibKO mice. Western blot of adult (Rac1 and Cdc42) or P7 (RhoA) whole brain lysate from control and RibKO mice shows that none of the GTPases differ in their activity (GTP bound states).

DISCUSSION

Constitutive deletion of *rictor* has been shown to be embryonically lethal [120]. Here, we show that deletion of *rictor* during brain development causes microcephaly that is induced by reduced cell size. Moreover, we find a pronounced phenotype in Purkinje cells affecting their morphology and connectivity, both of which might contribute to the severe motor deficits. Because the size of the neurospheres derived from RibKO mice is indifferent from those of control mice, this suggests, that growth rather than initial cell size is regulated by mTORC2.

Rictor has been removed in several other organs including skeletal muscle [122,123] and adipose tissue [124]. In all those tissues, the effect was rather small and never affected cell size or actin cytoskeletal modifications. mTOR has been recently shown to be involved in dendrite morphology in cultured hippocampal neurons [131]. However, this effect of mTOR knockdown by RNAi was attributed to mTORC1. In our group, we have investigated the role of mTORC1 by deletion of *raptor*, the essential mTORC1 component, in the developing brain. Those mice die at birth and show several phenotypic changes such as microcephaly, caused by reduced cell size and defects in proliferation, delayed glial differentiation and aberrations in cortical layering. Our results now show that deletion of *rictor* in the entire CNS and in specific subpopulations of neurons causes a rather severe phenotype with structural abnormalities in the soma, the axons and the dendrites. Because of the supposed functional crosstalk of mTORC1 and mTORC2 (via Akt and S6K) it was of major importance to evaluate the contribution of mTORC1 in the phenotype of RibKO mice. It was previously suggested that mTOR when assembled in mTORC1 affects neurite outgrowth and branching. Furthermore, results obtained from hippocampal neuron cultures showed that mTOR inhibition by RNAi had an effect on the number and complexity of neuronal branches [131]. However, Higuchi and colleagues showed that the neurite length, the branching and the number of neurites in NGF treated PC12 cells was not influenced by rapamycin [81] indicating for an mTORC1 independent mechanism of neuronal outgrowth. Although those studies have been performed in cell culture and in addition in different cell types, the notion appears that mTOR activity on growth and branching might also involve mTORC2 signaling.

mTORC1 is known to regulate cell size and translation by controlling the activities of the S6K and the 4EBP. Here, we analyzed mTORC1 signaling in rictor-deficient brains but found the mTORC1 signaling pathway towards those proteins to be unaffected. In addition we found that mTORC1 activity was not changed as indicated by normal phosphorylation levels of mTOR at Ser2448. These data provide strong evidence that mTORC1 is not involved in the phenotypic changes (neuronal size reduction and the abnormal dendrite morphology) in rictor-deficient brains. Hence, mTORC2 as well appears to play an unprecedented important role for the signaling and morphology of neurons *in vitro* and *in vivo*.

The two kinases, Akt and PKC whose activity is regulated by mTORC2 are known to influence neuronal morphology [79,161-163]. In RibKO mice, Akt activity is substantially diminished as indicated by diminished phosphorylation of Akt at Ser473 and lowered phosphorylation at Thr308. The Akt/PI3K pathway has been revealed as key mediator of various aspects of neurite outgrowth, including elongation, caliber and branching of neurites [79,133]. Akt is also implicated in various functions during development and growth of neurons and dysfunction of Akt is thought to cause neurodevelopmental disorders [134]. Hyper-activation of the Akt/PI3K pathway in specific

neuron populations was mediated by deletion of the upstream effector tumor suppressor protein PTEN and resulted in a pronounced increase in soma size and overgrowth of the affected brain area [164]. In contrast, we have observed reduced neuronal soma size and microcephaly in RibKO mice. The opposing phenotype of PTEN and neuronal rictor knockout mice would thus implicate a functional correlation coalescing on Akt. Furthermore, one study showed that specific down-regulation of the Ser473 phosphorylation site in Akt by polyphosphate 5-phosphatase (PIPP) which hydrolyses PIP3, reduces neurite elongation whereas overexpression of the phosphatase generates longer neurites [165]. This would indicate that specifically the phosphorylation of Akt at Ser-473 is important in the growth process in neurons which consequently assigns mTORC2 as an important player in this process. However, the regulating function of Akt on growth and morphology is exerted via the regulation of mTORC1, GSK3β or Pak1/2 and we have not detected a reduction in the phosphorylation levels of those Akt downstream targets in rictor-deficient mice. Although we cannot exclude that other Akt targets might play a role in the phenotype of RibKO mice but due to the lack of changes in Akt downstream targets our data so far indicates that Akt is not majorly involved in the brain size reduction and the morphological alteration in rictor deficient cells.

On the other hand our work points towards an important role of mTORC2 in the regulation of neuron morphology by controlling PKC activity. Different PKC isoforms exert important functions in a tissue, isoform and stimulus-specific manner [166]. Absent phosphorylation of PKCs causes rapid ubiquitin-dependent degradation of the protein and was shown to be the reason for PKC deficiency in *rictor*-depleted cells [150]. Loss of one PKC isoform generally induces a compensatory up-regulation of another isoform. In *rictor*-deficient neurons, however, all conventional PKC isoforms are largely lost. PKC signaling is known to have important functions during development and growth of Purkinje cells, and insufficient PKC activity in developing neurons causes defects in dendrite arborisation. PKCγ, which is specifically expressed in cerebellar Purkinje cells [161-163], was shown to induce extensive branching of primary dendrites upon pharmacological inhibition in mouse cerebellar slice cultures [135] and also PKCγ-knockout in mouse Purkinje neurons is characterized by the maintenance of several primary dendrites [23]. We also observe an increase in the number of primary dendrites in Purkinje cells of both, RibKO and L7rictor$^{-/-}$ mice which is a strong indication that deregulation of PKCs by loss of rictor causes the maintenance of multiple primary dendrites.

Another PKC which is highly expressed in brain tissue is PKCε [101] with highest production in hippocampus, cerebellum, frontal cortex, striatum and nucleus accumbens.[100]. PKCε has been found to promote neurite outgrowth without involvement of its kinase domain[167]. Although the mechanism of how PKCε influences neurite growth is not elucidated its presynaptic location indicates that it might also be important in the formation of synapses. In RibKO mice we have observed a profound loss of mEPSC and mIPSC amplitude and frequency which could be ascribed partially to defects in presynaptic function. In summary, the defects in dendrite morphology and synaptic function observed in the RibKO and in the L7rictor$^{-/-}$ mice might be based on the profound loss of all conventional PKCs and of PKCε. However, mice carrying deletions in multiple PKC isoforms have not been generated so far and therefore comparison to RibKO mice cannot be adopted.

Furthermore, PKC signaling was also implicated in mediating actin cytoskeleton rearrangements in a rictor dependent way [51]. In HeLa cells, rictor knockdown was shown to yield

similar actin morphology as PKCα knockdown and it was concluded that there might be a common mechanism in actin cytoskeletal organization [51]. However, this observation was thus far only observed in culture and could not be confirmed *in vivo*. The structuring of the actin cytoskeleton by PKC is mediated directly by PKCs and indirectly through phosphorylation of PKC substrates [168]. Some of these PKC substrates directly influence the actin morphology and the binding of actin to the plasma membrane such as GAP43, MARCKS and fascin [14,152,169]. As we have shown here, phosphorylation of those proteins is reduced in neurons of RibKO mice *in vitro* and *in vivo*. Thus, it is intriguing to speculate that in rictor deficient brains the reduced neurite growth as observed in cultured hippocampal neurons and in organotypic cerebellar slices is caused by the inefficient phosphorylation capacity of PKC towards those proteins. For GAP-43 this would mean that the barbed end capping function of unphosphorylated GAP-43 would inhibit the severing of actin and the rigidity of actin would thus prevent fast growth cone extensions.

In hippocampal culture, the axonal network is a prerequisite for the formation of elaborate dendritic arbors and spine formation. The reduced connectivity and the missing electrical signals from axons to the dendrites would thus also inhibit dendritic arbor formation in RibKO mice. The same could be true for the organotypic cerebellar slice cultures where the axonal network is greatly diminished in brains of RibKO mice and could also hold true for the *in vivo* observed dendritic spine reductions and the malformed dendritic tree of Purkinje cells. Purkinje cells are known to develop elaborate dendritic trees even in the absence of synaptic input from parallel fibers. However, when the parallel fiber input is absent a reduction in the branching of distal dendrites and the complexity of the dendritic tree is observed. In RibKO mice, the dendritic tree of Purkinje cells is already deformed at early developmental stages (P7) when parallel fiber input is not yet established which rather points to a cell autonomous growth defect. However, adult Purkinje cells exhibit strongly reduced excitatory and inhibitory input as measured by reduced EPSCs and IPSCs. This reduction can either be caused by a decrease in the number or size of synapses onto Purkinje cells or a reduction in the amount of transmitter vesicles released into the synaptic cleft. We observe a reduction in the number and size of climbing fiber terminals in RibKO mice. In addition, the reduced number of spines in hippocampal neurons and in Purkinje cells and the simplification of higher order branches in Purkinje cells points to a reduction in the number and/or size of afferent fibers. Moreover, in organotypic cerebellar slice cultures we observed a chaotic axonal growth which is a strong indication that the development of the presynaptic compartment is also disturbed. Excitatory synaptic efficacy is, however, dependent on proper neurotransmitter vesicle trafficking and quantal release of neurotransmitter at the presynaptic site [170]. Glutamate is secreted from the presynaptic terminal (parallel and climbing fibers in the cerebellum) by fusion of glutamate containing vesicles with the membrane. These presynaptic vesicles contain glutamate transporters that mediate the uptake of glutamate. There are three known vesicular glutamate transporters (vGLUTs) in the vertebrate CNS termed vGLUT1-vGLUT3 and their distribution is temporally and spatially regulated. In the adult brain their expression profiles differ and vGLUT1 and vGLUT2 show roughly complementary expression patterns[170]. vGLUT1 predominately functions in the cerebellar and the cerebral cortex and the hippocampus whereas vGLUT2 is mainly expressed in neurons of the spinal cord, brainstem and midbrain [170]. A reduction in the content of vGLUT proteins reduces the level of glutamate that can be released from the presynaptic terminal and consequently decreases the excitatory potential of a synapse and thus, reduces the possibility for the formation of spines. On

the other hand, a reduced synaptic terminal size will have less vGLUT proteins and this seems to be the case in the brains of RibKO mice. Hence, the Purkinje cell phenotype might be partially induced by deficient parallel fiber and climbing fiber axonal growth and synapse formation onto Purkinje cells.

Interesting also in this context is the prominent disruption of the cerebellar lobules. Mis-localization of cells in the cerebellum suggests that neurons of RibKO mice have defects in cell migration. The anchorage of Purkinje cell axons to the base of the fissures is, however, a prerequisite for proper cerebellar folia development. In organotypic cerebellar slice cultures of RibKO mice we have observed that the axonal outgrowth of Purkinje cells is majorly affected. Hence, inefficient anchorage of Purkinje cell axons may cause the disruption of cerebellar lobule structure. The defects in lobule structure are already visible at P7 when Purkinje cell migration is just about finished, whereas granule cell migration will proceed until about P20. This indicates that defective Purkinje cell axonal attachment to the base of the fissure and inaccurate Purkinje cell migration is the major cause for the defective foliation in RibKO mice. This is also supported by the finding that cerebellar lobule structure is normal in L7rictor$^{-/-}$ mice. There recombination takes place at later developmental stages than in RibKO mice and axonal growth, path-finding and anchorage might already have developed before the majority of cells are knocked out.

In the brain, rictor is expressed in neurons with highest expression in cerebellar Purkinje cells[120]. Hence, it is not surprising that this cell type features the strongest phenotypic alteration. In RibKO mice, *rictor* is deleted during early embryonic development. In contrast, deletion of rictor in the L7/Pcp2 mice starts during late embryonic development and peaks postnatally, when Purkinje cell migration is virtually finished [157]. Presuming that the cerebellar defects in RibKO mice are generated mainly postnatally during Purkinje cell migration, this would explain why the cerebellar foliation phenotype of L7rictor$^{-/-}$ mice is considerably weaker and the mice show no overt motor phenotype. However, Purkinje cells do exhibit the same morphological changes with smaller soma sizes, decreased dendrite diameter and abnormal branching pattern in both mouse lines. Dendrite and soma growth is mediated later during postnatal cerebellar development than migration and thus explains the milder phenotype of L7rictor$^{-/-}$ mice. Those data therefore support the consistency and cell autonomy of the rictor phenotype in different knockout systems.

Although, the reduction of cell size was mainly analyzed in detail in cerebellar Purkinje cells and in pyramidal cells of the CA1 layer of the hippocampus, a reduction in soma size was also observed in other neuron types as measured in the ventral tegmental area. The pronounced and global microcephaly of RibKO mice therefore strongly suggests that the decrease in cell size is valid for all neuron populations in RibKO mice.

Interestingly, brain-specific deletion of *rictor* caused not only a massive reduction in brain mass but also a reduced body size. Furthermore, we found a massively decreased testis size and recognized that also female mice are infertile. Because the brain regulates its body functions including body growth and maturation of sexual characteristics by coordinated secretion of various hormones, minor morphological changes in hormone sensing and secreting brain regions may affect the entire body. In healthy mammals the cells of the pituitary are stimulated by axons from the thalamus and this stimulus leads to the secretion of the luteinizing hormone from the pituitary. This consequently causes the secretion of testosterone in the testicles that is necessary for testis maturation and growth. Also other hormones which are important for growth and sexual development such as the growth hormone, follicle stimulating hormone and the lutenizing

hormone are produced by the thalamic stimulus and deficiency of those hormones causes dwarfism and failure to develop adult sexual functions. Thus, infertility and the reduction of body size in RibKO mice might be induced by insufficient hormonal secretion owing to the altered thalamic size. Although we did not test this hypothesis it is interesting that also in human patients microcephaly is often accompanied by a reduction in body size which can be caused by reduced growth hormone levels. Thus, it would be interesting to analyze the hormonal levels in RibKO mice and hopefully, further studies will address this question.

The motor deficits and the constant twitching that we observe in RibKO mice did not allow us to assess any other behavioral paradigms that would be necessary to analyze other brain disorders such as schizophrenia or autism spectrum disorders. Our results are therefore in stark contrast to an earlier report, published by Siuta and colleagues[130], who used the same Cre driver for deleting exon 3 of the *rictor* gene. In their paper, only a very specific phenotype in the prefrontal cortex related to the content of dopamine and serotonin was described while there is no mentioning of any overall phenotype. Interestingly, they linked the reported phenotype to schizophrenia as the mice also showed deficits in pre-pulse inhibition, a paradigm to assess the ability of the brain to filter out unnecessary information. Although we think that the paper reports an interesting aspect of mTORC2 function, we are wondering whether their interpretation is still valid given that *rictor* deletion leads to a rather drastic phenotype that affects the entire cell size, dendritic structure, synapse function and connectivity of neurons. It is well possible that the deletion of exon 3 leads to only partial recombination of the rictor gene which would explain the difference in phenotypic characteristics compared to our mice.

In summary, our data show that unlike other cell types, neurons are highly rictor-dependent. Although we are able to show that Akt and PKC activities are majorly diminished in RibKO mice, their contribution to the phenotype is still not clearly resolved. Both kinases are essential for neuronal development and function and both kinases regulate a multitude of other proteins and signaling cascades. In our study, we were able to expand the mTOR signaling pathway in neurons by adding GAP-43, MARCKS and fascin as possible players in the restructuring of the actin cytoskeleton. Because none of the other analyzed tissues such as fat and muscle have developed alterations in the cell size and shape upon loss of rictor function *in vivo*, this might indicate that PKC and its neuron specific downstream target GAP-43 are involved in the phenotype in RibKO mice. Although it cannot be excluded that other, yet unknown proteins also contribute to the phenotype, those data allude that the actin modifying activity of PKC and GAP-43 are involved in the morphological alterations in RibKO mice. In addition it provides first time evidence for the *in vivo* function of rictor in the regulation of the actin cytoskeleton. Because many CNS diseases are caused by dysfunctional neuronal connectivity, by alterations of dendritic arbors or reduced spine formation, it will be important to analyze other neuron type specific rictor knockout models for the contribution of rictor to psychiatric and neurological diseases including schizophrenia, autism spectrum disorders and Parkinson.

EXPERIMENTAL PROCEDURES

Generation of mice. Mice, homozygous for an allele containing LoxP sites flanking exon 4 and 5 of the *rictor* gene, were crossed with Nestin Cre transgenic mice to create heterozygous mice. These mice were then crossed with homozygously floxed *rictor* mice (*rictor* $^{fl/fl}$) to obtain *rictor* knockout mice (RibKO mice). Genotyping was performed by PCR on DNA isolated from toe using specific primers for the floxed region, the Cre transgenes or the recombined alleles as described in [122].

Tissue homogenization and Western blot analysis. Brains were dissected, transferred into protein lysate buffer (50 mM Tris; 150 mM NaCl; 1 mM EDTA; 1% Triton X100 supplemented with EDTA-free protease inhibitor cocktail tablets (Roche) and phosphatase inhibitor tablets PhosSTOP (Roche)) and homogenized with a Polytron using 10 strokes at 800 rpm. The homogenate was centrifuged at 13,600 g for 15 min. at 4°C. Cleared lysates were then used to determine total protein amount (BCA Protein Assay, Pierce). After dilution with 4x SDS sample buffer, equal protein amounts were loaded onto SDS gels.

Antibodies. Rabbit polyclonal antibodies were as follows: P-FoxO1 (Ser256), P-mTOR (Ser2448), P-mTOR (2481), P-PKCα (Ser657), PKCγ, GAP-43 (Ser41) and Cdc42 from Santa Cruz, Akt, Phospho- Akt (Thr308), Phospho-GSK-3b (Ser9), mTOR, PKCα, S6 Ribosomal Protein, Phospho-S6 Ribosomal Protein (Ser235/236), pS6 kinase and S6K, Phospho-MARCKS (Ser152/156), P-PAK1 (Thr423)/PAK2 (Thr402), Tyrosinhydroxylase from Cell Signaling. Phospho-PKCβ2 (T641) and Phospho-PKCε (S729) from abcam. Phospho-fascin (Ser39) from Covolab. Rabbit monoclonal antibodies were as follows: PKCε. β-actin, Phospho-Akt (Ser473), GSK-3β, Raptor and Rictor from Cell Signaling. PKCβII from abcam. Mouse monoclonal antibodies are as follows β-tubulin, Calbindin D-28K from Swant and PCNA from Abcam, GAP-43 from Invitrogen, GLUR2 and NR1 from BD Pharmingen and GAD67 from Chemicon. Guinea pig polyclonal antibodies were as follows: vGLUT1, vGLUT2 and vGAT from Synaptic Systems and GLAST from Chemicon. Rac1 and RhoA antibodies were derived from Active RhoA and Rac1 Pull-Down and Detection kits from Thermo scientific.

Histology and immunohistochemistry. Mice were anesthetized with a lethal dose of Pentobarbital (300 mg/kg) and transcardially perfused with 4% PFA. Brains were removed and tissue processed with a Shandon Pathcenter and embedded in paraffin (Merck). Paraffin blocks were cut with a microtome into 3 - 5 µm-thick sagittal or coronal sections. Antigen retrieval was performed before immunostaining by cooking the brain sections in sodium citrate buffer (10 mM sodium citrate in H_2O; 0.05% Tween 20, pH 6) for 20 min. Sections were rinsed twice in PBS, blocked with blocking buffer (5% BSA in PBS, 0.2% Triton) for 30 min. and incubated with primary antibody overnight at 4°C. Samples were washed three times with PBS and then stained with appropriate fluorescently labeled, secondary antibodies for 1 hr at room temperature. Samples were mounted with Kaiser's glycerol gelatin (Merck). General histology on sections was performed using Cresyl violet. Volumetric quantification of brain areas was performed in Cresyl violet-stained, 25 µm coronal paraffin sections. The arbitrary area of microscopic pictures taken at 2.5 x resolution was analyzed with Analysis software. Microscopy of immunohistochemically-

stained sections was performed with a fluorescence microscope or a confocal laser scanning microscope.

Golgi staining was performed by incubating freshly perfused mouse brains in Golgi solution (5% potassium dichromate, 5% potassium chromate, 5% mercuric chloride dissolved in H_2O) for 6 weeks. The solution was changed every two to three days. Brains were then subsequently dehydrated in 50%, 70%, 90% and 100% ethanol each step for several days. Brains were transferred to 2%, 4% and 8% Celloidin solution. For embedding, 8% Celloidin was evaporated to 16%, hardened to a block and cut with a vibratome into 200 µm sagittal sections. The sections were transferred onto gelatinized slides and stained first in ammonium hydroxide (14%) for 30 min. followed by Kodak fix solution for 30 min. The sections were then dehydrated in 50%, 70%, 90% and 100% ethanol followed by 15 min. CXA solution (1:1:1chloroform / xylol / ethanol) and embedded with Merckoglas (Merck). Microscopy was performed with a light microscope (Leitz DM RB). Golgi-stained neurons were reconstructed by camera lucida. The obtained data was analyzed with Microsoft Exel.

BrdU labeling was performed by intraperitoneally injecting mice with 50 µg BrdU in Tris-HCl (0.1M, pH 7.4) per gram of body weight. P14 animals were euthanized 2h after BrdU injection. Immunostaining was performed as described.

Quantification. Quantification of Golgi-stained neurons was performed by camera lucida reconstruction and analysis with Neurolucida software. Volumetric quantification of brain areas was performed in Cresyl violet-stained, 25 µm coronal paraffin sections. The arbitrary area of microscopic pictures taken at 2.5 x resolution was analyzed with Analysis software. Analysis of cell density was performed on sagittal, NeuN-stained, 5 µm thick paraffin sections in the retrosplenial and visual cortex. Quantification of Western blot protein band intensity was performed with ImageJ program. Quantification of all other anatomical and cellular parameters described in this manuscript was performed with Analysis software.

Statistical analysis. Statistical significance was assessed with the Student's *t* test. Differences were considered to be statistically significant if the *P* value was less than 0.05. All quantitative data were presented as means ± s.e.m. or s.d. as indicated in the figure legends.

Electrophysiology. Mice of the age of 25 days were deeply sedated with isoflurane. After decapitation, the brain was rapidly removed and immediately transferred into ice-cold, oxygenated (95% O_2, 5% CO_2), artificial cerebrospinal fluid (ACSF) containing 119 mM NaCl, 1 mM NaH_2Po_4, 2.5 mM KCl, 2.5 mM $CaCl_2$, 1.3 mM $MgCl_2$, 11 mM D-glucose and 26.2 mM $NaHCO_3$. Cerebella were cut with a vibratome into 250 µm sagittal sections and retained at least for 1 h at room temperature in oxygenated ACSF before recording. Miniature events were recorded using an Axonpatch Multiclamp 700B amplifier and borosilicate glass pipettes (4-6 mΩ) filled with intracellular solution (135 mM $CsMeSO_4$, 8 mM NaCl, 10 mM HEPES, 0.5 mM EGTA, 4 mM Mg-ATP, 0.3 mM Na-GTP, 5 mM Lidocaine-N-ethylbromid). For mEPSC recording, the holding potential was set to -70 mV. For mIPSC recording the holding potential was set to 0 mV. In both conditions, the postsynaptic current was recorded for 10 min. in the presence of 0.5 µM TTX. Traces were further analyzed with Mini Analysis Program v6 (Synaptosoft).

Tissue cultures. Neurospheres were isolated from newborn (P0) mice. Pups were decapitated, brains removed and transferred into ice-cold HBSS. Under a dissection microscope, meninges were carefully removed and one brain half was transferred into freshly prepared neurosphere medium DMEM-F12 (1:1), supplemented with 1% penicillin/streptomycin, 0.2 mg/ml glutamine, 2% B27, 2 µg/ml heparin, 20 ng/ml EGF and 10 ng/ml FGF2. The brain was carefully homogenized and plated on a 6 cm dish containing 4 ml NM and incubated at 36.5°C, 5% CO_2 in an incubator. After 4-5 days, the neurospheres were split into a single cell suspension and secondary neurospheres were grown for 6 days. 24 h prior to fixation, 10 µM BrdU was added to the medium. Neurospheres were fixed with 4% PFA and imaged at low magnification to determine the diameter of the neurospheres. To assess the number of the BrdU-positive cells, neurospheres were embedded in cryoprotective material, cut into 12 µm-thick sections and immunostained with antibodies to BrdU. The number of BrdU-positive cells per sphere was counted and normalized to the sphere diameter.

Organotypic cerebellar slices were cultured as described elsewhere [171]. In brief, P0 brains were dissected and transferred into ice-cold Gey`s balanced salt solution. Meninges were carefully removed and cerebella dissected. With a tissue chopper (McIIwain) 350 µm-thick sagittal slices were cut and transferred into fresh Gey`s solution. Slices were cultured on 0.4 µm membranes in 1 ml culture medium (50% basal medium with Earl`s salts, 25% HBSS, 25% horse serum, 1 mM glutamine, 5 mg/ml glucose) for 14 days. Culture medium was changed every 2-3 days.

Cultures of dissociated hippocampal neurons were performed as follows: Brains of P0 mice were dissected and transferred into ice-cold HBSS. Hippocampi were removed, trypsinized for 15 min. and dissociated. Cells were plated on poly-L-lysine coated coverslips at a density of 90,000 cells per well in a 24 well plate. Neurons were grown for 14 days. After 7 days, neurons were transfected with constructs encoding GFP and actin-RFP-dimers under the synapsin promoter using Lipofectamine. After 14 days, cultures were fixed with 4% PFA in PBS, containing 120 mM sucrose, washed in PBS and embedded with Kaiser`s glycerol gelatine.

Mouse behavior. For hind limb clasping assessment, one year-old mice were lifted by the tail and held over the cage for up to 2 minutes. Clasping was scored when mice crossed hind limbs for more than 3 seconds. The rotarod test was performed by placing 10 week-old mice on a rod which started moving at 5 rpm shortly after placement. Speed was continuously increased from 5 to 30 rpm in 120 seconds. The time that mice were able to stay on the rotating rod was measured. Assessment of motor control by the balance beam was conducted by placing the mice on the one side of the bar (length: 30 cm, width: 1.2 mm) which was brightly illuminated and letting them run over to the other side which ended in a dark box to symbolize shelter. Performance of mice was evaluated and tail support, touching the bar with the abdomen, hopping or robbing and holding of the bar with the paws from the bottom was scored as defective motor control.

Active RhoA and Rac1 pull-down and detection kits

The detection of active RhoA and Rac1 was performed as described in the user manual of the detection kits (Thermo scientific, assay number 16118 and 89854). Cdc42 activity was assessed with antibodies to Cdc42 using the active Rac1 lysate.

Detection of PKC substrates by Mass spectrometric (MS) analysis

For detection of PKC substrates, 8% polyacrylamide gel was loaded with whole brain protein samples of control and RibKO mice. The gel was stained with Coomassie blue for 2 hours and then washed over night in filtered H_2H. A gel band between 40 and 50 kDa was excised for each genotype and digested for MS measurement. For the digestion, gel pieces were immersed in 50% n-propanol and then washed 2-3 times in 40% n-propanol. To de-stain, the gel pieces were washed 5 times in 50% acetonitrile / 0.1 M NH_4HCO_3 and then incubated in this solution for 2 hours. Afterwards, gels were dehydrated with 100% acetonitrile for 10 minutes and then dried for 30 min. After complete evaporation, gel pieces were incubated in 50 µl of 10 mM DTT in 100 mM Tris-HCl (pH 8) at 37°C for 1 hour. Then DTT was replaced by 50 µl of a solution containing 50 mM Iodoacetamide in 100 mM Tris-HCl (pH 8) and incubated for 15 min in the dark. The access solution was removed and the gels washed in 50% acetonitrile / 0.1 M NH_4HCO_3, again dehydrated in 100% acetonitrile for 10 min and then air dried until liquid was completely evaporated. For each digest, 10 µl of a trypsin solution (12.5 ng / µl trypsin in 50 mM NH4HCO3) was added to obtain a final concentration of 0.125 µg trypsin per digest. The digest was incubated for 12-20 hours at 37°C. The supernatant was transferred into another eppendorf tube and the digest extracted with 30-50 µl 50% acetonitrile / 0.1 formic acid for 5 min at room temperature. The supernatant of the latter digest was then pooled with the first supernatant and dried in a speedvac. The dried peptides were then dissolved in 30 µl 0.1% formic acid / 2% acetonitrile for MS measurement.

ACKNOWLEDGEMENTS

I would like to show my gratitude to all the people who have contributed directly or indirectly to the accomplishment of this dissertation. Although it bears my name, this thesis would not have been possible without their help.

First of all I want to thank my Professor, Markus Rüegg, for giving me the chance to work on such an interesting and versatile project, and for providing a high research standard. I have been fortunate that he gave me scope for development and the opportunity to explore freely.

I am grateful to all my colleagues who have accompanied me during my time at the Biocenter and who have created such a wonderful working atmosphere. They have aided in realizing this thesis not least by supporting me in times of frustration with personal encouragement and scientific advice. Especially I would like to express my gratitude to Dr. Dimitri Cloetta who has contributed scientifically in many discussions concerning this project. But more importantly he has provided emotional support and has become a friend during this time.

I also would like to thank Dr. Stephan Frank for his help in the initial analysis of the histology, for providing me with equipment and for reading the paper manuscript. I am also grateful for his persistent interest in the project, for the discussions and for his helpful suggestions.

I also want to thank Dr. Martin Gassmann and Dr. Joseph Kapfhammer for reading the manuscript. I thank Suzette Moes and Paul Jenö for measuring the Masspec samples and for their help in interpreting the data. I also would like to thank Dr. Peter Scheiffele for providing us with the Pcp2/L7-Cre mice and Dr. Andreas Lüthi for providing me the Neurolucida equipment. I also wish to thank Dr. Fatiha Boukhtouche for her help in setting up the cerebellar slice cultures and all the people from the animal facility for taking care of the mice.

I am truly thankful to my boyfriend Daniel for his patience, his support, his honesty and his thoughtfulness and above all for giving me his love. With understanding and humor he has helped me to maintain self-contentment in times when it was needed.

Most importantly, none of this would have been possible without my parents. They have been a current source of support, advice, encouragement and love and they have often given me the strength to carry on in demanding situations.

REFERENCES

1 Quintes, S., Goebbels, S., Saher, G., Schwab, M. H. & Nave, K. A. Neuron-glia signaling and the protection of axon function by Schwann cells. *J Peripher Nerv Syst* **15**, 10-16 (2010).

2 Eulenburg, V. & Gomeza, J. Neurotransmitter transporters expressed in glial cells as regulators of synapse function. *Brain research reviews* **63**, 103-112 (2010).

3 Pardo, C. A. & Eberhart, C. G. The neurobiology of autism. *Brain pathology (Zurich, Switzerland)* **17**, 434-447 (2007).

4 Benitez-King, G., Ramirez-Rodriguez, G., Ortiz, L. & Meza, I. The neuronal cytoskeleton as a potential therapeutical target in neurodegenerative diseases and schizophrenia. *Current drug targets* **3**, 515-533 (2004).

5 Knoblich, J. A. Mechanisms of asymmetric stem cell division. *Cell* **132**, 583-597 (2008).

6 Marin, O., Valiente, M., Ge, X. & Tsai, L. H. Guiding neuronal cell migrations. *Cold Spring Harbor perspectives in biology* **2**, a001834 (2010).

7 Bradke, F. & Dotti, C. G. The role of local actin instability in axon formation. *Science (New York, N.Y* **283**, 1931-1934 (1999).

8 Kunda, P., Paglini, G., Quiroga, S., Kosik, K. & Caceres, A. Evidence for the involvement of Tiam1 in axon formation. *J Neurosci* **21**, 2361-2372 (2001).

9 Craig, A. M. & Banker, G. Neuronal polarity. *Annual review of neuroscience* **17**, 267-310 (1994).

10 McAllister, A. K. Cellular and molecular mechanisms of dendrite growth. *Cereb Cortex* **10**, 963-973 (2000).

11 Luo, L. Actin cytoskeleton regulation in neuronal morphogenesis and structural plasticity. *Annual review of cell and developmental biology* **18**, 601-635 (2002).

12 Stiess, M. & Bradke, F. Neuronal polarization: The cytoskeleton leads the way. *Developmental neurobiology* (2010).

13 Denny, J. B. Molecular mechanisms, biological actions, and neuropharmacology of the growth-associated protein GAP-43. *Current neuropharmacology* **4**, 293-304 (2006).

14 He, Q., Dent, E. W. & Meiri, K. F. Modulation of actin filament behavior by GAP-43 (neuromodulin) is dependent on the phosphorylation status of serine 41, the protein kinase C site. *J Neurosci* **17**, 3515-3524 (1997).

15 Urbanska, M., Blazejczyk, M. & Jaworski, J. Molecular basis of dendritic arborization. *Acta neurobiologiae experimentalis* **68**, 264-288 (2008).

16 Gulledge, A. T., Kampa, B. M. & Stuart, G. J. Synaptic integration in dendritic trees. *Journal of neurobiology* **64**, 75-90 (2005).

17 Segev, I. & London, M. Untangling dendrites with quantitative models. *Science (New York, N.Y* **290**, 744-750 (2000).

18 Voogd, J. & Glickstein, M. The anatomy of the cerebellum. *Trends Neurosci* **21**, 370-375 (1998).

19 Sillitoe, R. V. & Joyner, A. L. Morphology, molecular codes, and circuitry produce the three-dimensional complexity of the cerebellum. *Annual review of cell and developmental biology* **23**, 549-577 (2007).

20 Miale, I. L. & Sidman, R. L. An autoradiographic analysis of histogenesis in the mouse cerebellum. *Exp Neurol* **4**, 277-296 (1961).

21 Edwards, M. A., Yamamoto, M. & Caviness, V. S., Jr. Organization of radial glia and related cells in the developing murine CNS. An analysis based upon a new monoclonal antibody marker. *Neuroscience* **36**, 121-144 (1990).

22 Morales, D. & Hatten, M. E. Molecular markers of neuronal progenitors in the embryonic cerebellar anlage. *J Neurosci* **26**, 12226-12236 (2006).

23 Kapfhammer, J. P. Cellular and molecular control of dendritic growth and development of cerebellar Purkinje cells. *Prog Histochem Cytochem* **39**, 131-182 (2004).

24 Mason, C. A., Christakos, S. & Catalano, S. M. Early climbing fiber interactions with Purkinje cells in the postnatal mouse cerebellum. *J Comp Neurol* **297**, 77-90 (1990).

25 Altman, J. Postnatal development of the cerebellar cortex in the rat. II. Phases in the maturation of Purkinje cells and of the molecular layer. *J Comp Neurol* **145**, 399-463 (1972).

26 Hendelman, W. J. & Aggerwal, A. S. The Purkinje neuron: I. A Golgi study of its development in the mouse and in culture. *J Comp Neurol* **193**, 1063-1079 (1980).

27 Machold, R. & Fishell, G. Math1 is expressed in temporally discrete pools of cerebellar rhombic-lip neural progenitors. *Neuron* **48**, 17-24 (2005).

28 Wingate, R. J. The rhombic lip and early cerebellar development. *Curr Opin Neurobiol* **11**, 82-88 (2001).

29 Evans, G. J. Synaptic signalling in cerebellar plasticity. *Biol Cell* **99**, 363-378 (2007).

30 Fujita, S. Quantitative analysis of cell proliferation and differentiation in the cortex of the postnatal mouse cerebellum. *J Cell Biol* **32**, 277-287 (1967).

31 Wang, J., Arbuzova, A., Hangyas-Mihalyne, G. & McLaughlin, S. The effector domain of myristoylated alanine-rich C kinase substrate binds strongly to phosphatidylinositol 4,5-bisphosphate. *The Journal of biological chemistry* **276**, 5012-5019 (2001).

32 Goldowitz, D. & Hamre, K. The cells and molecules that make a cerebellum. *Trends Neurosci* **21**, 375-382 (1998).

33 Brown, G. E., Karpetsky, T. P., Rictor, K. & Rahman, A. Characterization of deoxyribonuclease activities derived from control and inflammation-associated mouse peritoneal macrophages. *The Biochemical journal* **220**, 561-568 (1984).

34 Watanabe, M. Molecular mechanisms governing competitive synaptic wiring in cerebellar Purkinje cells. *Tohoku J Exp Med* **214**, 175-190 (2008).

35 Napper, R. M. & Harvey, R. J. Number of parallel fiber synapses on an individual Purkinje cell in the cerebellum of the rat. *The Journal of comparative neurology* **274**, 168-177 (1988).

36 Bosman, L. W. & Konnerth, A. Activity-dependent plasticity of developing climbing fiber-Purkinje cell synapses. *Neuroscience* **162**, 612-623 (2009).

37 Doughty, M. L., Delhaye-Bouchaud, N. & Mariani, J. Quantitative analysis of cerebellar lobulation in normal and agranular rats. *J Comp Neurol* **399**, 306-320 (1998).

38 Rakic, P. & Sidman, R. L. Organization of cerebellar cortex secondary to deficit of granule cells in weaver mutant mice. *J Comp Neurol* **152**, 133-161 (1973).

39 Vincent, J., Legrand, C., Rabie, A. & Legrand, J. Effects of thyroid hormone on synaptogenesis in the molecular layer of the developing rat cerebellum. *J Physiol (Paris)* **78**, 729-738 (1982).

40 Tsutsui, K., Ukena, K., Usui, M., Sakamoto, H. & Takase, M. Novel brain function: biosynthesis and actions of neurosteroids in neurons. *Neurosci Res* **36**, 261-273 (2000).

41 Sakamoto, H., Mezaki, Y., Shikimi, H., Ukena, K. & Tsutsui, K. Dendritic growth and spine formation in response to estrogen in the developing Purkinje cell. *Endocrinology* **144**, 4466-4477 (2003).

42 Mount, H. T., Elkabes, S., Dreyfus, C. F. & Black, I. B. Differential involvement of metabotropic and p75 neurotrophin receptors in effects of nerve growth factor and neurotrophin-3 on cultured Purkinje cell survival. *J Neurochem* **70**, 1045-1053 (1998).

43 Schilling, K., Dickinson, M. H., Connor, J. A. & Morgan, J. I. Electrical activity in cerebellar cultures determines Purkinje cell dendritic growth patterns. *Neuron* **7**, 891-902 (1991).

44 Larsell, O. The morphogenesis and adult pattern of the lobules and fissures of the cerebellum of the white rat. *J Comp Neurol* **97**, 281-356 (1952).

45 Sudarov, A. & Joyner, A. L. Cerebellum morphogenesis: the foliation pattern is orchestrated by multi-cellular anchoring centers. *Neural development* **2**, 26 (2007).

46 He, C. & Klionsky, D. J. Regulation mechanisms and signaling pathways of autophagy. *Annual review of genetics* **43**, 67-93 (2009).

47 Zoncu, R., Efeyan, A. & Sabatini, D. M. mTOR: from growth signal integration to cancer, diabetes and ageing. *Nat Rev Mol Cell Biol* **12**, 21-35 (2011).

48 Heitman, J., Movva, N. R. & Hall, M. N. Targets for cell cycle arrest by the immunosuppressant rapamycin in yeast. *Science (New York, N.Y* **253**, 905-909. (1991).

49 Jacinto, E. & Hall, M. N. Tor signalling in bugs, brain and brawn. *Nat Rev Mol Cell Biol* **4**, 117-126 (2003).

50 Kim, D. H. *et al.* mTOR interacts with raptor to form a nutrient-sensitive complex that signals to the cell growth machinery. *Cell* **110**, 163-175 (2002).

51 Sarbassov, D. D. *et al.* Rictor, a novel binding partner of mTOR, defines a rapamycin-insensitive and raptor-independent pathway that regulates the cytoskeleton. *Curr Biol* **14**, 1296-1302 (2004).

52 Sarbassov, D. D. *et al.* Prolonged rapamycin treatment inhibits mTORC2 assembly and Akt/PKB. *Molecular cell* **22**, 159-168 (2006).

53 Wullschleger, S., Loewith, R. & Hall, M. N. TOR signaling in growth and metabolism. *Cell* **124**, 471-484 (2006).

54 Sabatini, D. M. mTOR and cancer: insights into a complex relationship. *Nature reviews* **6**, 729-734 (2006).

55 Martin, D. E. & Hall, M. N. The expanding TOR signaling network. *Current opinion in cell biology* **17**, 158-166 (2005).

56 Wang, L., Harris, T. E., Roth, R. A. & Lawrence, J. C., Jr. PRAS40 regulates mTORC1 kinase activity by functioning as a direct inhibitor of substrate binding. *J Biol Chem* **282**, 20036-20044 (2007).

57 Pearce, L. R. *et al.* Identification of Protor as a novel Rictor-binding component of mTOR complex-2. *Biochem J* **405**, 513-522 (2007).

58 Frias, M. A. *et al.* mSin1 is necessary for Akt/PKB phosphorylation, and its isoforms define three distinct mTORC2s. *Curr Biol* **16**, 1865-1870 (2006).

59 Yang, Q., Inoki, K., Ikenoue, T. & Guan, K. L. Identification of Sin1 as an essential TORC2 component required for complex formation and kinase activity. *Genes Dev* **20**, 2820-2832 (2006).

60 Loewith, R. *et al.* Two TOR complexes, only one of which is rapamycin sensitive, have distinct roles in cell growth control. *Mol Cell* **10**, 457-468 (2002).

61 Peterson, T. R. *et al.* DEPTOR is an mTOR inhibitor frequently overexpressed in multiple myeloma cells and required for their survival. *Cell* **137**, 873-886 (2009).

62 Sarbassov, D. D., Guertin, D. A., Ali, S. M. & Sabatini, D. M. Phosphorylation and regulation of Akt/PKB by the rictor-mTOR complex. *Science* **307**, 1098-1101 (2005).

63 Ikenoue, T., Inoki, K., Yang, Q., Zhou, X. & Guan, K. L. Essential function of TORC2 in PKC and Akt turn motif phosphorylation, maturation and signalling. *Embo J* **27**, 1919-1931 (2008).

64 Hietakangas, V. & Cohen, S. M. Re-evaluating AKT regulation: role of TOR complex 2 in tissue growth. *Genes Dev* **21**, 632-637 (2007).

65 Alessi, D. R. *et al.* Mechanism of activation of protein kinase B by insulin and IGF-1. *Embo J* **15**, 6541-6551 (1996).

66 Long, X., Lin, Y., Ortiz-Vega, S., Yonezawa, K. & Avruch, J. Rheb binds and regulates the mTOR kinase. *Curr Biol* **15**, 702-713 (2005).

67 Long, X., Ortiz-Vega, S., Lin, Y. & Avruch, J. Rheb binding to mammalian target of rapamycin (mTOR) is regulated by amino acid sufficiency. *J Biol Chem* **280**, 23433-23436 (2005).

68 Vander Haar, E., Lee, S. I., Bandhakavi, S., Griffin, T. J. & Kim, D. H. Insulin signalling to mTOR mediated by the Akt/PKB substrate PRAS40. *Nat Cell Biol* **9**, 316-323 (2007).

69 Garami, A. *et al.* Insulin activation of Rheb, a mediator of mTOR/S6K/4E-BP signaling, is inhibited by TSC1 and 2. *Mol Cell* **11**, 1457-1466 (2003).

70 Inoki, K., Li, Y., Xu, T. & Guan, K. L. Rheb GTPase is a direct target of TSC2 GAP activity and regulates mTOR signaling. *Genes Dev* **17**, 1829-1834 (2003).

71 Zhang, Y. *et al.* Rheb is a direct target of the tuberous sclerosis tumour suppressor proteins. *Nat Cell Biol* **5**, 578-581 (2003).

72 Tee, A. R., Manning, B. D., Roux, P. P., Cantley, L. C. & Blenis, J. Tuberous sclerosis complex gene products, Tuberin and Hamartin, control mTOR signaling by acting as a GTPase-activating protein complex toward Rheb. *Curr Biol* **13**, 1259-1268 (2003).

73 Inoki, K., Li, Y., Zhu, T., Wu, J. & Guan, K. L. TSC2 is phosphorylated and inhibited by Akt and suppresses mTOR signalling. *Nat Cell Biol* **4**, 648-657 (2002).

74 Ma, X. M. & Blenis, J. Molecular mechanisms of mTOR-mediated translational control. *Nat Rev Mol Cell Biol* **10**, 307-318 (2009).

75 Birkenkamp, K. U. & Coffer, P. J. Regulation of cell survival and proliferation by the FOXO (Forkhead box, class O) subfamily of Forkhead transcription factors. *Biochem Soc Trans* **31**, 292-297 (2003).

76 Biggs, W. H., 3rd, Meisenhelder, J., Hunter, T., Cavenee, W. K. & Arden, K. C. Protein kinase B/Akt-mediated phosphorylation promotes nuclear exclusion of the winged helix transcription factor FKHR1. *Proc Natl Acad Sci U S A* **96**, 7421-7426 (1999).

77 Guertin, D. A. *et al.* Ablation in mice of the mTORC components raptor, rictor, or mLST8 reveals that mTORC2 is required for signaling to Akt-FOXO and PKCalpha, but not S6K1. *Dev Cell* **11**, 859-871 (2006).

78 Jacinto, E. *et al.* SIN1/MIP1 maintains rictor-mTOR complex integrity and regulates Akt phosphorylation and substrate specificity. *Cell* **127**, 125-137 (2006).

79 Read, D. E. & Gorman, A. M. Involvement of Akt in neurite outgrowth. *Cell Mol Life Sci* **66**, 2975-2984 (2009).

80 Easton, R. M. *et al.* Role for Akt3/protein kinase Bgamma in attainment of normal brain size. *Molecular and cellular biology* **25**, 1869-1878 (2005).

81 Higuchi, M., Onishi, K., Masuyama, N. & Gotoh, Y. The phosphatidylinositol-3 kinase (PI3K)-Akt pathway suppresses neurite branch formation in NGF-treated PC12 cells. *Genes Cells* **8**, 657-669 (2003).

82 Beaulieu, J. M., Gainetdinov, R. R. & Caron, M. G. Akt/GSK3 signaling in the action of psychotropic drugs. *Annual review of pharmacology and toxicology* **49**, 327-347 (2009).

83 Huang, E. J. & Reichardt, L. F. Trk receptors: roles in neuronal signal transduction. *Annual review of biochemistry* **72**, 609-642 (2003).

84 Qi, X. J., Wildey, G. M. & Howe, P. H. Evidence that Ser87 of BimEL is phosphorylated by Akt and regulates BimEL apoptotic function. *The Journal of biological chemistry* **281**, 813-823 (2006).

85 Datta, S. R. *et al.* Akt phosphorylation of BAD couples survival signals to the cell-intrinsic death machinery. *Cell* **91**, 231-241 (1997).

86 Du, K. & Montminy, M. CREB is a regulatory target for the protein kinase Akt/PKB. *The Journal of biological chemistry* **273**, 32377-32379 (1998).

87 Asnaghi, L., Bruno, P., Priulla, M. & Nicolin, A. mTOR: a protein kinase switching between life and death. *Pharmacol Res* **50**, 545-549 (2004).

88 Ksiezak-Reding, H., Pyo, H. K., Feinstein, B. & Pasinetti, G. M. Akt/PKB kinase phosphorylates separately Thr212 and Ser214 of tau protein in vitro. *Biochimica et biophysica acta* **1639**, 159-168 (2003).

89 Enomoto, A. *et al.* Akt/PKB regulates actin organization and cell motility via Girdin/APE. *Developmental cell* **9**, 389-402 (2005).

90 Shiue, H., Musch, M. W., Wang, Y., Chang, E. B. & Turner, J. R. Akt2 phosphorylates ezrin to trigger NHE3 translocation and activation. *The Journal of biological chemistry* **280**, 1688-1695 (2005).

91 Bokoch, G. M. Biology of the p21-activated kinases. *Annual review of biochemistry* **72**, 743-781 (2003).

92 Facchinetti, V. *et al.* The mammalian target of rapamycin complex 2 controls folding and stability of Akt and protein kinase C. *The EMBO journal* **27**, 1932-1943 (2008).

93 Nishizuka, Y. Protein kinase C and lipid signaling for sustained cellular responses. *Faseb J* **9**, 484-496 (1995).

94 Ohno, S. & Nishizuka, Y. Protein kinase C isotypes and their specific functions: prologue. *Journal of biochemistry* **132**, 509-511 (2002).

95 Balendran, A. *et al.* A 3-phosphoinositide-dependent protein kinase-1 (PDK1) docking site is required for the phosphorylation of protein kinase Czeta (PKCzeta) and PKC-related kinase 2 by PDK1. *J Biol Chem* **275**, 20806-20813 (2000).

96 Newton, A. C. Regulation of the ABC kinases by phosphorylation: protein kinase C as a paradigm. *Biochem J* **370**, 361-371 (2003).

97 Edwards, A. S., Faux, M. C., Scott, J. D. & Newton, A. C. Carboxyl-terminal phosphorylation regulates the function and subcellular localization of protein kinase C betaII. *J Biol Chem* **274**, 6461-6468 (1999).

98 Dutil, E. M., Keranen, L. M., DePaoli-Roach, A. A. & Newton, A. C. In vivo regulation of protein kinase C by trans-phosphorylation followed by autophosphorylation. *J Biol Chem* **269**, 29359-29362 (1994).

99 Le Good, J. A. *et al.* Protein kinase C isotypes controlled by phosphoinositide 3-kinase through the protein kinase PDK1. *Science* **281**, 2042-2045 (1998).

100 Minami, H., Owada, Y., Suzuki, R., Handa, Y. & Kondo, H. Localization of mRNAs for novel, atypical as well as conventional protein kinase C (PKC) isoforms in the brain of developing and mature rats. *J Mol Neurosci* **15**, 121-135 (2000).

101 Chen, G., Masana, M. I. & Manji, H. K. Lithium regulates PKC-mediated intracellular cross-talk and gene expression in the CNS in vivo. *Bipolar disorders* **2**, 217-236 (2000).

102 Van Kolen, K., Pullan, S., Neefs, J. M. & Dautzenberg, F. M. Nociceptive and behavioural sensitisation by protein kinase Cepsilon signalling in the CNS. *Journal of neurochemistry* **104**, 1-13 (2008).

103 Leitges, M., Kovac, J., Plomann, M. & Linden, D. J. A unique PDZ ligand in PKCalpha confers induction of cerebellar long-term synaptic depression. *Neuron* **44**, 585-594 (2004).

104 Saito, N. & Shirai, Y. Protein kinase C gamma (PKC gamma): function of neuron specific isotype. *J Biochem* **132**, 683-687 (2002).

105 Weeber, E. J. *et al.* A role for the beta isoform of protein kinase C in fear conditioning. *J Neurosci* **20**, 5906-5914 (2000).

106 Khasar, S. G. *et al.* A novel nociceptor signaling pathway revealed in protein kinase C epsilon mutant mice. *Neuron* **24**, 253-260 (1999).

107 Jacinto, E. *et al.* Mammalian TOR complex 2 controls the actin cytoskeleton and is rapamycin insensitive. *Nature cell biology* **6**, 1122-1128 (2004).

108 Aigner, L. & Caroni, P. Absence of persistent spreading, branching, and adhesion in GAP-43-depleted growth cones. *The Journal of cell biology* **128**, 647-660 (1995).

109 Akers, R. F. & Routtenberg, A. Protein kinase C phosphorylates a 47 Mr protein (F1) directly related to synaptic plasticity. *Brain Res* **334**, 147-151 (1985).

110 Skene, J. H. & Willard, M. Changes in axonally transported proteins during axon regeneration in toad retinal ganglion cells. *The Journal of cell biology* **89**, 86-95 (1981).

111 Skene, J. H. *et al.* A protein induced during nerve growth (GAP-43) is a major component of growth-cone membranes. *Science (New York, N.Y* **233**, 783-786 (1986).

112 Caroni, P. New EMBO members' review: actin cytoskeleton regulation through modulation of PI(4,5)P(2) rafts. *The EMBO journal* **20**, 4332-4336 (2001).

113 Hens, J. J. *et al.* B-50/GAP-43 binds to actin filaments without affecting actin polymerization and filament organization. *Journal of neurochemistry* **61**, 1530-1533 (1993).

114 Shen, Y., Mishra, R., Mani, S. & Meiri, K. F. Both cell-autonomous and cell non-autonomous functions of GAP-43 are required for normal patterning of the cerebellum in vivo. *Cerebellum (London, England)* **7**, 451-466 (2008).

115 Gan, X., Wang, J., Su, B. & Wu, D. Evidence for direct activation of mTORC2 kinase activity by phosphatidylinositol 3,4,5-trisphosphate. *The Journal of biological chemistry* **286**, 10998-11002 (2011).

116 Zinzalla, V., Stracka, D., Oppliger, W. & Hall, M. N. Activation of mTORC2 by association with the ribosome. *Cell* **144**, 757-768 (2011).

117 Saci, A., Cantley, L. C. & Carpenter, C. L. Rac1 regulates the activity of mTORC1 and mTORC2 and controls cellular size. *Molecular cell* **42**, 50-61 (2011).

118 Huang, J., Dibble, C. C., Matsuzaki, M. & Manning, B. D. The TSC1-TSC2 complex is required for proper activation of mTOR complex 2. *Molecular and cellular biology* **28**, 4104-4115 (2008).

119 Cybulski, N. & Hall, M. N. TOR complex 2: a signaling pathway of its own. *Trends in biochemical sciences* **34**, 620-627 (2009).

120 Shiota, C., Woo, J. T., Lindner, J., Shelton, K. D. & Magnuson, M. A. Multiallelic disruption of the rictor gene in mice reveals that mTOR complex 2 is essential for fetal growth and viability. *Developmental cell* **11**, 583-589 (2006).

121 Jones, K. T., Greer, E. R., Pearce, D. & Ashrafi, K. Rictor/TORC2 regulates Caenorhabditis elegans fat storage, body size, and development through sgk-1. *PLoS Biol* **7**, e60 (2009).

122 Bentzinger, C. F. *et al.* Skeletal muscle-specific ablation of raptor, but not of rictor, causes metabolic changes and results in muscle dystrophy. *Cell metabolism* **8**, 411-424 (2008).

123 Kumar, A. *et al.* Muscle-specific deletion of rictor impairs insulin-stimulated glucose transport and enhances Basal glycogen synthase activity. *Molecular and cellular biology* **28**, 61-70 (2008).

124 Cybulski, N., Polak, P., Auwerx, J., Ruegg, M. A. & Hall, M. N. mTOR complex 2 in adipose tissue negatively controls whole-body growth. *Proceedings of the National Academy of Sciences of the United States of America* **106**, 9902-9907 (2009).

125 Gu, Y., Lindner, J., Kumar, A., Yuan, W. & Magnuson, M. A. Rictor/mTORC2 is essential for maintaining a balance between beta-cell proliferation and cell size. *Diabetes* **60**, 827-837 (2011).

126 Guertin, D. A. *et al.* mTOR complex 2 is required for the development of prostate cancer induced by Pten loss in mice. *Cancer cell* **15**, 148-159 (2009).

127 Cota, D. *et al.* Hypothalamic mTOR signaling regulates food intake. *Science (New York, N.Y* **312**, 927-930 (2006).

128 Swiech, L., Perycz, M., Malik, A. & Jaworski, J. Role of mTOR in physiology and pathology of the nervous system. *Biochim Biophys Acta* **1784**, 116-132 (2008).

129 Fan, Q. W. & Weiss, W. A. Autophagy and Akt promote survival in glioma. *Autophagy* **7**, 536-538 (2011).

130 Siuta, M. A. *et al.* Dysregulation of the norepinephrine transporter sustains cortical hypodopaminergia and schizophrenia-like behaviors in neuronal rictor null mice. *PLoS biology* **8**, e1000393 (2010).

131 Jaworski, J., Spangler, S., Seeburg, D. P., Hoogenraad, C. C. & Sheng, M. Control of dendritic arborization by the phosphoinositide-3'-kinase-Akt-mammalian target of rapamycin pathway. *J Neurosci* **25**, 11300-11312 (2005).

132 Kumar, V., Zhang, M. X., Swank, M. W., Kunz, J. & Wu, G. Y. Regulation of dendritic morphogenesis by Ras-PI3K-Akt-mTOR and Ras-MAPK signaling pathways. *J Neurosci* **25**, 11288-11299 (2005).

133 Tucker, B. A., Rahimtula, M. & Mearow, K. M. Laminin and growth factor receptor activation stimulates differential growth responses in subpopulations of adult DRG neurons. *The European journal of neuroscience* **24**, 676-690 (2006).

134 Levitt, P. & Campbell, D. B. The genetic and neurobiologic compass points toward common signaling dysfunctions in autism spectrum disorders. *The Journal of clinical investigation* **119**, 747-754 (2009).

135 Schrenk, K., Kapfhammer, J. P. & Metzger, F. Altered dendritic development of cerebellar Purkinje cells in slice cultures from protein kinase Cgamma-deficient mice. *Neuroscience* **110**, 675-689 (2002).

136 Laplante, M. & Sabatini, D. M. mTOR signaling at a glance. *J Cell Sci* **122**, 3589-3594 (2009).

137 Nicklin, P. *et al.* Bidirectional transport of amino acids regulates mTOR and autophagy. *Cell* **136**, 521-534 (2009).

138 Avruch, J. *et al.* Insulin and amino-acid regulation of mTOR signaling and kinase activity through the Rheb GTPase. *Oncogene* **25**, 6361-6372 (2006).

139 Zimmerman, L. *et al.* Independent regulatory elements in the nestin gene direct transgene expression to neural stem cells or muscle precursors. *Neuron* **12**, 11-24 (1994).

140 Sands, J., Dobbing, J. & Gratrix, C. A. Cell number and cell size: organ growth and development and the control of catch-up growth in rats. *Lancet* **2**, 503-505 (1979).

141 Reynolds, B. A. & Weiss, S. Clonal and population analyses demonstrate that an EGF-responsive mammalian embryonic CNS precursor is a stem cell. *Developmental biology* **175**, 1-13 (1996).

142 Mori, H. *et al.* Effect of neurosphere size on the growth rate of human neural stem/progenitor cells. *Journal of neuroscience research* **84**, 1682-1691 (2006).

143 Wetts, R. & Herrup, K. Interaction of granule, Purkinje and inferior olivary neurons in lurcher chimeric mice. II. Granule cell death. *Brain Res* **250**, 358-362 (1982).

144 Sidman, R. L., Lane, P. W. & Dickie, M. M. Staggerer, a new mutation in the mouse affecting the cerebellum. *Science (New York, N.Y* **137**, 610-612 (1962).

145 Fremeau, R. T., Jr. *et al.* The expression of vesicular glutamate transporters defines two classes of excitatory synapse. *Neuron* **31**, 247-260 (2001).

146 Hisano, S. *et al.* Expression of inorganic phosphate/vesicular glutamate transporters (BNPI/VGLUT1 and DNPI/VGLUT2) in the cerebellum and precerebellar nuclei of the rat. *Brain Res Mol Brain Res* **107**, 23-31 (2002).

147 Copp, J., Manning, G. & Hunter, T. TORC-specific phosphorylation of mammalian target of rapamycin (mTOR): phospho-Ser2481 is a marker for intact mTOR signaling complex 2. *Cancer research* **69**, 1821-1827 (2009).

148 Brunet, A. *et al.* Akt promotes cell survival by phosphorylating and inhibiting a Forkhead transcription factor. *Cell* **96**, 857-868 (1999).

149 Vivanco, I. & Sawyers, C. L. The phosphatidylinositol 3-Kinase AKT pathway in human cancer. *Nature reviews* **2**, 489-501 (2002).

150 Ikenoue, T., Hong, S. & Inoki, K. Monitoring mammalian target of rapamycin (mTOR) activity. *Methods Enzymol* **452**, 165-180 (2009).

151 Aarts, L. H., Schotman, P., Verhaagen, J., Schrama, L. H. & Gispen, W. H. The role of the neural growth associated protein B-50/GAP-43 in morphogenesis. *Advances in experimental medicine and biology* **446**, 85-106 (1998).

152 Hartwig, J. H. *et al.* MARCKS is an actin filament crosslinking protein regulated by protein kinase C and calcium-calmodulin. *Nature* **356**, 618-622 (1992).

153 Machesky, L. M. & Li, A. Fascin: Invasive filopodia promoting metastasis. *Communicative & integrative biology* **3**, 263-270 (2010).

154 Li, A. *et al.* The actin-bundling protein fascin stabilizes actin in invadopodia and potentiates protrusive invasion. *Curr Biol* **20**, 339-345 (2010).

155 Ono, S. *et al.* Identification of an actin binding region and a protein kinase C phosphorylation site on human fascin. *The Journal of biological chemistry* **272**, 2527-2533 (1997).

156 Nordquist, D. T., Kozak, C. A. & Orr, H. T. cDNA cloning and characterization of three genes uniquely expressed in cerebellum by Purkinje neurons. *J Neurosci* **8**, 4780-4789 (1988).

157 Saito, H. *et al.* L7/Pcp-2-specific expression of Cre recombinase using knock-in approach. *Biochemical and biophysical research communications* **331**, 1216-1221 (2005).

158 Bandeira, F., Lent, R. & Herculano-Houzel, S. Changing numbers of neuronal and non-neuronal cells underlie postnatal brain growth in the rat. *Proceedings of the National Academy of Sciences of the United States of America* **106**, 14108-14113 (2009).

159 Pilpel, Y. & Segal, M. Activation of PKC induces rapid morphological plasticity in dendrites of hippocampal neurons via Rac and Rho-dependent mechanisms. *The European journal of neuroscience* **19**, 3151-3164 (2004).

160 Kwon, T., Kwon, D. Y., Chun, J., Kim, J. H. & Kang, S. S. Akt protein kinase inhibits Rac1-GTP binding through phosphorylation at serine 71 of Rac1. *The Journal of biological chemistry* **275**, 423-428 (2000).

161 Barmack, N. H., Qian, Z. & Yoshimura, J. Regional and cellular distribution of protein kinase C in rat cerebellar Purkinje cells. *The Journal of comparative neurology* **427**, 235-254 (2000).

162 Hashimoto, T. *et al.* Postnatal development of a brain-specific subspecies of protein kinase C in rat. *J Neurosci* **8**, 1678-1683 (1988).

163 Saito, N., Kikkawa, U., Nishizuka, Y. & Tanaka, C. Distribution of protein kinase C-like immunoreactive neurons in rat brain. *J Neurosci* **8**, 369-382 (1988).

164 Kwon, C. H. *et al.* Pten regulates neuronal soma size: a mouse model of Lhermitte-Duclos disease. *Nature genetics* **29**, 404-411 (2001).

165 Ooms, L. M. *et al.* The inositol polyphosphate 5-phosphatase, PIPP, Is a novel regulator of phosphoinositide 3-kinase-dependent neurite elongation. *Molecular biology of the cell* **17**, 607-622 (2006).

166 Casabona, G. Intracellular signal modulation: a pivotal role for protein kinase C. *Progress in neuro-psychopharmacology & biological psychiatry* **21**, 407-425 (1997).

167 Ling, M., Troller, U., Zeidman, R., Lundberg, C. & Larsson, C. Induction of neurites by the regulatory domains of PKCdelta and epsilon is counteracted by PKC catalytic activity and by the RhoA pathway. *Experimental cell research* **292**, 135-150 (2004).

168 Larsson, C. Protein kinase C and the regulation of the actin cytoskeleton. *Cell Signal* **18**, 276-284 (2006).

169 Jansen, S. *et al.* Mechanism of Actin Filament Bundling by Fascin. *The Journal of biological chemistry* (2011).

170 Wojcik, S. M. *et al.* An essential role for vesicular glutamate transporter 1 (VGLUT1) in postnatal development and control of quantal size. *Proceedings of the National Academy of Sciences of the United States of America* **101**, 7158-7163 (2004).

171 Boukhtouche, F. *et al.* Retinoid-related orphan receptor alpha controls the early steps of Purkinje cell dendritic differentiation. *J Neurosci* **26**, 1531-1538 (2006).